

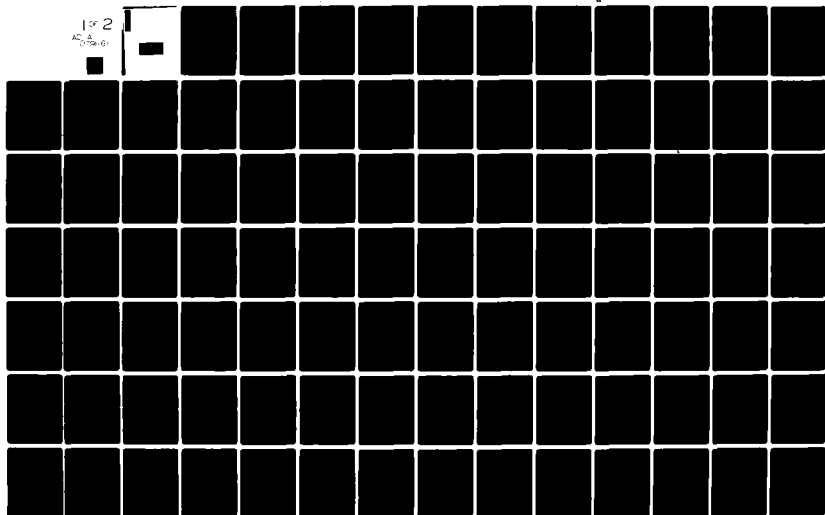
AD-A079 861

AIR FORCE INST OF TECH WRIGHT-PATTERSON AFB OH SCHOOL--ETC F/G 12/1
COMPARISON OF NUMERICAL ANALYSIS METHODS FOR SOLVING ONE-DIMENS--ETC(U)
DEC 79 R A SMITH
AFIT/GAE/AA/79D-17

UNCLASSIFIED

NL

1 of 2
AC 8
D79-61



14 AFIT/GAE/AA/79D-17

6

COMPARISON OF NUMERICAL ANALYSIS
METHODS FOR SOLVING ONE-DIMENSIONAL
ELLIPTIC DIFFERENTIAL EQUATIONS.

9 Poster's THESIS,

AFIT/GAE/AA/79D-17

10

Randy A. Smith
USAF

11 Dec 79

12
158

D D C
RECEIVED
JAN 28 1980
A

Approved for public release; distribution unlimited

012,225

11

COMPARISON OF NUMERICAL ANALYSIS METHODS FOR
SOLVING ONE-DIMENSIONAL, ELLIPTIC
DIFFERENTIAL EQUATIONS

THESIS

Presented to the Faculty of the School of Engineering
of the Air Force Institute of Technology

Air University
in Partial Fulfillment of the
Requirements for the Degree of
Master of Science

by

Randy A. Smith, B.S.
2nd Lt USAF

Graduate Aeronautical Engineering

December 1979

Approved for public release; distribution unlimited

Accession For	
NTIS GAAI	<input checked="checked" type="checkbox"/>
DDC TAB	<input type="checkbox"/>
Unannounced	<input type="checkbox"/>
Justification	
By	
Distribution/	
Available by Date	
Dist	Available/or special
A	

Preface

In any study of the relative value of one particular method compared with another, one must always consider the context in which the methods were compared. The four methods compared in this study: collocation, finite differences, Galerkin, and least squares, have been bent, folded, and mutilated by the pencil and erasure of a young aspiring engineer. Fortunately, the methods and the engineer are still operating today and I have several people to thank for that.

The gentleman who has patiently guided me through this project is Captain James E. Marsh. His guidance and understanding were of great value to me. Dr. John Jones, Jr. and Major Stephen J. Koob also contributed significantly to my understanding of this project. On the nontechnical aspects of the project, my wife Marisa was a true inspiration. Her thoughtful support was priceless to me. And to Ms. Phyllis Reynolds my very capable typist, I owe my most sincere thanks for her patience and perseverance.

Contents

	Page
Preface	ii
List of Figures	iv
List of Tables	v
Abstract	vii
I. Introduction	1
Background	1
Approach	6
II. Problem Set	8
Second-Order Linear--Axial Rod	8
Fourth-Order Linear--Beam in Bending	10
Second-Order Nonlinear	16
III. Computer System and Program Information	19
IV. Results and Discussion	21
Second-Order Linear	23
Fourth-Order Linear	28
Nonlinear	32
V. Conclusions	36
Bibliography	38
Appendix A: Numerical and Graphical Data	39
Appendix B: Finite Difference Expressions	94
Appendix C: Derivation of Finite Element Equations for the Axial Rod	102
Appendix D: Derivation of Finite Element Equations for the Beam in Bending	119
Appendix E: Shape Functions and Derivatives	131
Appendix F: Derivation of Finite Element Equations for the Nonlinear Problem	138
Vita	147

List of Figures

Figure	Page
1. Uniaxial Deflection of a Rod	9
2. Transverse Bending Displacement of a Beam . . .	11
3. Exact solution to the General Nonlinear Problem	17
4. Exact solution to Nonlinear Problem Studied . .	18
5. Main Program Flow Chart	20
B-1. Discretization of One-Dimensional Domain for Finite Difference Method	94
B-2. Symmetry of Approximate Displacement About a Clamped End	95
C-1. Global Illustration of a Clamped-Free Uniform Rod Approximated by Two C^1 Line-Elements with a Half-Sin Load Distribution . .	108
C-2. Global Illustration of a Clamped-Free Uniform Rod Approximated by Two C^0 Line-Elements with a Half-Sin Load Distribution . .	113
E-1. C^0 Line Element	131
E-2. Linear Shape Functions	133
E-3. C^1 Line Element	133
E-4. Cubic Shape Functions	134
E-5. Septic Shape Functions	136
F-1. Discretized Domain for Nonlinear Problem . . .	139

List of Tables

Table	Page
I. Axial Rod Problems--Exact Solutions	12
II. Beam Problems--Exact Solutions	13
III. Performance Criteria Used for Comparing the Numerical Methods for Linear Problems . . .	22
IV. Results--Problem 1; Uniform Clamped- Clamped Rod, Uniform Load	24
V. Results--Problem 2; Uniform Clamped- Free Rod, Uniform Load	24
VI. Results--Problem 3; Variable Clamped- Clamped Rod, Uniform Load, $\alpha=0.5$	25
VII. Results--Problem 4; Variable Clamped- Free Rod, Uniform Load, $\alpha=0.5$	25
VIII. Results--Problem 5; Uniform Clamped- Clamped Rod, Half-Sin Load	26
IX. Results--Problem 6; Uniform Clamped- Free Rod, Half-Sin Load	26
X. Results--Problem 7; Uniform Clamped Clamped Beam, Uniform Load	29
XI. Results--Problem 8; Uniform Clamped- Free Beam, Uniform Load	29
XII. Results--Problem 9; Variable Clamped- Clamped Beam, Uniform Load, $\alpha=0.5$	30
XIII. Results--Problem 10; Variable Clamped- Free Beam, Uniform Load, $\alpha=0.5$	30
XIV. Results--Problem 11; Uniform Clamped- Clamped Beam, Half-Sin Load	31
XV. Results--Problem 12; Uniform Clamped- Free Beam, Half-Sin Load	31

Table	Page
XVI. Nodal Displacements for Nonlinear Problem by Galerkin's Method	33
XVII. Nodal Displacements for Nonlinear Problem by Collocation Method	34
A-I. Uniform Clamped-Clamped Rod, Uniform Load	40
A-II. Uniform Clamped-Free Rod, Uniform Load	42
A-III. Variable Clamped-Clamped Rod, Uniform Load, Taper Ratio $\alpha=0.5$	44
A-IV. Variable Clamped-Free Rod, Uniform Load, Taper Ratio $\alpha=0.5$	46
A-V. Uniform Clamped-Clamped Rod, Half-Sin Load	48
A-VI. Uniform Clamped-Free Rod, Half-Sin Load	50
A-VII. Uniform Clamped-Clamped Beam, Uniform Load	52
A-VIII. Uniform Clamped-Free Beam, Uniform Load	54
A-IX. Variable Clamped-Clamped Beam, Uniform Load, Taper Ratio $\alpha=0.5$	56
A-X. Variable Clamped-Free Beam, Uniform Load, Taper Ratio $\alpha=0.5$	58
A-XI. Uniform Clamped-Clamped Beam, Half-Sin Load	60
A-XII. Uniform Clamped-Free Beam, Half-Sin Load	62
E-I. Linear and Cubic Shape Functions with Derivatives of Specific Interest	135
E-II. Septic Shape Functions with Derivatives of Specific Interest	137

Abstract

Four numerical methods are used to solve a specific set of problems and then the methods are compared for accuracy and efficiency.

The methods are: standard finite differences, collocation, Galerkin, and least squares. The latter three methods are finite element methods which use either Lagrange linear, Hermite cubic, or Hermite septic piecewise polynomials as interpolation functions.

The problem set consists of second- and fourth-order, linear and nonlinear, differential equations with constant and variable coefficients. The linear equations govern elementary structural members and the nonlinear equation is a one-dimensional analog for transonic flow past an airfoil.

The three major conclusions are: (1) the least squares method with Hermite cubic polynomials was the method of choice for the second-order linear equations, (2) the collocation method was chosen over the Galerkin and the finite difference methods for the fourth-order equations, and (3) Galerkin method was chosen over the collocation method for the nonlinear problem.

A

COMPARISON OF NUMERICAL ANALYSIS METHODS FOR
SOLVING ONE-DIMENSIONAL, ELLIPTIC
DIFFERENTIAL EQUATIONS

I. Introduction

Background

Comparisons of numerical analysis methods for solving differential equations have been of interest for many years. One of the most recent studies was performed by Houstis et al. (Ref 5). In this study four methods were evaluated for solving second-order, linear, elliptic, partial differential equations. The four methods were: standard finite differences; collocation; Galerkin; and least squares using Hermite cubic piecewise polynomials. They concluded that:

1. There is normally a "crossover point" at low accuracy beyond which collocation is more efficient than standard finite differences. Even when finite differences is more efficient, it is by a small amount while collocation is sometimes dramatically more efficient than finite differences. Collocation is much superior for problems whose boundary conditions involved derivatives.
2. There is practically no difference at all between Galerkin and least squares performance. They tend to be slightly more accurate than collocation but are very much less efficient because of the increased work to compute the coefficients in the matrix problem to be solved [Ref 5:324-325].

In view of this work the question arises, will these results hold for higher-order linear and nonlinear differential equations?

The three differential equations selected for comparison analysis in this thesis are equations which govern elementary problems from the field of aeronautical engineering. The first problem, the axial deflection of a rod, is governed by a second-order, linear, ordinary differential equation. The second problem, the bending of a beam, is governed by a fourth-order, linear, ordinary differential equation. In practice these two structural members are used to model more complicated structures. For example, in the computer program "ANALYZE," used by the Air Force Flight Dynamics Laboratory for analysis of aerospace structures, the rod member is used to model spar and rib caps and other line elements (Ref 11:18). The third differential equation is second-order and nonlinear; it represents a one-dimensional, steady, analog to the problem of transonic flow over an airfoil. Fung, et al. (Ref 3), solved this equation with unsteady perturbations using a finite difference method. The finite element methods included in this thesis have not been used previously to solve this nonlinear equation. The purpose of this thesis is to determine if the results of Houstis (Ref 5) apply to these three problems.

The numerical methods evaluated by Houstis and used in this study can be classified into two categories: finite

difference methods, and finite element methods. Three formulation techniques were used to obtain the finite element equations. They are: collocation, Galerkin, and least squares methods. These numerical methods as used in this study transform the original continuous differential equation into a system of algebraic equations. These equations can be solved to yield an approximate solution to the original continuous problem. Although the four methods all yield algebraic equations, the approaches are very different for finite element methods as compared to finite difference methods.

The finite difference method approximates the derivatives appearing in the governing differential equation by difference quotients (Ref 4:222-228). These quotients are formulated at N (a finite number) points in the problem domain. This process generates N equations, nonlinear in general, with N unknowns. After implementing the boundary conditions, the resulting equations can be solved for the remaining unknown values. These values of the function at N points form a discrete approximation to the solution of the problem.

Unlike the finite difference method, the finite element methods yield a piecewise continuous approximation to the solution (Ref 6:3-9). The approximation is achieved by discretizing the domain into E elements, with N nodes and M nodal parameters. The approximate solution in a "global" sense is given by:

$$\tilde{\phi} = \sum_{j=1}^M N_j \phi_j \quad (1)$$

where

$\tilde{\phi}$ = global approximate solution,
 N_j = global shape (interpolation) functions, and
 ϕ_j = nodal parameters (field variables)

When Eq (1) is substituted into the continuous differential equation there will be some error for all cases except where the number of parameters M is infinite, or where the shape functions contain all terms of the exact solution. The error ϵ is given by

$$\tilde{\epsilon} = \mathcal{L}(\tilde{\phi}) - \tilde{f} \quad (2)$$

where

$\tilde{\epsilon}$ = vector of nodal errors,
 \mathcal{L} = differential operator, and
 \tilde{f} = vector of equivalent nodal forces.

The finite element equations are derived in this thesis by the method of weighted residuals (Ref 6). This method requires the residual error ϵ be zero in some average sense. The generalized orthogonality condition is used to achieve this result. In general, the error is forced to satisfy the following equations

$$\int_{\Omega} \epsilon \psi_i d\Omega = 0 \quad i=1,2,\dots,M \quad (3)$$

where

Ω = problem domain,

ψ_i = weighting functions.

The procedure yields M algebraic equations with M unknown nodal parameters. When solved for, the parameters can be substituted in Eq (1) to give the approximate solution to the problem. These equations can be simplified by writing Eq (3) as the sum of integrals over each element. By using an appropriate coordinate transformation each integral can be evaluated on a local basis. Likewise, the approximate global solution $\tilde{\phi}$ is assumed to be the sum of the approximate solutions within each element.

Thus

$$\tilde{\phi} = \sum_{e=1}^{\bar{E}} \tilde{\phi}(e) \quad (4)$$

where $\tilde{\phi}(e)$ is the approximate "local" solution in element e . These local solutions are related to the elemental nodal parameters by the following equation:

$$\tilde{\phi}(e) = \sum_{j=1}^m N_j \phi_j \quad (5)$$

where

m = number of nodal unknowns associated with element e ,

N_j = local shape functions defined for element e ,
and

ϕ_j = nodal parameters associated with element e .

Then if the residual error in each element is forced to satisfy Eq (3) over the element's domain, the result is m equations in m unknowns. These m equations will have the same form for all like elements. Thus, the equations for other like elements are easily generated, and the global equations can be assembled from the \bar{E} sets of local equations. This similarity between like elements greatly reduces the amount of work required to formulate the global equations. More of the details for the finite element techniques are given in Appendices C and D.

Approach

The general approach followed by Houstis (Ref 5) is used in this work. This approach consists of choosing: a problem set from the specified domain, the numerical methods, and the performance criteria for evaluating the methods. The next step is to select and solve specific problems; and, lastly, evaluate each method according to the criteria established.

The problem set has been briefly described in the previous section. It consists of second- and fourth-order, linear differential equations with both constant and variable coefficients. The last problem is a second-order nonlinear differential equation. The two constant coefficient, linear equations are solved for two sets of boundary conditions and two different forcing functions. The two variable coefficient equations are solved for the

same two sets of boundary conditions and for one forcing function. The problem set is described in greater detail in Chapter II.

The standard finite difference method is used only to solve the linear problems whereas the finite element methods are used for all of the problems. The finite difference formulations for each problem are presented in Appendix B. The finite element formulations for each problem are described in Appendices C and D.

The performance criteria chosen are: ease of formulation, accuracy of the solution, computational time required, and "efficiency" of the numerical method. Efficiency was chosen in this study as a function of formation time versus accuracy achieved; where accuracy was defined as the maximum error at any node or grid point. The implementation of the methods and the evaluation of their performance was done with the use of computer programs written by the author in FORTRAN EXTENDED. Several routines were used from the International Mathematical and Statistical Library (Ref 7) for solving the systems of equations and for matrix manipulations. The programs were executed on the Aeronautical Systems Division Computer at Wright-Patterson Air Force Base, Ohio.

II. Problem Set From One-Dimensional Elliptic Differential Equations

Second-Order Linear--Axial Rod

The axial deflection of a rod under the influence of an axially distributed force is illustrated in Fig. 1. This system is governed by the differential equation:

$$\frac{d}{dx} \left\{ A(x) E \frac{du(x)}{dx} \right\} = -F(x) \quad (6)$$

where

E = Young's modulus,

$u(x)$ = axial deflection,

$F(x)$ = axially distributed force, and

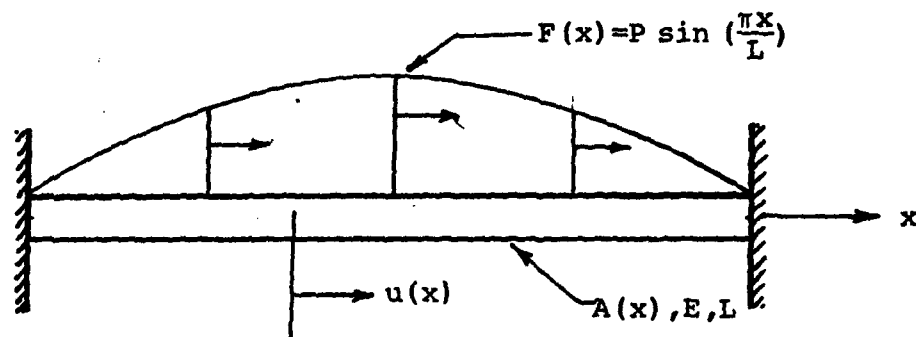
$A(x)$ = cross-sectional area.

For a tapered rod with a taper ratio α , the cross-sectional area is given by

$$A(x) = A \left(1 - \alpha \frac{x}{L} \right), \quad 0 \leq x \leq L \quad (7)$$

where A is the area at the root of the rod. If the taper ratio α is zero, the area is constant and the problem reduces to the uniform rod. Two possible boundary conditions at the ends are:

(a) Clamped-clamped, half-sin load, $\alpha=0$



(b) Clamped-free, uniform load, $\alpha=0.5$

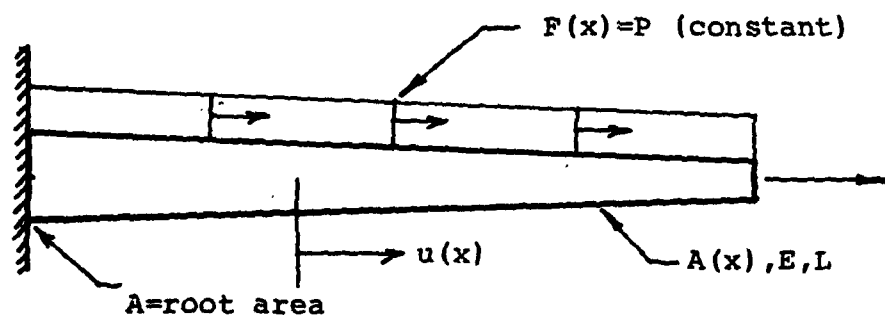


Fig. 1. Uniaxial Deflection of a Rod

$$u(x_k) = 0 \quad - \text{zero displacement} \quad (8)$$

$$A(x)E \left. \frac{du(x)}{dx} \right|_{x=x_k} = 0 \quad - \text{zero axial force} \quad (9)$$

where x_k is the coordinate at the particular end. The six cases of the axial rod studied are detailed in Table I, where the uniform load is $F(x) = P$ (constant); and the "half-sin" load is $F(x) = P \sin(\frac{\pi x}{L})$.

Fourth-Order Linear--Beam in Bending

The governing differential equation for the bending displacement of a beam subjected to a transverse load, as illustrated in Fig. 2 is fourth-order and linear. The equation is

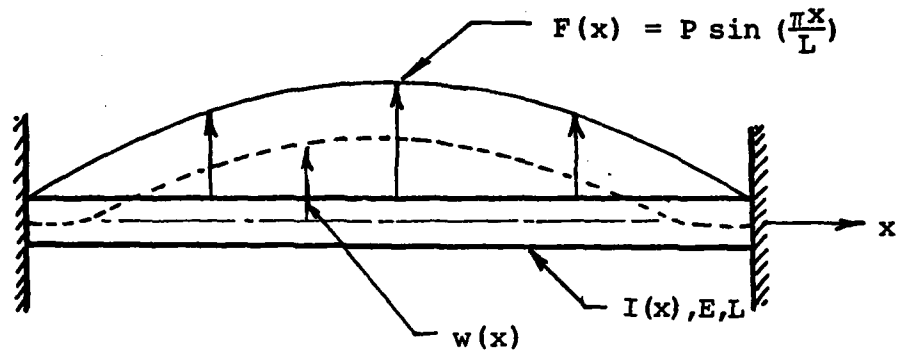
$$\frac{d^2}{dx^2} \left\{ I(x)E \frac{d^2 w(x)}{dx^2} \right\} = F(x) \quad (10)$$

where $w(x)$ is the transverse displacement and $I(x)$ is the cross-sectional moment of inertia. The moment of inertia is given by:

$$I(x) = I(1 - \alpha \frac{x}{L}), \quad 0 \leq x \leq L \quad (11)$$

where I is the moment of inertia at the root of the beam. The boundary conditions studied with Eq (10) represent the same end constraints as studied with the rod. The boundary conditions for a clamped end are:

(a) Clamped-clamped, half-sin load, $\alpha=0$



(b) Clamped-free, uniform load, $\alpha=0.5$

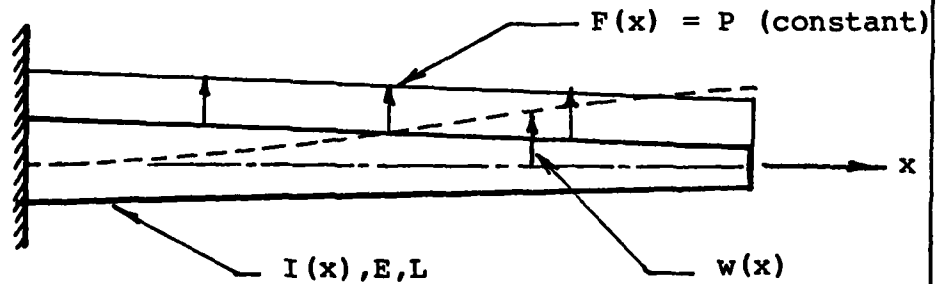


Fig. 2. Transverse Bending Displacement of a Beam

Table I
Axial Rod Problems--Exact Solutions

Description	Taper Ratio	BC Eqn $x=0$ k	BC Eqn $x=L$ k	Exact Solution $u(x)$: $0 \leq x \leq L$
Clamped-Clamped Uniform Rod, Uniform Load	0.0	(8)	(8)	$-\frac{Px}{2AE} (L-x)$
Clamped-Free Uniform Rod, Uniform Load	0.0	(8)	(9)	$-\frac{Px}{2AE} (2L-x)$
Clamped-Clamped Uniform Rod, Half-sin Load	0.0	(8)	(8)	$-\frac{PL^2}{\pi^2 AE} \sin \frac{\pi x}{L}$
Clamped-Free Uniform Rod, Half-sin Load	0.0	(8)	(9)	$-\frac{PL}{\pi AE} \left\{ x + \frac{L}{\pi} \sin \frac{\pi x}{L} \right\}$
Clamped-Clamped Variable Rod, Uniform Load	0.5	(8)	(8)	$-\frac{2PL^2}{AE} \left\{ \frac{x}{L} - \frac{\ln(1-x/2L)}{\ln(1/2)} \right\}$
Clamped-Free Variable Rod, Uniform Load	0.5	(8)	(9)	$-\frac{2PL^2}{AE} \left\{ \frac{x}{L} + \ln(1-x/2L) \right\}$

$$w(x_k) = 0 - \text{zero displacement}$$

(12)

$$\left. \frac{dw}{dx} \right|_{x=x_k} = 0 - \text{zero slope}$$

For a free end the boundary conditions are

$$I(x)E \left. \frac{d^2w}{dx^2} \right|_{x=x_k} = 0 - \text{zero bending moment}$$

(13)

$$I(x)E \left. \frac{d^3w}{dx^3} \right|_{x=x_k} = 0 - \text{zero shear force}$$

As with the axial rod, six cases are studied. In all cases the boundary conditions at the left end are given by Eq (12) with the coordinate $x_k = 0$. The details are given in Table II.

Table II

Beam Problems--Exact Solutions

Description	Taper Ratio	BC Eqn at $x=L_k$	Exact Sol Eqn No
Clamped-Clamped Uniform Beam, Uniform Load	0.0	(12)	(14)
$w(x) = \frac{P}{24EI} \left\{ x^4 - 4Lx^3 + 6L^2x^2 \right\}$			

Table II--Continued

Description	Taper Ratio	BC Eqn at $x=L_k$	Exact Sol Eqn No
Clamped-Free Uniform Beam, Uniform Load	0.0	(13)	
$w(x) = \frac{P}{24EI} \left\{ x^4 - 2Lx^3 + L^2x^2 \right\}$			(15)

Description	Taper Ratio	BC Eqn at $x=L_k$	Exact Sol Eqn No
Clamped-Clamped Uniform Beam, Half-Sin Load	0.0	(12)	
$x(x) = \frac{PL^2}{\pi^3AE} \left\{ \frac{L^2}{\pi} \sin \frac{\pi x}{L} + x^2 - xL \right\}$			(16)

Description	Taper Ratio	BC Eqn at $x=L_k$	Exact Sol Eqn No
Clamped-Free Uniform Beam, Half-Sin Load	0.0	(13)	
$x(x) = \frac{PL}{\pi AE} \left\{ \frac{L^3}{\pi^3} \sin \frac{\pi x}{L} - \frac{x^3}{6} + \frac{Lx^2}{2} - \frac{L^2x}{\pi^2} \right\}$			(17)

Table II--Continued

Description	Taper Ratio	BC Eqn at $x=L$ k	Exact Sol Eqn No
Clamped-Clamped Variable Beam, Uniform Load	0.5	(12)	(18)
$w(x) = \frac{4L^2}{EI} \left\{ -\frac{PLx^3}{24L} + \frac{x^2}{4L} (C1-PL) + [(2L-x) \ln(1-\frac{x}{2L}) + x] (PL-C1+\frac{C2}{2L}) \right\}$ $C1 = PL \left\{ \frac{5}{4} + \frac{11}{6} \ln 0.5 \right\}, C2 = PL^2 \left\{ \frac{\frac{11}{24} + \frac{2}{3} \ln 0.5}{1 + 1.5 \ln 0.5} \right\}$			

Description	Taper Ratio	BC Eqn at $x=L$ k	Exact Sol Eqn No
Clamped-Free Variable Beam, Uniform Load	0.5	(13)	
$w(x) = \frac{PL}{EI} \left\{ L^2 [(2L-x) \ln(1-\frac{x}{2L}) + x] - \frac{x^3}{6} \right\} \quad (19)$			

Second-Order Nonlinear

A one-dimensional, steady, second-order, nonlinear analog of the governing differential equation for transonic flow over an airfoil is given by

$$(1-\phi_{,x})\phi_{,xx} = 0 \quad 0 < x < 1 \quad (20)$$

where

$\phi(x)$ = field variable - potential,

$\phi_{,x}$ = first derivative with respect to x of the field variable ϕ , and

$\phi_{,xx}$ = second derivative with respect to x of the field variable ϕ .

The boundary conditions are

$$\begin{aligned} \phi(0) &= C_1 \\ \phi_{,x}(0) &= C_2 \end{aligned} \quad (21)$$

and either

$$\phi(1) = C_4 \quad (22)$$

or

$$\phi_{,x}(1) = C_3 \quad (23)$$

where C_1 , C_2 , C_3 , and C_4 are constants.

If the differential equation is solved with the two boundary conditions at $x=0$ and with either boundary condition at $x=1$, the exact solution may be discontinuous. This solution is illustrated in Fig. 3 for positive constants C_1 through C_4 .

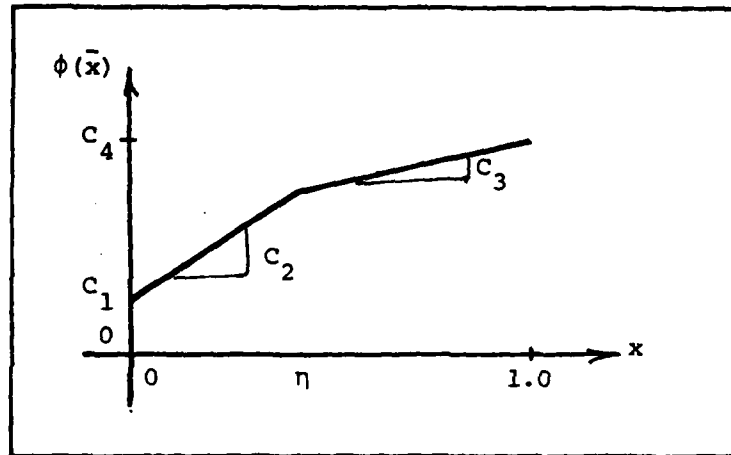


Fig. 3. Exact Solution to the General Nonlinear Problem

The coordinate of the discontinuity η is given by

$$\eta = \frac{C_1 + C_3 - C_4}{C_3 - C_2}, \quad C_2 \neq C_3 \quad (24)$$

The solution to the left of the discontinuity is

$$\phi_L(x) = C_2 x + C_1, \quad 0 \leq x \leq \eta \quad (25)$$

and to the right of the discontinuity the solution is

$$\phi_R(x) = C_4(1 - C_3 x), \quad \eta \leq x \leq 1 \quad (26)$$

The particular problem studied in this work has constants $C_1 = C_4 = 0$ and $C_2 = -C_3 = 1$, thus the break occurs at the coordinate $\eta = 0.5$. This solution is illustrated in Fig. 4.

The equations of the solution are:

$$\phi_L(x) = x, \quad 0 \leq x \leq .5$$

(27)

$$\phi_R(x) = 0.5 - x, \quad .5 \leq x \leq 1$$

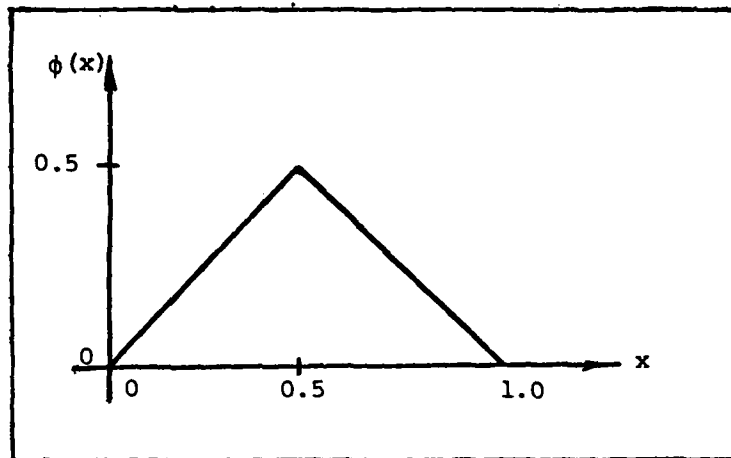


Fig. 4. Exact Solution to
Nonlinear Problem Studied

III. Computer System and Program Information

The use of a high speed digital computer is a must for any study of numerical analysis methods. The numerical calculations for the linear problems studied in this thesis were performed with the aid of the ASD computer system. This system has two Control Data Corporation central processors operating in parallel. The CDC 6613 and CDC CYBER 74 processors both have 131000_{10} 60-bit words of central memory.

The computer programs written by the author for this study perform all but three of the manipulations required to formulate, solve, and analyze the numerical solutions. These three manipulations are performed by subroutines from the IMSL code in operation on the ASD computer. The manipulations and associated subroutines are:

1. matrix multiplication -- VMULBB
2. linear equation solving -- LEQT1B
3. vector maximum value search -- VABMXF

All matrices are stored in band storage mode where only elements on the diagonals are stored. A flow chart of the main program is included as Fig 5.

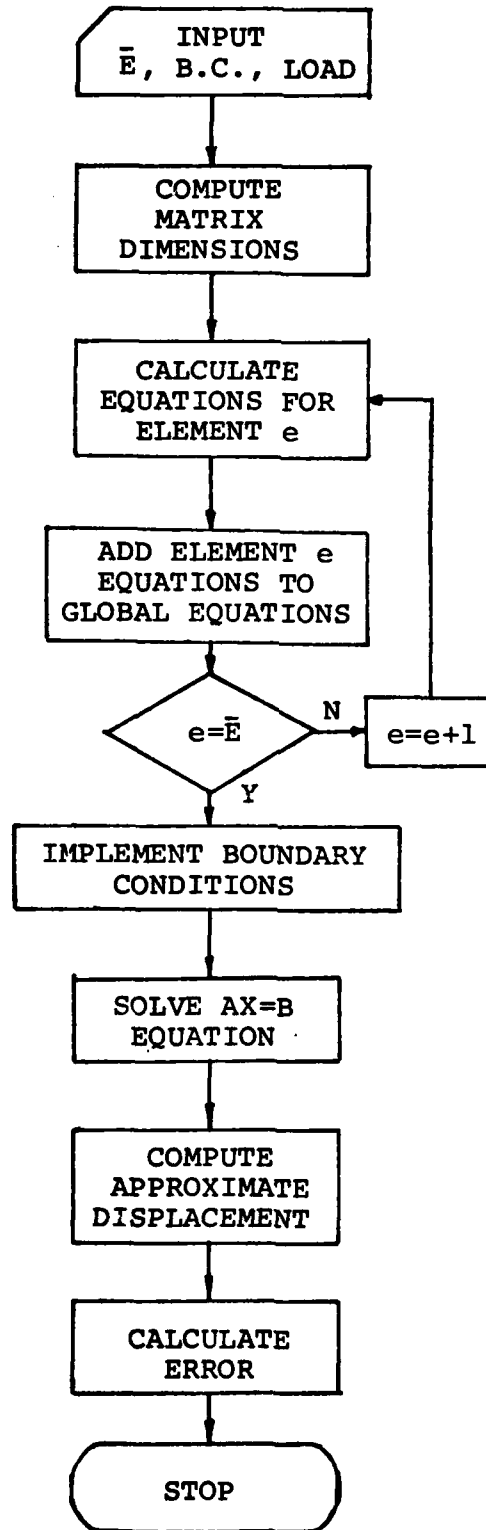


Fig. 5. Main Program Flow Chart

IV. Results and Discussion

The results of this study are analyzed according to the types of differential equations solved. Thus the results show which method performs best for each class of differential equations.

In addition to the performance criteria introduced in Chapter I, several other criteria are also included in the results, for they show a more complete trend than just the criteria stated in Chapter I. The entire list of criteria is given in Table III. When comparing errors the roundoff error must be considered. Because of roundoff error in the solutions, some entries in Tables A-I through A-XII are nonzero, but many orders of magnitude smaller than similar entries. The growth in these nonzero terms is of great importance for they indicate an unstable algorithm when the growth rate is exceptionally large. This phenomenon is discussed later. In all cases, the error compared is a relative error ϵ_R defined at a point as

$$\epsilon_R = \left| \frac{\tilde{\phi} - \phi}{\phi(x_1)} \right|$$

where

$\tilde{\phi}$ = approximate solution at a point in the domain,
 ϕ = exact solution at the same point in the domain,
and

Table III

Performance Criteria Used for Comparing the
Numerical Methods for Linear Problems

Table Entry		Description of Criteria
Max Nodal Error	--	Maximum relative error at any node or grid point
Max Point Error	--	Maximum relative error at any one of 97 equally spaced points in the domain--all nodes are included in this sample
Best Nodal Error	--	Best Maximum Nodal Error for each method and each problem
Best Point Error	--	Best Maximum Point Error for each method and each problem
Execution Time	--	Decimal seconds required to solve the global equations
Formation Time	--	Decimal seconds required to compute and assemble the global equations; and implement the boundary conditions
CF	--	Convergence factor for a particular halving of the stepsize $CF = \frac{\epsilon(h)}{\epsilon(h/2)}$ --the order of convergence is equal to \sqrt{CF} . If $CF < 1.0$ the algorithm diverges
CFN	--	Max Nodal Error convergence factor CF for smallest stepsize studied
CFP	--	Max Point Error Convergence factor CF for smallest stepsize studied
Efficiency Point	--	Maximum efficiency for each method and each problem where efficiency is the $\log \{ [\text{Max Point Error (Formation Time)}^5] - 1 \}$
Number of Elements	--	Number of Elements corresponding to maximum efficiency

$(x)_1$ = exact solution at $X_1=0.5$ for clamped-clamped boundary conditions and $X_1=1.0$ for clamped-free conditions.

These points give an exact solution that is either the maximum or very near the maximum displacement.

Second-Order Linear--Axial Rod

The results presented in Tables IV through IX indicate a general trend. That is, the higher-order finite element methods, collocation and least squares, are more accurate throughout the domain than are finite differences and Galerkin's method. This is evidenced by small pointwise errors for the higher-order methods. Least squares is by far the most accurate and most efficient method studied for this second-order problem.

Finite Differences and Galerkin's. These two methods both use a linear approximation for the field variable. This order of approximation is not as accurate as the cubics even though the solution at the nodes matches the exact solution identically. For Problems 1 and 2, the values recorded in Table IV and V for these two methods correspond to a solution with thirty-nodes. The Best Point Error indicates the maximum error at one of 97 equally spaced points in the domain. This quantity reveals an accuracy of only two digits for these methods. Both methods proved to be accurate to the order h^2 as expected, for all the second-order problems except for Problem 1

Table IV
Results--Problem 1; Uniform Clamped-Clamped Rod, Uniform Load

Method	Max CFN	Best Nodal Error	Max CFP	Best Point Error	Efficiency (Point)	Number of Elements
COLL	.18	0	.28	.278E-13	20.06	1
FD	.118	0	4.51	.868E-3	7.43	32
GAL	.119	0	4.51	.868E-3	5.35	32
LS	.093	0	.094	.278E-13	20.10	1

Table V
Results--Problem 2; Uniform Clamped-Free Rod, Uniform Load

Method	Max CFN	Best Nodal Error	Max CFP	Best Point Error	Efficiency (Point)	Number of Elements
COLL	.16	.711E-14	.17	.142E-13	20.40	1
FD	.449	0	4.50	.217E-3	8.09	32
GAL	.449	.711E-14	4.50	.217E-3	5.96	32
LS	.073	.213E-13	.073	.426E-13	19.79	1

Table VI

Results--Problem 3; Variable Clamped-Clamped Rod, Uniform Load, $\alpha=0.5$

Method	Max CFN	Best Nodal Error	Max CFP	Best Point Error	Efficiency (Point)	Number of Elements
COLL	3.88	0	4.3	.351E-3	5.21	16
FD	3.99	.874E-4	4.37	.180E-2	7.09	32
GAL	3.99	.874E4	4.37	.180E-2	5.09	16
LS	15.4	.336E-6	14.4	.366E-5	7.21	16

Table VII

Results--Problem 4; Variable Clamped-Free Rod, Uniform Load, $\alpha=0.5$

Method	Max CFN	Best Nodal Error	Max CFP	Best Point Error	Efficiency (Point)	Number of Elements
COLL	2.8	.251E-3	2.87	.252E-3	5.39	16
FD	3.99	.651E-3	3.99	.651E-3	7.62	32
GAL	3.99	.994E-4	4.56	.248E-3	5.92	32
LS	16.0	.619E-6	16.0	.619E-6	8.03	16

Table VIII

Results--Problem 5; Uniform Clamped-Clamped Rod, Half-Sin Load

Method	Max CFN	Best Nodal Error	Max CFP	Best Point Error	Efficiency (Point)	Number of Elements
COLL	4.16	.343E-14	4.17	.109E-2	4.74	16
FD	4.01	.804E-3	4.01	.804E-3	7.41	32
GAL	.123	.438E-14	4.48	.107E-2	5.23	32
LS	.100	.343E-14	15.7	.385E-5	7.18	16

Table IX

Results--Problem 6; Uniform Clamped-Free Rod, Half-Sin Load

Method	Max CFN	Best Nodal Error	Max CFP	Best Point Error	Efficiency (Point)	Number of Elements
COLL	3.99	.107E-2	4.01	.107E-2	4.76	16
FD	4.00	.803E-3	4.00	.803E-3	7.44	32
GAL	.411	.112E-13	4.50	.340E-3	5.77	32
LS	.074	.223E-13	15.8	.122E-5	7.69	16

where the nodal error increased at a rate proportional to $h^{-\sqrt{5.6}} = h^{-2.4}$. According to Fix (Ref 2:205-215), the round-off error is bound by the condition number of the Toeplitz matrix. This upper bound is h^{-2m} where m is the order of the differential equation. In this case, the round-off error should be less than Ch^{-4} ; C =constant. Therefore, the errors present in these problems are acceptable considering that the error present is in the thirteenth digit on a machine with fourteen significant digits.

Collocation and Least Squares. These two methods give excellent accuracy for Problems 1 and 2 but are definitely unstable. This is due to the fact that the cubic approximation with two boundary conditions will solve the governing differential equation for Problems 1 and 2 exactly with only one element. By increasing the number of elements one simply increases the probability that the discretization error and/or the roundoff error will be increased. On the other hand, for the four remaining rod problems the exact solutions are either functions of natural logarithms or trigonometric functions. These solutions can not be modeled exactly with a third-order polynomial. For these four problems the collocation method is only of order h^2 where as the least squares method approaches an order of accuracy h^4 . It is also interesting to note that the order of the approximation polynomial does not noticeably

affect the round-off error. This can be seen from the results of Problems 1 and 2, where for the collocation method the error grows at approximately the same rate as for the finite difference and Galerkin methods. This observation is also made by Fix (Ref 2:215).

Fourth-Order Linear--Beam in Bending

The results for this system are given in Tables X through XV. The tables show that for the simple cases of Problems 7 and 8 the methods using a septic approximation are exceptionally accurate and very efficient. But as the problem becomes more complex the septic shape functions do not guarantee a more accurate solution than is obtained by the Galerkin's method with cubic shape functions. It is also apparent that the order of convergence is very strongly dependent on the particular problem being solved. This fact is substantiated by examining the convergence factors CF for the Galerkin method in Tables X through XV. For the tapered beam the algorithm is only of order h^2 whereas for the uniform beam with a half-sin load the method is of order h^4 . In Problems 7 and 8 the change from $O(h^4)$ to $O(h^2)$ is brought about by simply freeing the right end of the beam. As with the Axial Rod, the higher-order methods are unstable for the cases where the exact solution is of less order than the approximation function. The explanation of this is the same as for the axial rod. For the simple cases the collocation or least squares methods

Table X

Results--Problem 7; Uniform Clamped-Clamped Beam, Uniform Load

Method	Max CFN	Best Nodal Error	Max CFP	Best Point Error	Efficiency (Point)	Number of Elements
COLL	.458	0	.506	.201E-11	15.85	1
FD	4.01	.781E-2	4.01	.781E-2	5.82	32
GAL	.033	0	15.9	.153E-4	6.70	16
LS	5E-4	0	5E-4	.373E-12	15.40	1

Table XI

Results--Problem 8; Uniform Clamped-Free Beam, Uniform Load

Method	Max CFN	Best Nodal Error	Max CFP	Best Point Error	Efficiency (Point)	Number of Elements
COLL	2.68	.168E-10	2.64	.168E-10	15.03	1
FD	4.00	.977E-3	4.00	.977E-3	6.70	32
GAL	4.01	.130E-2	4.01	.130E-2	4.76	16
LS	.001	.906E-11	.001	.906E-11	15.08	1

Table XII

Results--Problem 9; Variable Clamped-Clamped Beam, Uniform Load, $\alpha=0.5$

Method	Max CFN	Best Nodal Error	Max CFP	Best Point Error	Efficiency (Point)	Number of Elements
COLL	1.55	.875E-11	1.54	.232E-1	5.94	1
FD	3.98	.849E-2	3.98	.849E-2	5.82	32
GAL	3.88	.800E-11	3.95	.128E-2	4.75	16

Table XIII

Results--Problem 10; Variable Clamped-Free Beam, Uniform Load, $\alpha=0.5$

Method	Max CFN	Best Nodal Error	Max CFP	Best Point Error	Efficiency (Point)	Number of Elements
COLL	1.65	.149E-1	1.65	.149E-1	6.04	1
FD	4.01	.207E-2	4.01	.207E-2	6.38	32
GAL	4.01	.739E-3	4.01	.739E-3	4.98	16

Table XIV
Results--Problem 11; Uniform Clamped-Clamped Beam, Half-Sin Load

Method	Max CFN	Best Nodal Error	Max CFP	Best Point Error	Efficiency (Point)	Number of Elements
COLL	46.0	.337E-12	47.3	.755E-5	5.74	8
FD	4.02	.749E-2	4.02	.749E-2	5.86	32
GAL	.057	.104E-12	15.8	.179E-4	6.60	16

Table XV
Results--Problem 12; Uniform Clamped-Free Beam, Half-Sin Load

Method	Max CFN	Best Nodal Error	Max CFP	Best Point Error	Efficiency (Point)	Number of Elements
COLL	9.80	.344E-5	9.80	.344E-5	6.09	8
FD	4.32	.502E-3	4.32	.502E-3	6.96	32
GAL	.048	.601E-14	15.7	.535E-6	8.07	16

give good results with only one element. The collocation method is the most accurate and efficient method for all of the problems except the half-sin loaded beams. For these last two problems the Galerkin method was more efficient due to the more simple calculations required to form the global equations. The collocation method exhibited very poor convergence for the variable beams.

Nonlinear Problem

The nonlinear problem was solved without the aid of the digital computer due to a lack of time. The two approximate methods used were the Galerkin method and the collocation method. Two iterative formulations of the original differential equation were used as detailed in Appendix F; each proved to behave quite differently. It was expected that formulation A, which does not have an iterative forcing term, would give the fastest convergence. This was, in fact, the case; formulation A gave the exact solution after one iteration. Formulation B converged to the correct solution but took several iterations. The numerical results for this problem by the Galerkin method are given in Table XVI, and for the collocation method in Table XVII. The process of solving the equations using a hand calculator forces one to place more emphasis on the "efficiency" of the method. Efficiency in this context could be defined as the number of keystrokes required to obtain the solution for each iteration. By this measure the Galerkin technique is definitely easier to work with.

Table XVI
Nodal Displacements for Nonlinear Problem by Galerkin's Method

	ϕ_1	ϕ_2	ϕ_3	ϕ_4	ϕ_5	ϕ_6	ϕ_7	ϕ_8
exact	0	1	.500	1	.500	-1	0	-1
initial guess	0	1	1	1	1	-1	0	-1
A-1*	0	1	.500	1	.500	-1	0	-1
A-2	0	1	.500	1	.500	-1	0	-1
B-1	0	1	.662	1.22	.662	-1.22	0	-1
B-2	0	1	.5006	1.0015	.5006	-1.0015	0	-1

*A-1 indicates the solution by formulation A with one iteration, etc.

Table XVII
Nodal Displacements for Nonlinear Problem by Collocation Method

	ϕ_1	ϕ_2	ϕ_3	ϕ_4	ϕ_5	ϕ_6	ϕ_7	ϕ_8
exact	0	1	.500	1	.500	-1	0	-1
initial guess	0	1	1	1	1	-1	0	-1
A-1*	0	1	.500	1	.500	-1	0	-1
A-2	0	1	.500	1	.500	-1	0	-1
B-1								
B-2								

*A-1 indicates the solution by formulation A with on iteration, etc.

The nonlinear problem studied required some knowledge of the physical process that Eq (F-1) is used as an analog for. The boundary conditions chosen are mathematically convenient but not physically desirable. The condition $\phi(1)=0$ implies that the function itself goes to zero at $x=1$. A better choice for the boundary condition at $x=1$ would have been $\phi_x(1)=C_4$. This implies that the function is nonzero at the boundary. Another aspect of the problem which must be understood is the condition that a jump in the first derivative of ϕ must occur in the flow field. The function is continuous but the derivative changes discontinuously, which models the idealized behavior caused by a shock in the flow field. This behavior requires an approximation to the field variable which has first derivatives as nodal parameters. Such an approximation disqualifies linear shape functions even though the exact solution can be represented by two straight lines.

V. Conclusions

One of the objectives of the study was to determine if comparisons made by Houstis (Ref 5) based on a second-order, two dimensional, constant coefficient problem set would hold for a set of higher-order variable coefficient problems or nonlinear problems. In searching for an answer to this question several other conclusions were also obtained. The conclusions of this study are:

1. For the second-order linear problem studied, the least squares method, with Hermite cubic polynomials, is more accurate and also more efficient than the collocation, Galerkin, or finite difference methods studied. The least squares method outperformed the other four methods for all six cases of the axial rod studied. The most heavily weighted performance criteria were efficiency and accuracy, in that order.

2. For the fourth-order linear problem studied, the least squares method with Hermite septic polynomials was only used for the constant coefficient case with a constant forcing term. In this case least squares performed equally as well as collocation, with the same interpolation functions; and significantly better than finite differences and Galerkin with lower-order interpolation functions. For the variable coefficient case collocation was slightly

less efficient than the other two methods. In general, collocation was the method of choice.

3. For the nonlinear problem the Galerkin and collocation methods both perform similarly. The number of calculations required for each iteration was much greater for the collocation method than for the Galerkin method.

The second conclusion obtained by Houstis varies significantly from those of this study. This difference can possibly be accounted for by the fact that Houstis used a numerical integration scheme for the Galerkin and least squares methods. Since the methods were formulated with polynomials, the integration is trivial and numerical integration is not called for.

Bibliography

1. Collatz, Lothar. The Numerical Treatment of Differential Equations (third edition). New York: Springer-Verlag New York, Inc., 1966.
2. Fix, George J. and Gilbert Strang. An Analysis of the Finite Element Method. Englewood Cliffs, N.J.: Prentice-Hall, Inc., 1968.
3. Fung, K-Y, et al. "Small Unsteady Perturbations in Transonic Flows," AIAA Journal, 16:815-822 (August 1978).
4. Hornbeck, Robert W. Numerical Methods. New York: Quantum Publishers, Inc., 1975.
5. Houstis, E. N., et al. "Evaluation of Numerical Methods for Elliptic Partial Differential Equations," Journal of Computational Physics, 27:323-350 (December 1978).
6. Huebner, Kenneth H. The Finite Element Method for Engineers. New York: John Wiley and Sons, 1975.
7. International Mathematical and Statistical Library. Houston, Tx: IMSL, Inc., 1979
8. Ketter, Robert L., and Sherwood P. Prawel, Jr. Modern Methods of Engineering Computation. New York: McGraw-Hill Book Co., 1969.
9. Popov, Egor P. Introduction to Mechanics of Solids. Englewood Cliffs, N.J.: Prentice-Hall, Inc., 1968.
10. Prenter, P. M. Splines and Variational Methods. New York: John Wiley and Sons, 1975.
11. Venkayya, Vipperla B., et al. "ANALYZE"--Analysis of Aerospace Structures with Membrane Elements. Technical Report. Wright-Patterson AFB, Ohio: Air Force Flight Dynamics Laboratory, December 1978. (AFFDL-TR-78-170).
12. Zienkiewicz, O. C. The Finite Element Method. New York: McGraw-Hill Book Co. (U.K.) Limited, 1977.

Appendix A
Numerical and Graphical Data

This appendix contains all of the numerical results for the linear problems. These results are given in Tables A-I through A-XII for which the headings are defined in Chapter IV. Each table presents data for one specific problem as solved using the various numerical methods.

The graphical data shows two aspects of the study. The first six graphs are representative of the way in which the methods approximate the solutions to the various problems. The next twenty-four graphs are plots of the relative error at 97 points in the domain. This number of points was chosen because it insures that the plotted solution will not "skip over" any nodes for the values of \bar{E} studied.

Table A-I
Uniform Clamped-Clamped Rod, Uniform Load

Method	$\frac{l}{h}$	Max Nodal Error	CF	Max Point Error	CF	Seconds Formation	Seconds Execution
COLL	1	0	-	.278E-13	-	.050	.004
	2	0	0	.391E-13	0.71	.075	.003
	4	.142E-13	0	.320E-13	1.22	.124	.004
	8	.213E-13	.67	.391E-13	0.82	.231	.006
	16	.121E-12	.18	.142E-12	0.28	.429	.011
FD	2	0	-	.25	-	.023	.001
	4	0	0	.625E-1	4	.031	.001
	8	.213E-13	0	.156E-1	4.01	.045	.002
	16	.426E-13	.50	.391E-2	3.99	.076	.003
	32	.359E-12	.119	.868E-3	4.51	.134	.001

Table A-I--Continued

Method	$\frac{1}{h}$	Max Nodal Error	CF	Max Point Error	CF	Seconds Formation	Seconds Execution
GAL	4	0	-	.625E-1	-	.053	.003
	8	.213E-13	0	.156E-1	4.01	.101	.003
	16	.426E-13	.50	.391E-2	3.99	.182	.004
	32	.359E-12	.119	.868E-3	4.51	.349	.100
LS	1	0	-	.278E-13	-	.049	.003
	2	0	-	.391E-13	.711	.077	.003
	4	.107E-13	0	.320E-13	1.22	.124	.005
	8	.522E-11	.002	.525E-11	.006	.232	.008
	16	.560E-10	.093	.561E-10	.094	.433	.010

Table A-II
Uniform Clamped-Free Rod, Uniform Load

Method	$\frac{1}{h}$	Max Nodal Error	CF	Max Point Error	CF	Seconds Formation	Seconds Execution
COLL	1	.142E-13	-	.142E-13	-	.049	.002
	2	.711E-14	2.00	.178E-13	0.80	.076	.004
	4	.142E-13	0.50	.391E-13	0.46	.124	.004
	8	.675E-13	0.21	.146E-12	0.27	.233	.004
	16	.419E-12	0.16	.838E-12	0.17	.435	.013
FD	2	0	-	.625E-1	-	.024	.001
	4	.711E-14	0	.156E-1	4.01	.033	.001
	8	.142E-13	.501	.391E-2	3.99	.046	.001
	16	.512E-12	.028	.977E-3	4.00	.078	.002
	32	.114E-11	.449	.217E-3	4.50	.130	.006

Table A-II--Continued

Method	$\frac{l}{h}$	Max Nodal Error	CF	Max Point Error	CF	Seconds Formation	Seconds Execution
GAL	4	.711E-14	-	.156E-1	-	.058	.003
	8	.142E-13	.501	.391E-2	3.99	.100	.003
	16	.512E-12	.028	.977E-3	4.002	.170	.005
	32	.114E-11	.449	.217E-3	4.50	.348	.006
LS	1	.213E-13	-	.426E-13	-	.052	.003
	2	.355E-13	.60	.391E-13	1.09	.078	.004
	4	.438E-11	.008	.438E-11	.009	.123	.005
	8	.524E-10	.084	.524E-10	.084	.222	.008
	16	.717E-9	.073	.717E-9	.073	.442	.011

Table A-III
Variable Clamped-Clamped Rod, Uniform Load, Taper Ratio $\alpha=0.5$

Method	$\frac{1}{h}$	Max Nodal Error	CF	Max Point Error	CF	Seconds Formation	Seconds Execution
COLL	1	0	-	.1282	-	.051	.003
	2	.394E-1	0	.723E-1	1.77	.077	.003
	4	.493E-2	7.99	.751E-2	9.63	.128	.004
	8	.134E-2	3.68	.151E-2	4.97	.230	.008
	16	.345E-3	3.88	.351E-3	4.30	.445	.012
FD	2	.192E-1	-	.357	-	.026	.001
	4	.512E-2	3.75	.108	3.31	.033	.001
	8	.139E-2	3.68	.299E-1	3.61	.045	.002
	16	.349E-3	3.98	.787E-2	3.80	.079	.004
	32	.874E-4	3.99	.180E-2	4.37	.135	.006

Table A-III--Continued

Method	$\frac{1}{h}$	Max Nodal Error	CF	Max Point Error	CF	Seconds Formation	Seconds Execution
GAL	2	.512E-3	-	.108	-	.055	.003
	4	.139E-2	.368	.299E-1	3.61	.092	.004
	8	.349E-3	3.98	.787E-2	3.80	.171	.004
	16	.874E-4	3.99	.180E-2	4.37	.339	.008
LS	1	0	-	.427E-1	-	.052	.003
	2	.784E-3	0	.681E-2	6.27	.076	.003
	4	.761E-4	10.3	.675E-3	10.1	.128	.006
	8	.519E-5	14.7	.526E-4	12.8	.228	.008
	16	.336E-6	15.4	.366E-5	14.4	.441	.011

Table A-IV

Variable Clamped-Free Rod, Uniform Load, Taper Ratio $\alpha=0.5$

Method	$\frac{l}{h}$	Max Nodal Error	CF	Max Point Error	CF	Seconds Formation	Seconds Execution
COLL	1	.566E-1	-	.566E-1	-	.051	.002
	2	.852E-2	6.64	.852E-2	6.64	.075	.004
	4	.102E-2	8.35	.118E-2	7.22	.127	.003
	8	.704E-3	1.45	.722E-3	1.63	.230	.007
	16	.251E-3	2.80	.252E-3	2.87	.439	.012
FD	2	.164	-	.164	-	.023	.001
	4	.415E-1	3.95	.415E-1	3.95	.031	.001
	8	.104E-1	3.99	.104E-1	3.99	.049	.002
	16	.260E-2	4.00	.260E-2	4.00	.074	.002
	32	.651E-3	3.99	.651E-3	3.99	.130	.004

Table A-IV--Continued

Method	$\frac{1}{h}$	Max Nodal Error	CF	Max Point Error	CF	Seconds Formation	Seconds Execution
GAL	4	.628E-2	-	.155E-1	-	.053	.003
	8	.158E-2	3.98	.428E-2	3.62	.098	.004
	16	.397E-3	3.98	.113E-2	3.79	.178	.004
	32	.994E-4	3.99	.248E-3	4.56	.345	.007
LS	1	.206E-1	-	.206E-1	-	.050	.002
	2	.202E-2	10.2	.202E-2	10.2	.074	.002
	4	.149E-3	13.6	.149E-3	13.6	.123	.004
	8	.977E-5	15.3	.977E-5	15.3	.227	.007
	16	.619E-6	16.0	.619E-6	16.0	.932	.011

Table A-V
Uniform Clamped-Clamped Rod, Half-Sin Load

Method	$\frac{l}{h}$	Max Nodal Error	CF	Max Point Error	CF	Seconds Formation	Seconds Execution
COLL	1	.343E-14	-	.2354	-	.048	.003
	2	.596E-1	0	.833E-1	2.83	.073	.003
	4	.214E-1	2.79	.218E-1	3.82	.124	.005
	8	.453E-2	4.72	.455E-2	4.79	.228	.008
	16	.109E-2	4.16	.109E-2	4.17	.441	.011
FD	2	.234	-	.234	-	.020	.002
	4	.530E-1	4.42	.530E-1	4.42	.031	.001
	8	.130E-1	4.08	.130E-1	4.08	.047	.001
	16	.322E-2	4.04	.322E-2	4.04	.076	.003
	32	.809E-3	4.01	.804E-3	4.01	.137	.005

Table A-V--Continued

Method	$\frac{1}{h}$	Max Nodal Error	CF	Max Point Error	CF	Seconds Formation	Seconds Execution
GAL	4	.438E-14	-	.703E-1	-	.058	.002
	8	.131E-13	.334	.188E-1	3.74	.096	.003
	16	.438E-13	.299	.479E-2	3.93	.182	.004
	32	.355E-12	.123	.107E-2	4.48	.353	.006
LS	1	.343E-14	-	.215	-	.053	.003
	2	.343E-14	1.0	.108E-1	19.9	.077	.004
	4	.394E-13	.087	.906E-3	11.9	.130	.004
	8	.539E-11	.007	.606E-4	15.0	.231	.007
	16	.541E-10	.100	.385E-5	15.7	.444	.010

Table A-VI
Uniform Clamped-Free Rod, Half-Sin Load

Method	$\frac{l}{h}$	Max Nodal Error	CF	Max Point Error	CF	Seconds Formation	Seconds Execution
COLL	1	.360	-	.360	-	.047	.003
	2	.121E-1	29.8	.121E-1	29.8	.073	.005
	4	.163E-1	.74	.168E-1	.72	.125	.005
	8	.427E-2	3.82	.429E-2	3.92	.229	.008
	16	.107E-2	3.99	.107E-2	4.01	.438	.012
FD	2	.215	-	.215	-	.026	.001
	4	.519E-1	4.14	.519E-1	4.14	.033	.002
	8	.129E-1	4.02	.129E-1	4.02	.047	.002
	16	.321E-2	4.02	.321E-2	4.02	.077	.003
	32	.803E-3	4.00	.803E-3	4.00	.135	.005

Table A-VI--Continued

Method	$\frac{1}{h}$	Max Nodal Error	CF	Max Point Error	CF	Seconds Formation	Seconds Execution
GAL	4	.112E-13	-	.224E-1	-	.057	.003
	8	.167E-13	.671	.600E-2	3.73	.095	.003
	16	.525E-12	.032	.153E-2	3.92	.182	.003
	32	.119E-11	.441	.340E-3	4.50	.346	.006
LS	1	.223E-13	-	.683E-1	-	.052	.002
	2	.335E-13	.666	.343E-2	19.9	.078	.002
	4	.454E-11	.007	.288E-3	15.4	.127	.003
	8	.564E-10	.080	.193E-4	11.6	.234	.008
	16	.758E-9	.074	.22E-5	15.8	.442	.012

Table A-VII
Uniform Clamped-Clamped Beam, Uniform Load

Method	$\frac{l}{h}$	Max Nodal Error	CF	Max Point Error	CF	Seconds Formation	Seconds Execution
COLL	1	0	-	.201E-11	-	.148	.006
	2	.634E-12	0	.201E-11	1.00	.228	.008
	4	.696E-10	.009	.921E-10	.002	.408	.016
	8	.152E-9	.458	.182E-9	.506	.751	.028
FD	4	.5	-	.5	-	.039	.002
	8	.125	4.00	.125	4.00	.058	.002
	16	.313E-1	3.99	.313E-1	3.99	.100	.005
	32	.781E-2	4.01	.781E-2	4.01	.181	.008

Table A-VII--Continued

Method	$\frac{1}{h}$	Max Nodal Error	CF	Max Point Error	CF	Seconds Formation	Seconds Execution
GAL	2	0	-	.625E-1	-	.072	.004
	4	.266E-14	0	.391E-2	8.3	.118	.006
	8	.346E-12	.008	.244E-3	16.0	.216	.008
	16	.104E-10	.033	.153E-4	15.9	.420	.010
LS	1	0	-	.199E-11	-	.155	.006
	2	.139E-12	0	.373E-12	5.34	.254	.009
	4	.225E-10	.01	.225E-10	.02	.442	.016
	8	.414E-7	5E-4	.414E-7	5E-4	.847	.028

Table A-VIII
Uniform Clamped-Free Beam, Uniform Load

Method	$\frac{l}{h}$	Max Nodal Error	CF	Max Point Error	CF	Seconds Formation	Seconds Execution
COLL	1	.168E-10	-	.168E-10	-	.141	.007
	2	.493E-10	.341	.423E-10	.326	.232	.007
	4	.330E-9	.149	.330E-9	.128	.397	.018
	8	.123E-9	2.68	.125E-9	2.64	.756	.024
FD	4	.625E-1	-	.625E-1	-	.038	.001
	8	.156E-1	4.01	.156E-1	4.01	.062	.003
	16	.391E-2	3.99	.391E-2	3.99	.098	.004
	32	.977E-3	4.00	.977E-3	4.00	.183	.007

Table A-VIII--Continued

Method	$\frac{1}{h}$	Max Nodal Error	CF	Max Point Error	CF	Seconds Formation	Seconds Execution
GAL	1	.333	-	.333	-	.051	.003
	2	.833E-1	3.96	.833E-1	3.96	.077	.004
	4	.208E-1	4.01	.208E-1	4.01	.123	.006
	8	.521E-2	3.99	.521E-2	3.99	.224	.006
	16	.130E-2	4.01	.130E-2	4.01	.421	.011
LS	1	.906E-11	-	.906E-11	-	.156	.005
	2	.112E-8	.008	.112E-8	.008	.249	.010
	4	.202E-7	.055	.202E-7	.055	.449	.015
	8	.572E-4	.001	.572E-4	.001	.855	.026

Table A-IX
Variable Clamped-Clamped Beam, Uniform Load, Taper Ratio $\alpha=0.5$

Method	$\frac{l}{h}$	Max Nodal Error	CF	Max Point Error	CF	Seconds Formation	Seconds Execution
COLL	1	.875E-11	-	.232E-1	-	.138	.006
	2	.119	0	.121	.192	.225	.010
	4	.104	1.14	.105	1.15	.408	.017
	8	.671E-1	1.55	.684E-1	1.54	.763	.027
FD	4	.509	-	.509	-	.039	.002
	8	.134	3.80	.134	3.80	.056	.002
	16	.338E-1	3.96	.338E-1	3.96	.100	.005
	32	.849E-2	3.98	.849E-2	3.98	.178	.008

Table A-IX--Continued

Method	$\frac{1}{h}$	Max Nodal Error	CF	Max Point Error	CF	Seconds Formation	Seconds Execution
GAL	2	.215E-2	-	.973E-1	-	.071	.002
	4	.173E-1	.124	.194E-1	5.02	.124	.005
	8	.493E-2	3.51	.505E-2	3.84	.222	.007
	16	.127E-2	3.88	.128E-2	3.95	.426	.011

Table A-X

Variable Clamped-Free Beam, Uniform Load, Taper Ratio $\alpha=0.5$

Method	$\frac{l}{h}$	Max Nodal Error	CF	Max Point Error	CF	Seconds Formation	Seconds Execution
COLL	1	.149E-1	-	.149E-1	-	.144	.006
	2	.124	.120	.124	.120	.226	.009
	4	.986E-1	1.26	.986E-1	1.26	.394	.015
	8	.596E-1	1.65	.596E-1	1.65	.742	.028
FD	4	.134	-	.134	-	.038	.002
	8	.333E-1	4.02	.333E-1	4.02	.059	.003
	16	.829E-2	4.02	.829E-2	4.02	.098	.006
	32	.207E-2	4.01	.207E-2	4.01	.182	.008

Table A-X--Continued

Method	$\frac{1}{h}$	Max Nodal Error	CF	Max Point Error	CF	Seconds Formation	Seconds Execution
GAL	1	.207	-	.207	-	.051	.003
	2	.489E-1	4.23	.489E-1	4.23	.076	.003
	4	.119E-1	4.11	.119E-1	4.11	.114	.005
	8	.296E-2	4.02	.296E-2	4.02	.213	.008
	16	.739E-3	4.01	.739E-3	4.01	.426	.012

Table A-XI
Uniform Clamped-Clamped Beam, Half-Sin Load

Method	$\frac{l}{h}$	Max Nodal Error	CF	Max Point Error	CF	Seconds Formation	Seconds Execution
COLL	1	.377E-12	-	.156E-1	-	.140	.005
	2	.720E-3	0	.137E-2	11.4	.228	.009
	4	.347E-3	2.08	.357E-3	3.84	.396	.015
	8	.754E-5	46.0	.755E-5	47.3	.751	.028
FD	4	.513	-	.513	-	.038	.002
	8	.122	4.21	.122	4.21	.060	.002
	16	.301E-1	4.05	.301E-1	4.05	.101	.006
	32	.749E-2	4.02	.749E-2	4.02	.179	.008

Table A-XI--Continued

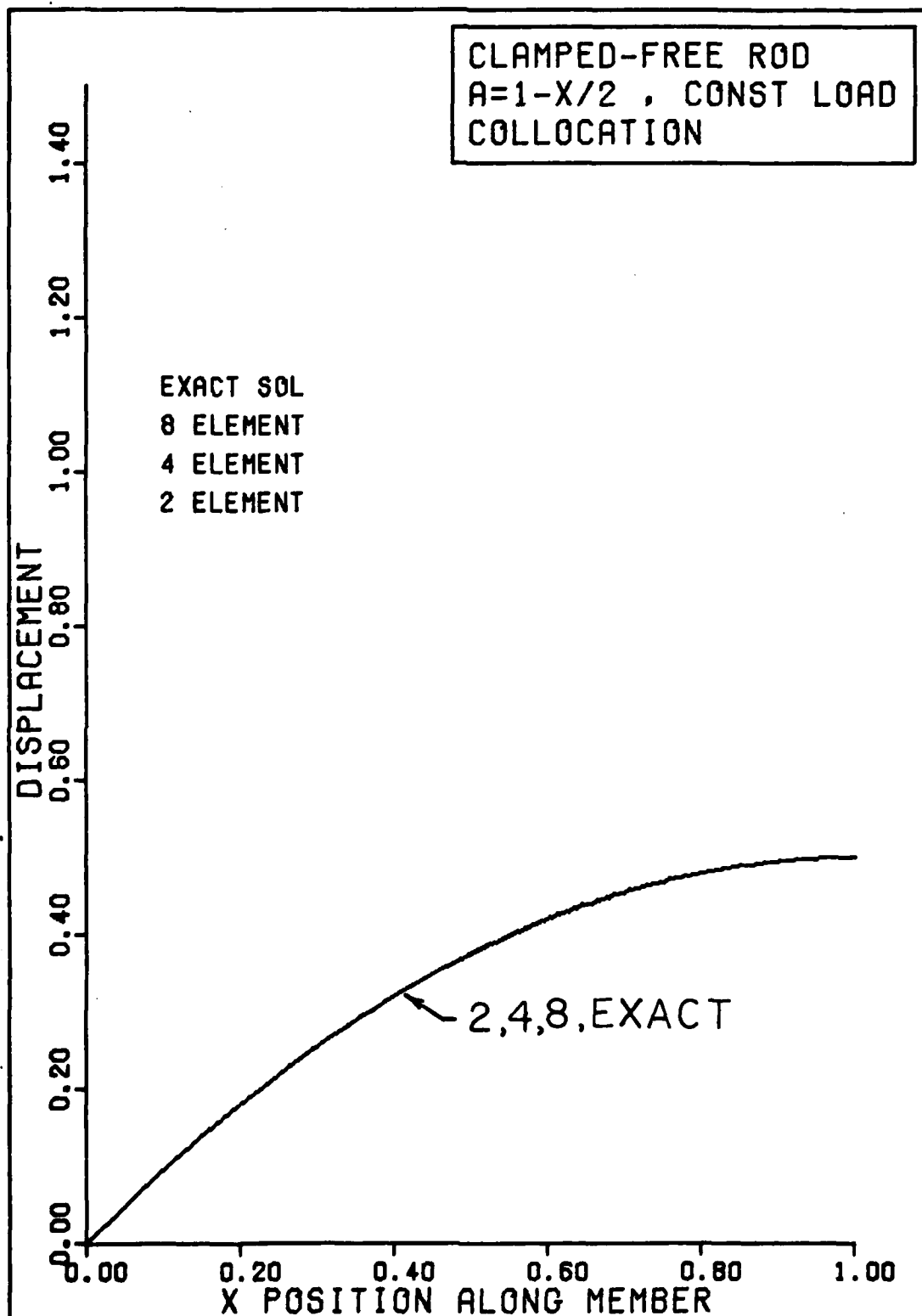
Method	$\frac{1}{h}$	Max Nodal Error	CF	Max Point Error	CF	Seconds Formation	Seconds Execution
GAL	2	.104E-12	-	.503E-1	-	.078	.004
	4	.104E-12	1.0	.422E-2	11.9	.122	.006
	8	.312E-12	.333	.282E-3	15.0	.225	.003
	16	.543E-11	.057	.179E-4	15.8	.427	.013

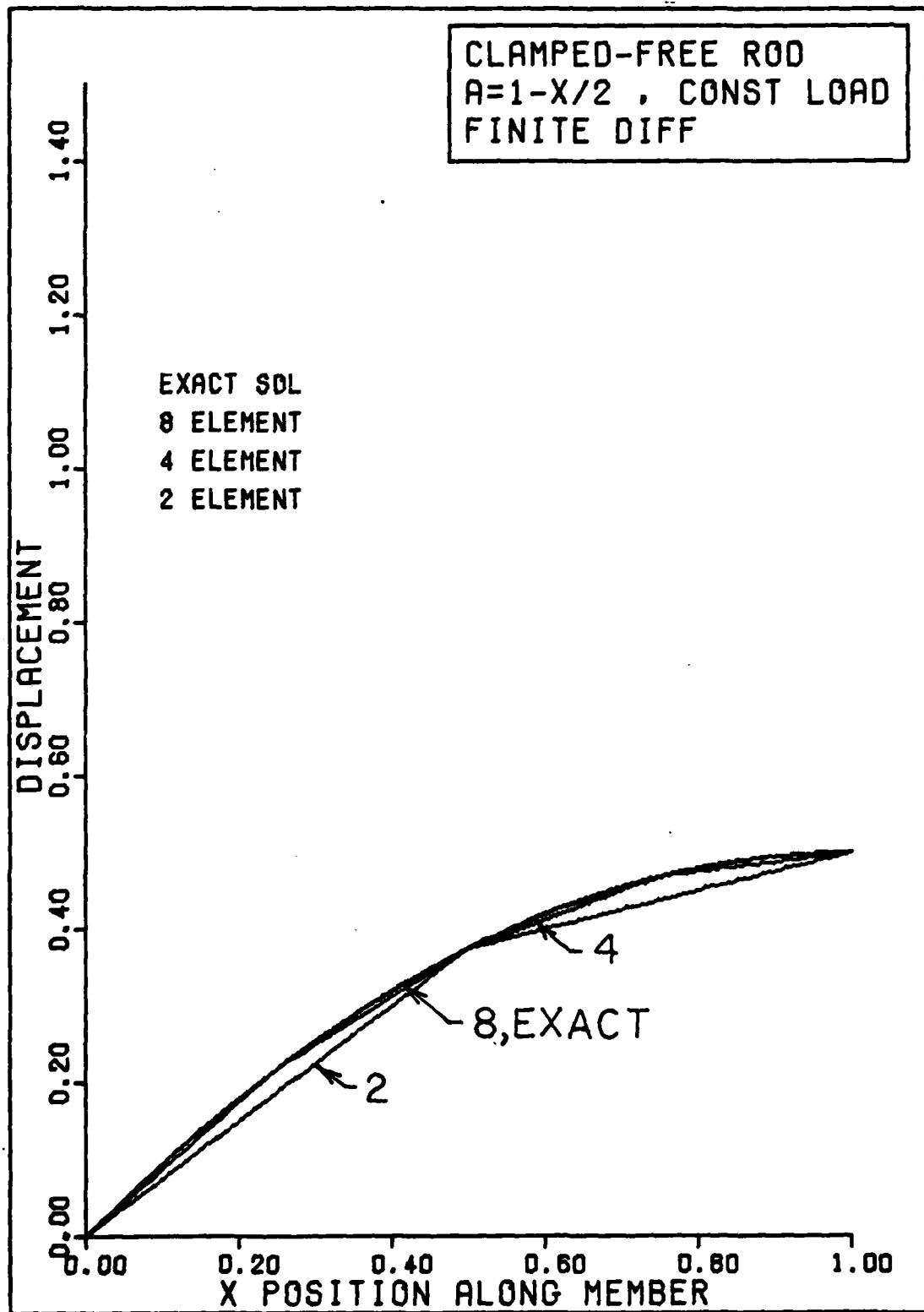
Table A-XII
Uniform Clamped-Free Beam, Half-Sin Load

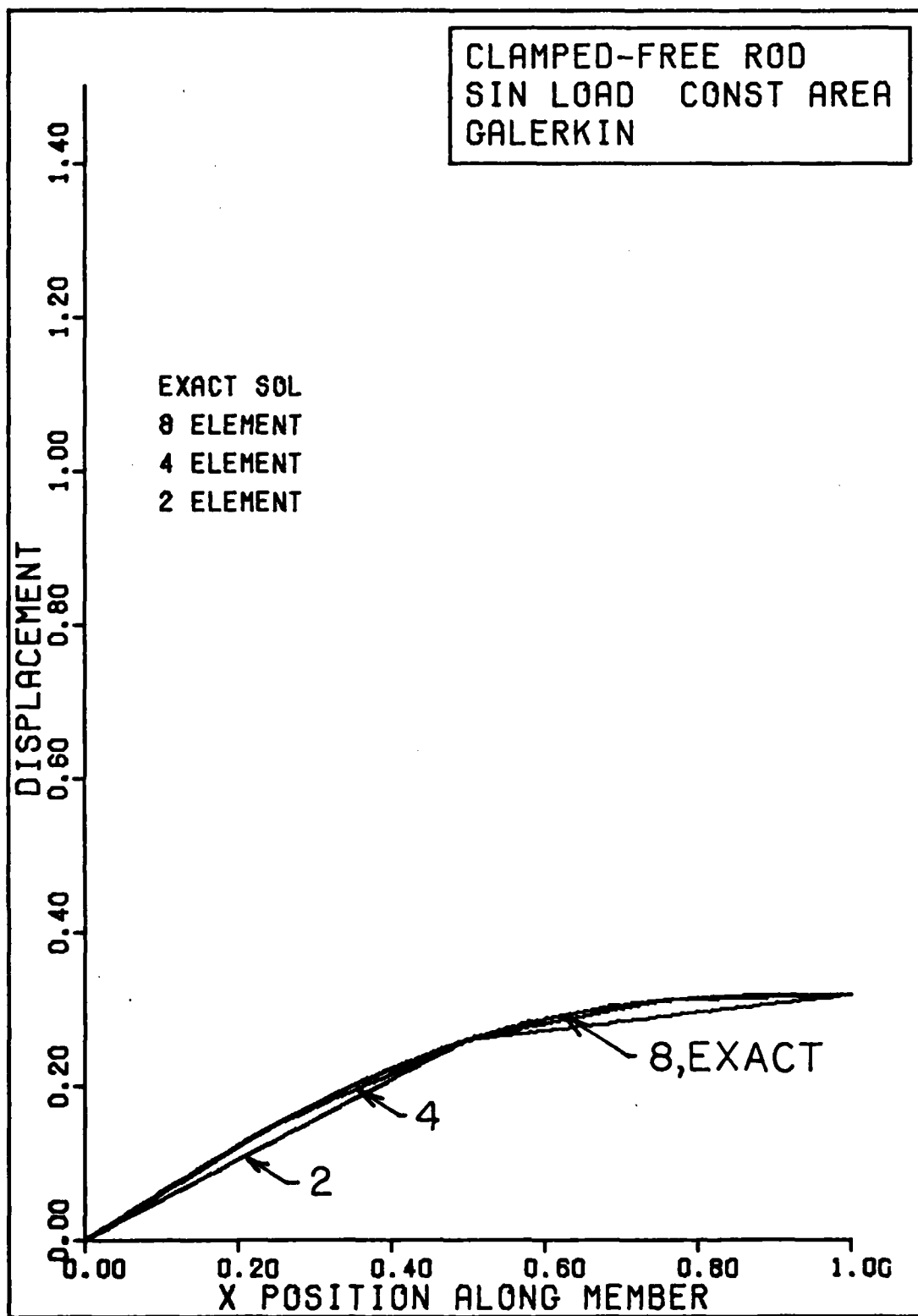
Method	$\frac{1}{h}$	Max Nodal Error	CF	Max Point Error	CF	Seconds Formation	Seconds Execution
COLL	1	.653E-1	-	.653E-1	-	.143	.005
	2	.369E-2	17.7	.369E-2	17.7	.225	.009
	4	.337E-4	109	.337E-4	109	.398	.016
	8	.344E-5	9.80	.344E-5	9.8	.749	.029
FD	4	.332E-1	-	.322E-1	-	.038	.002
	8	.855E-2	3.77	.855E-2	3.77	.060	.004
	16	.217E-2	3.94	.217E-2	3.94	.098	.006
	32	.502E-3	4.32	.502E-3	4.32	.185	.008

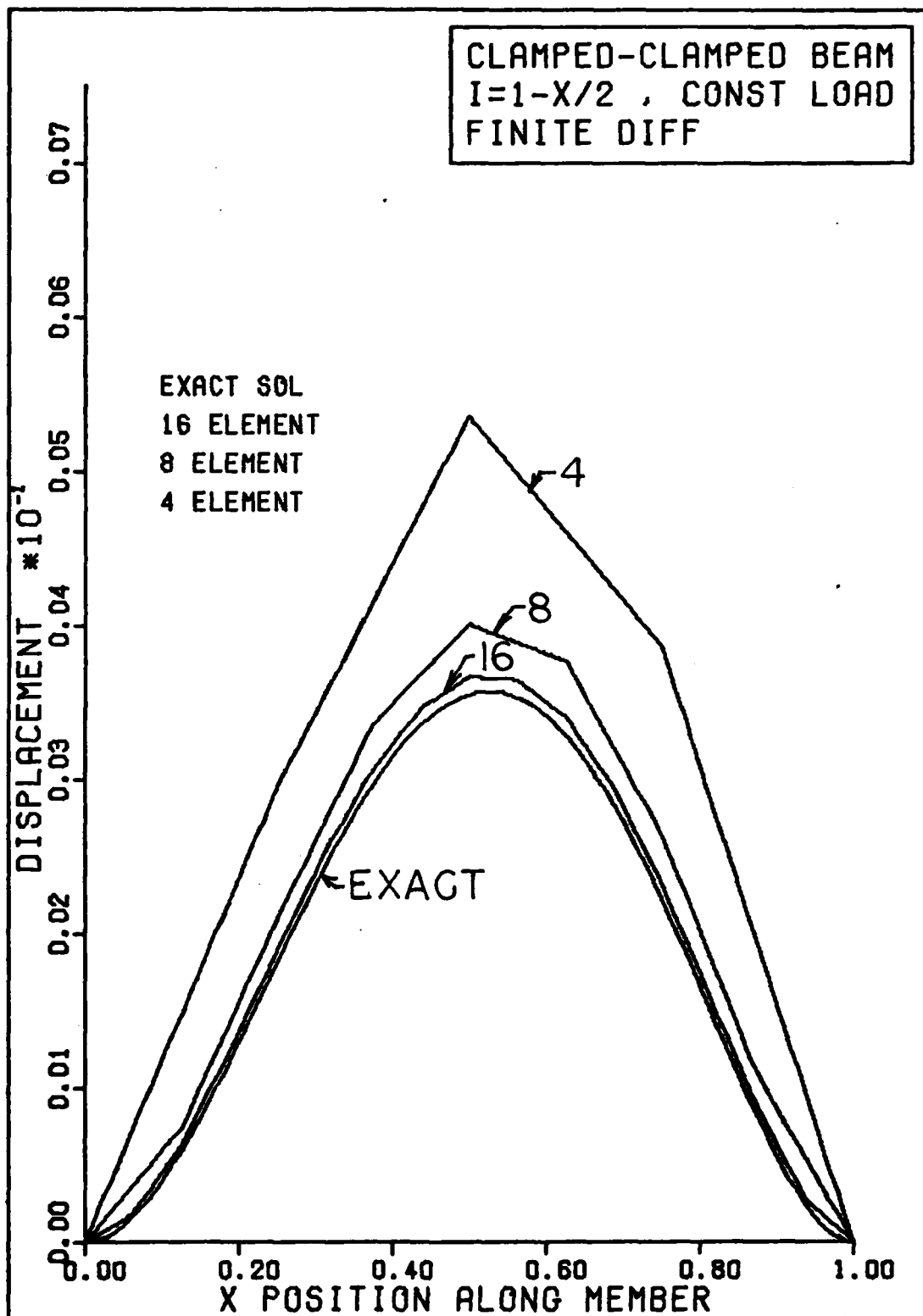
Table A-XII--Continued

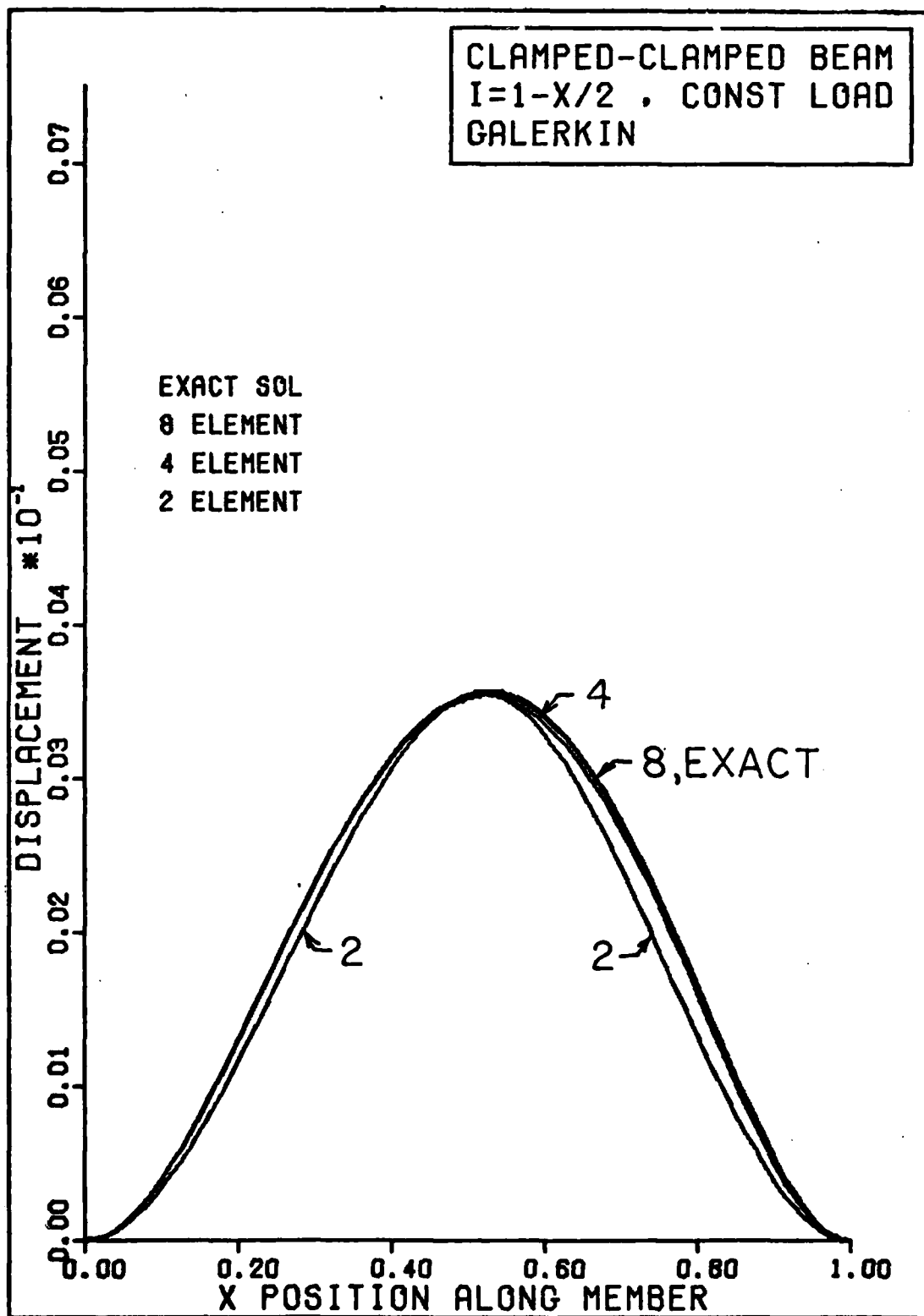
Method	$\frac{1}{h}$	Max Nodal Error	CF	Max Point Error	CF	Seconds Formation	Seconds Execution
GAL	1	.601E-14	-	.298E-1	-	.046	.001
	2	.601E-14	1.0	.150E-2	19.9	.077	.003
	4	.926E-12	.006	.126E-3	11.9	.122	.005
	8	.198E-10	.047	.842E-5	15.0	.223	.008
	16	.412E-9	.048	.535E-6	15.7	.436	.011

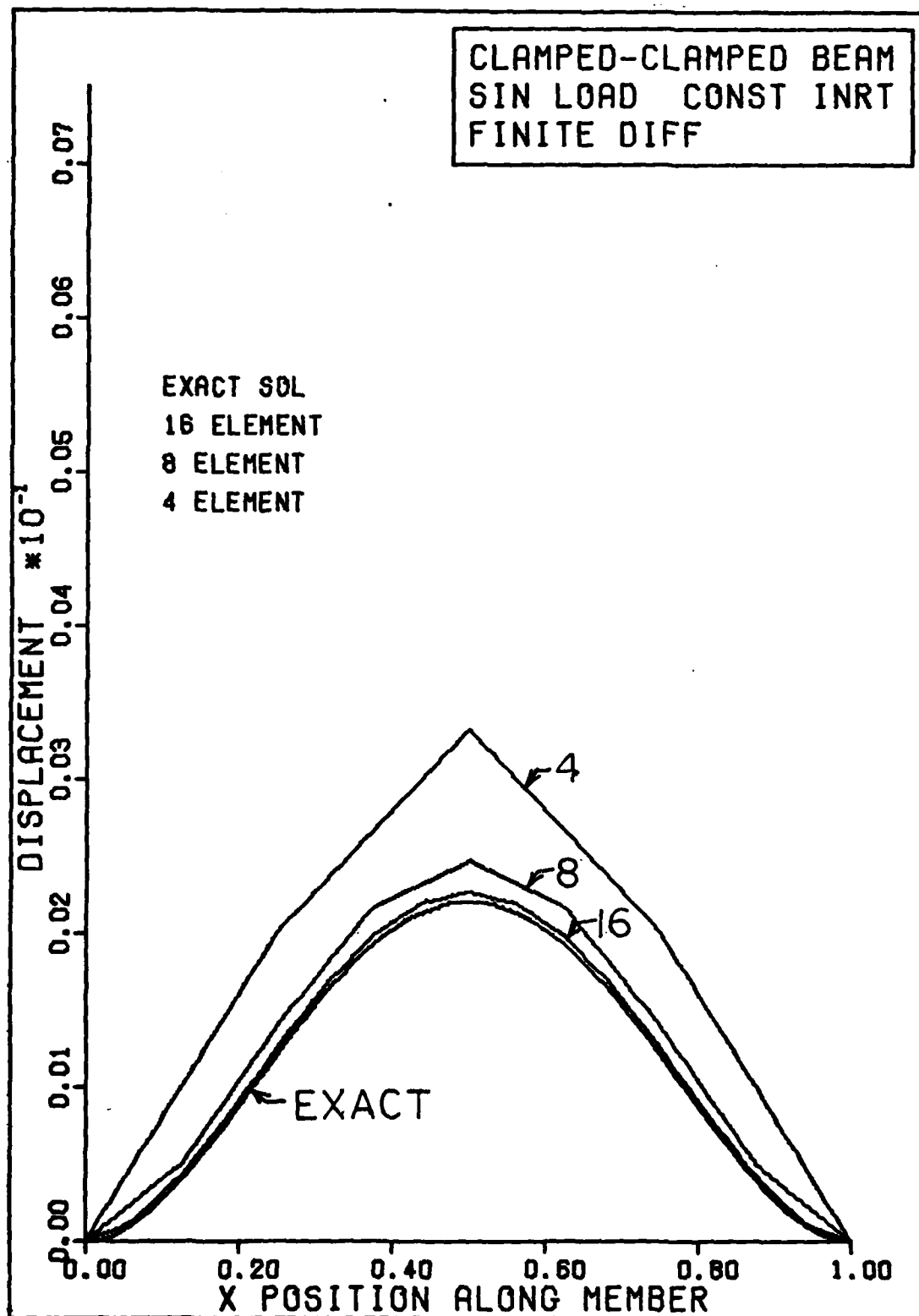


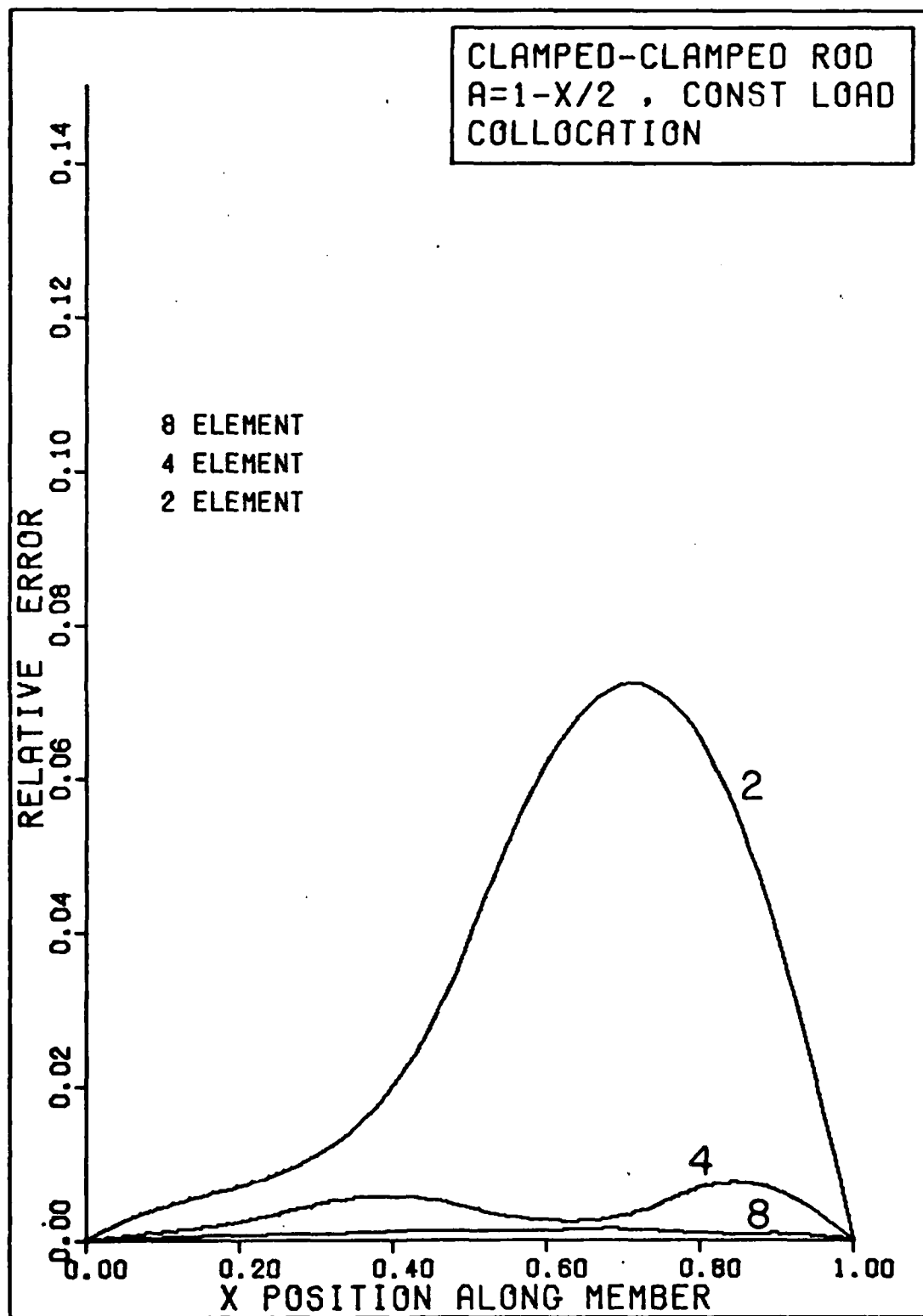


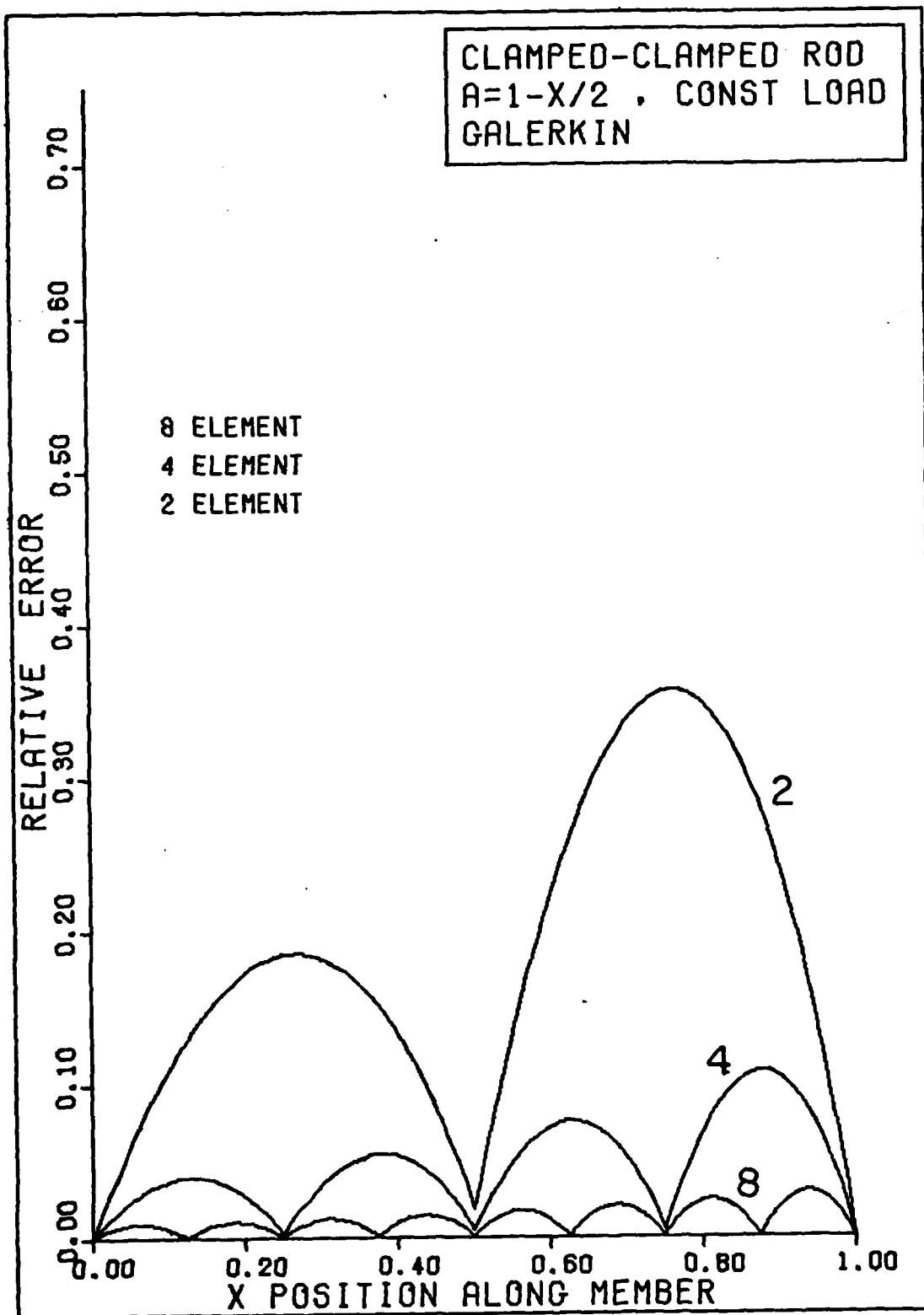


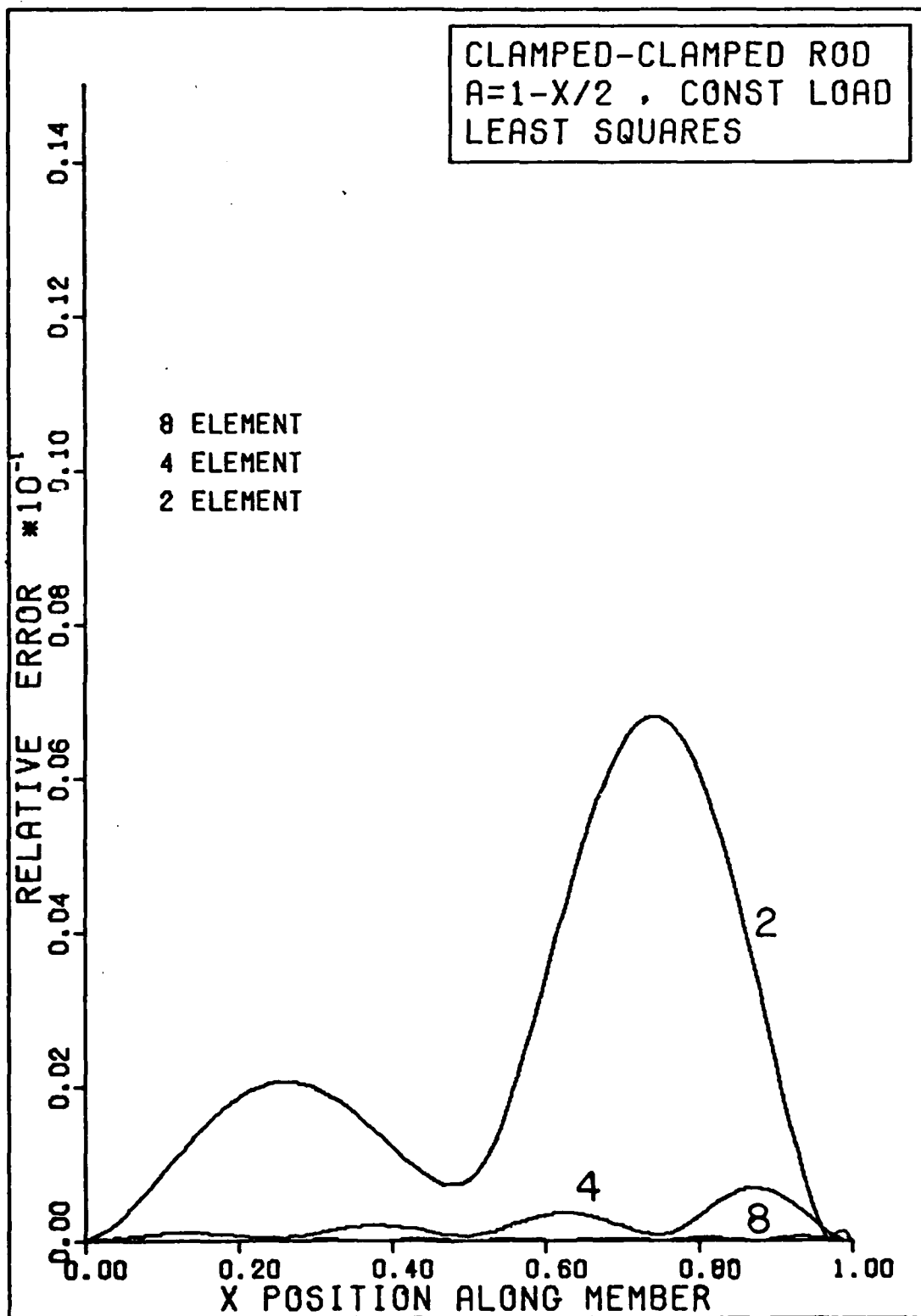


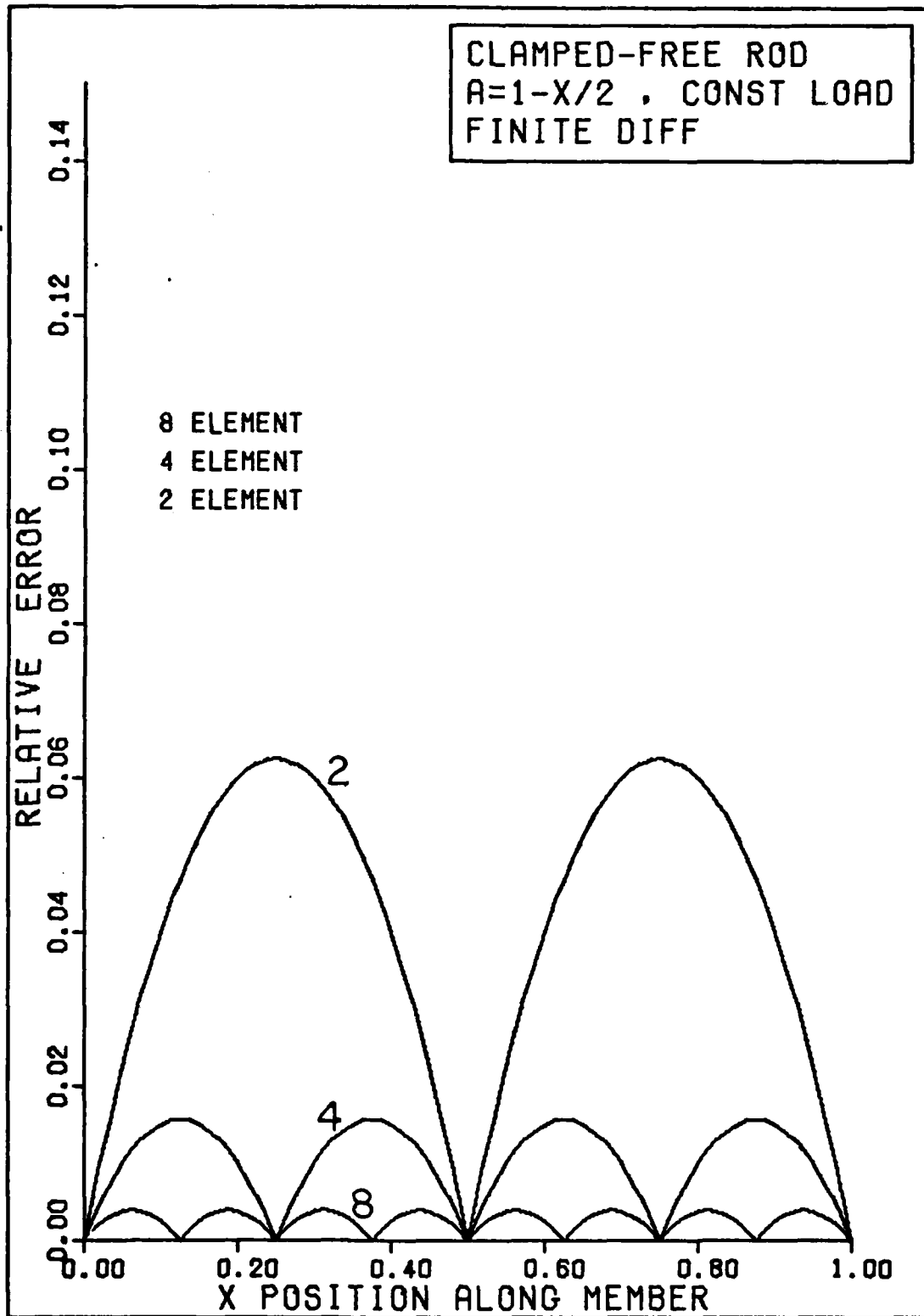


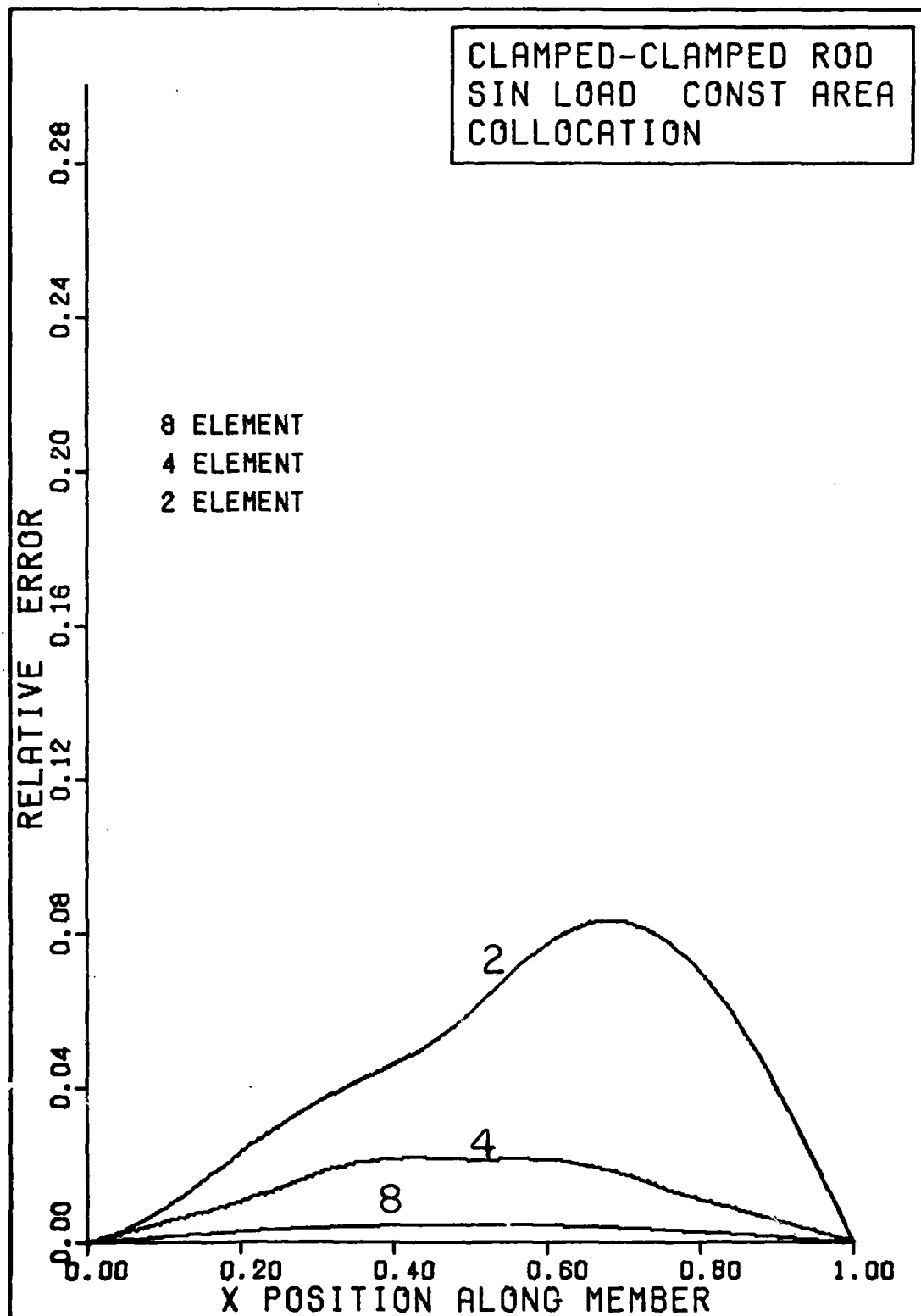


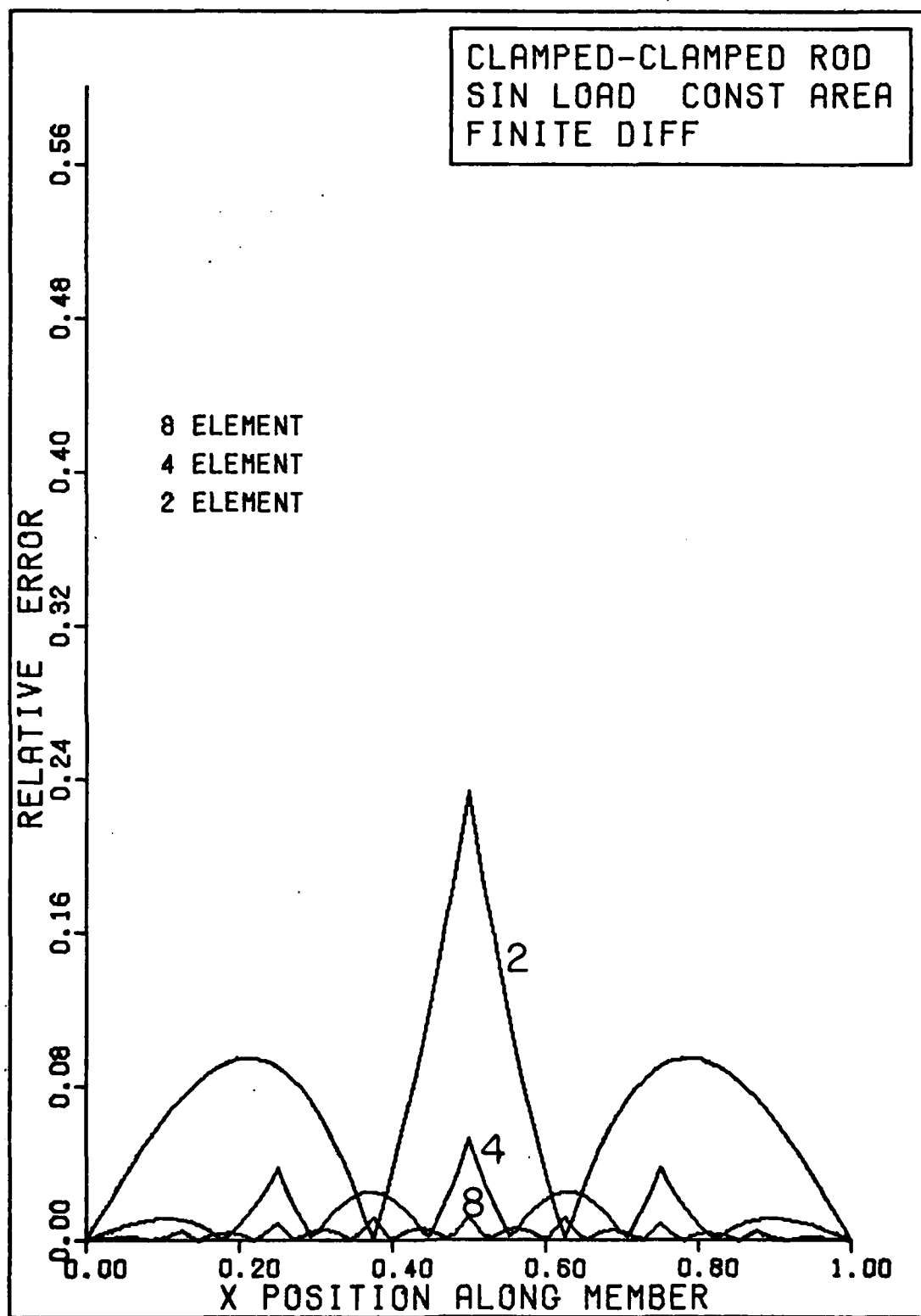


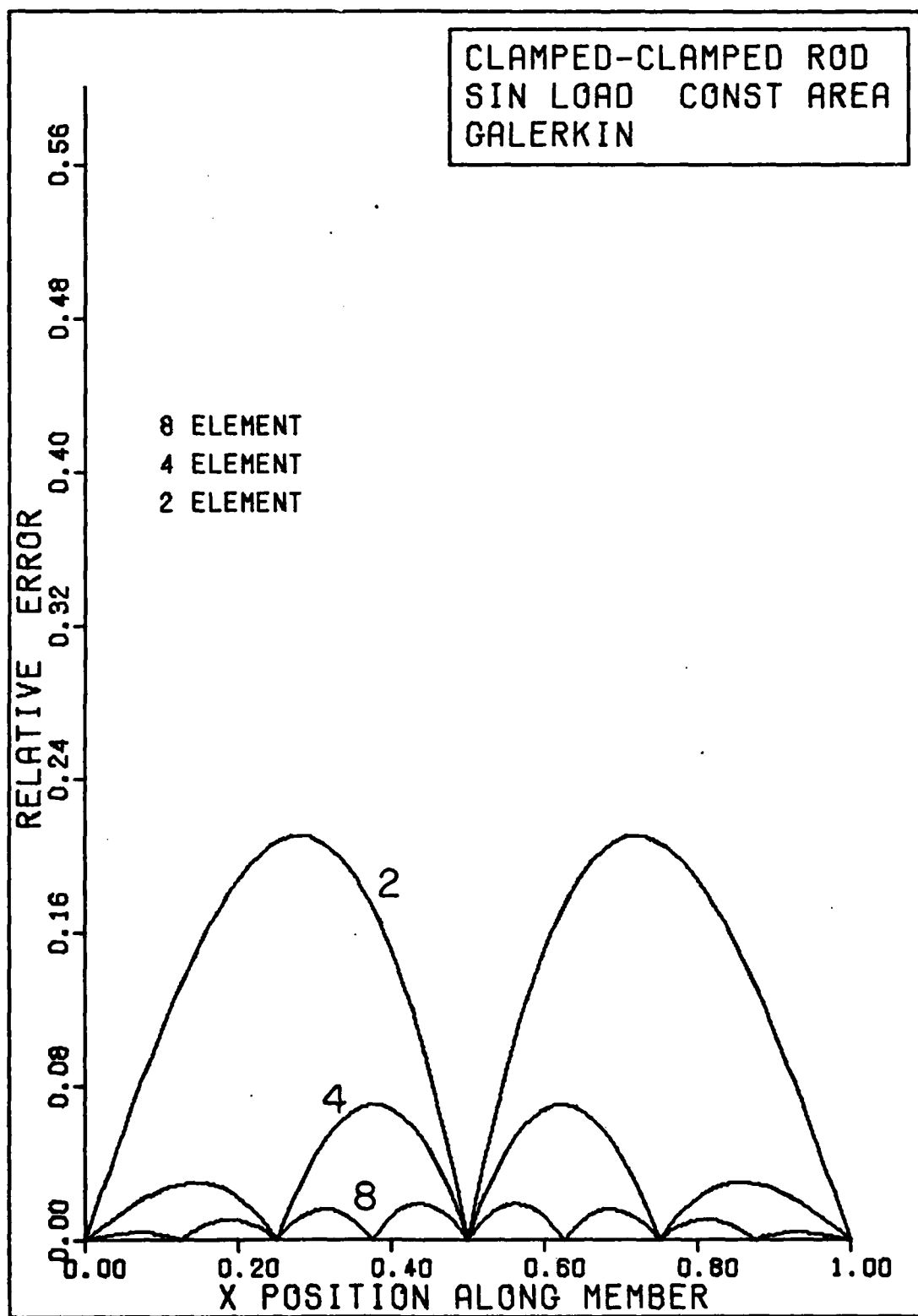


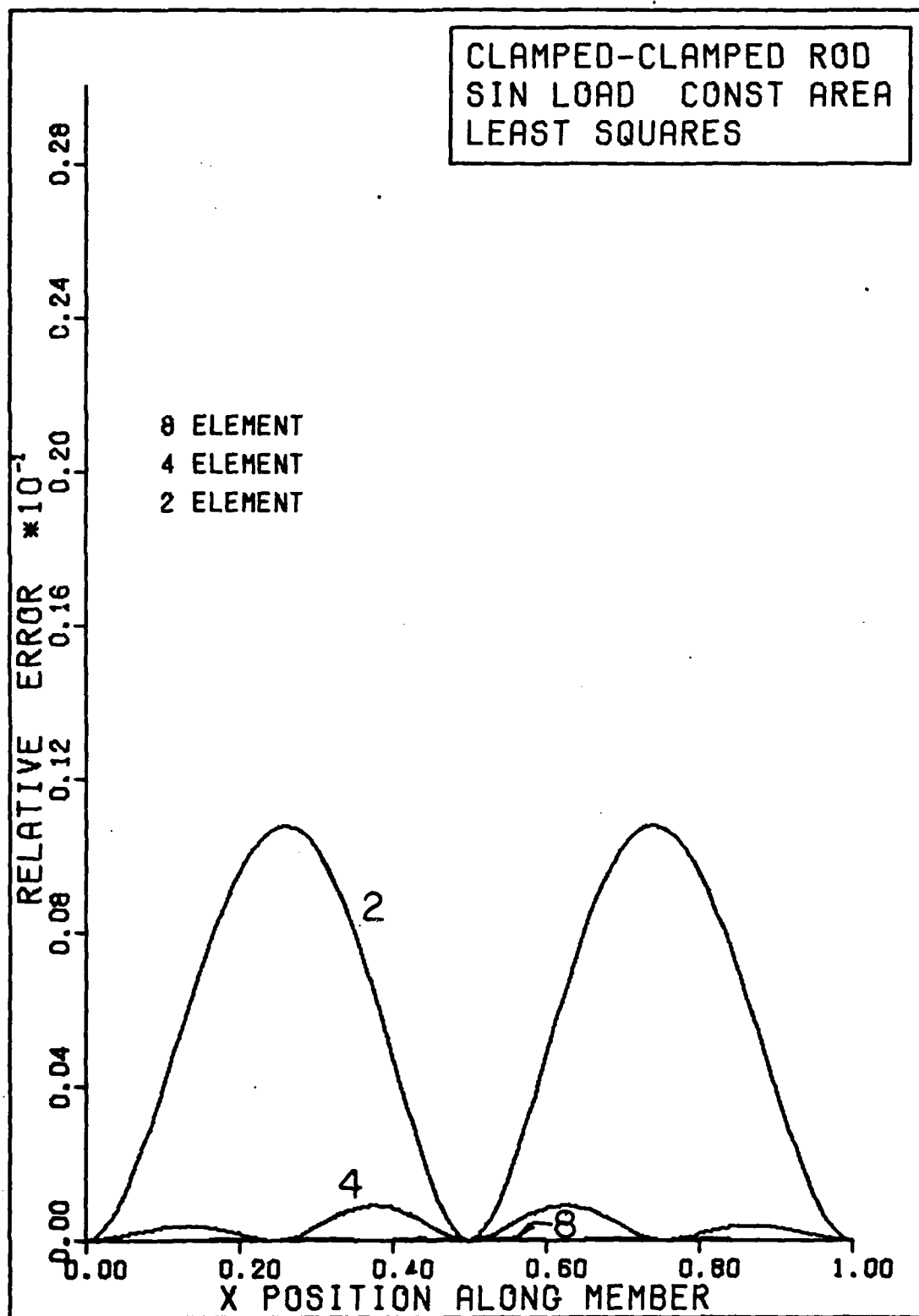


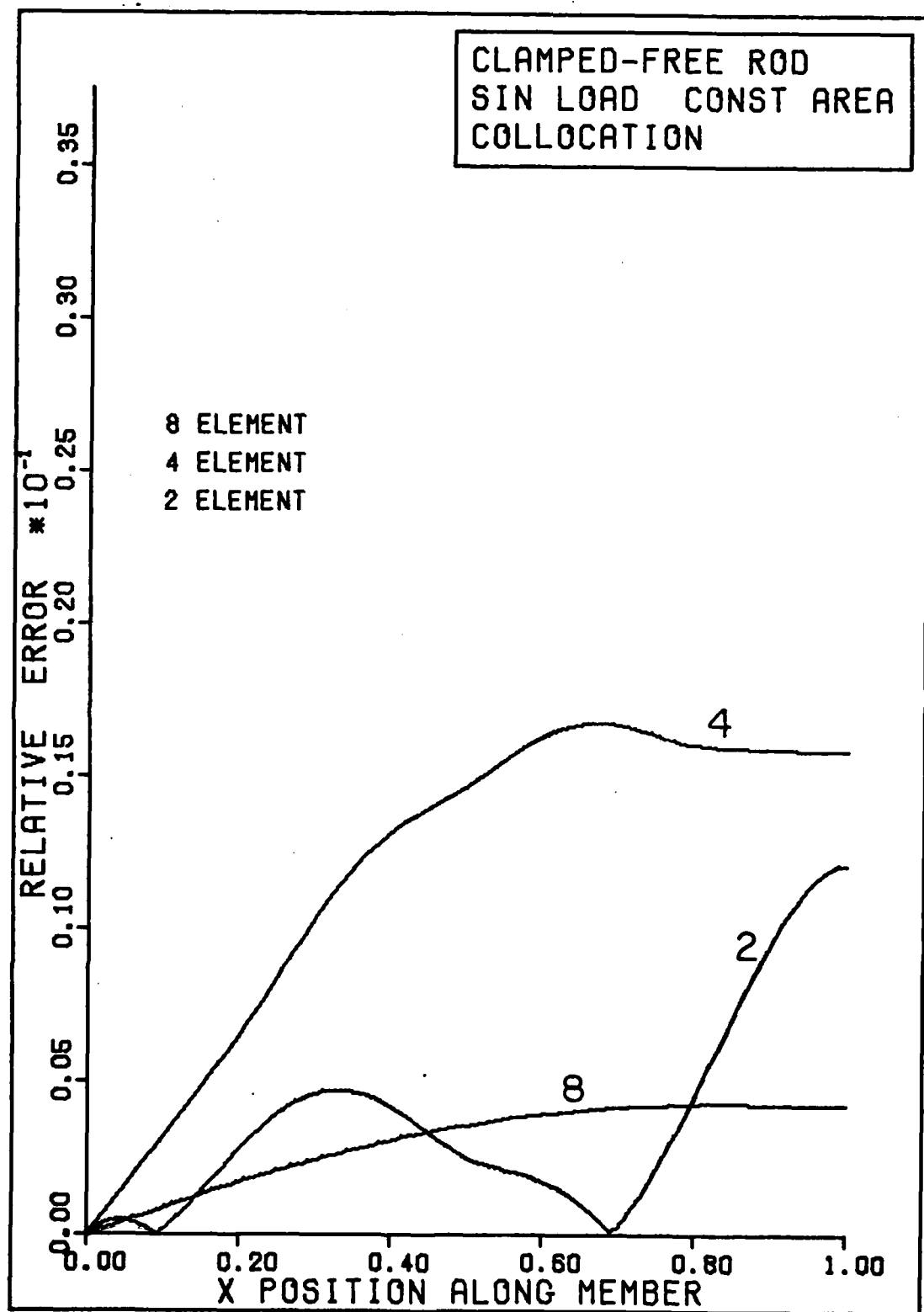


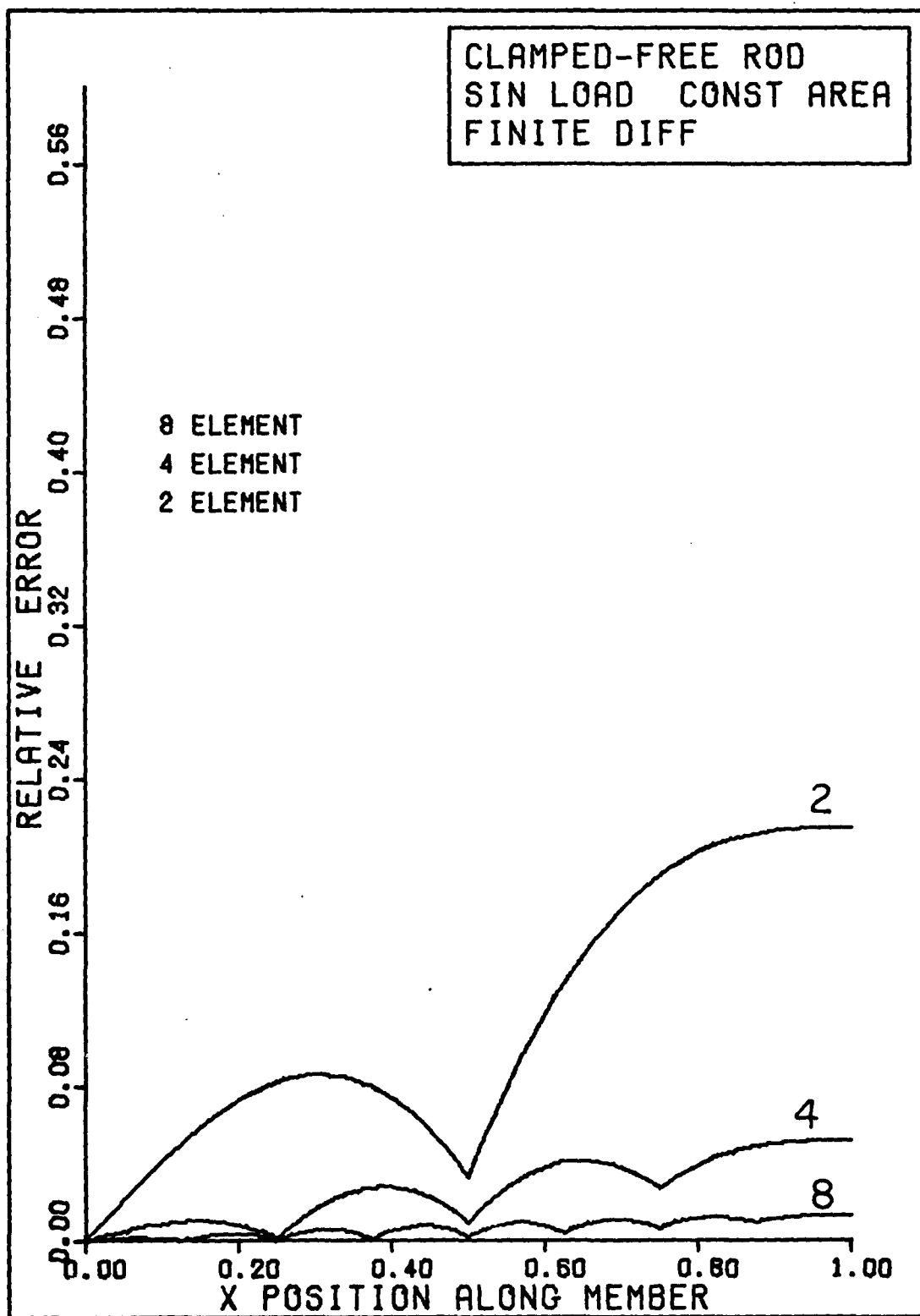


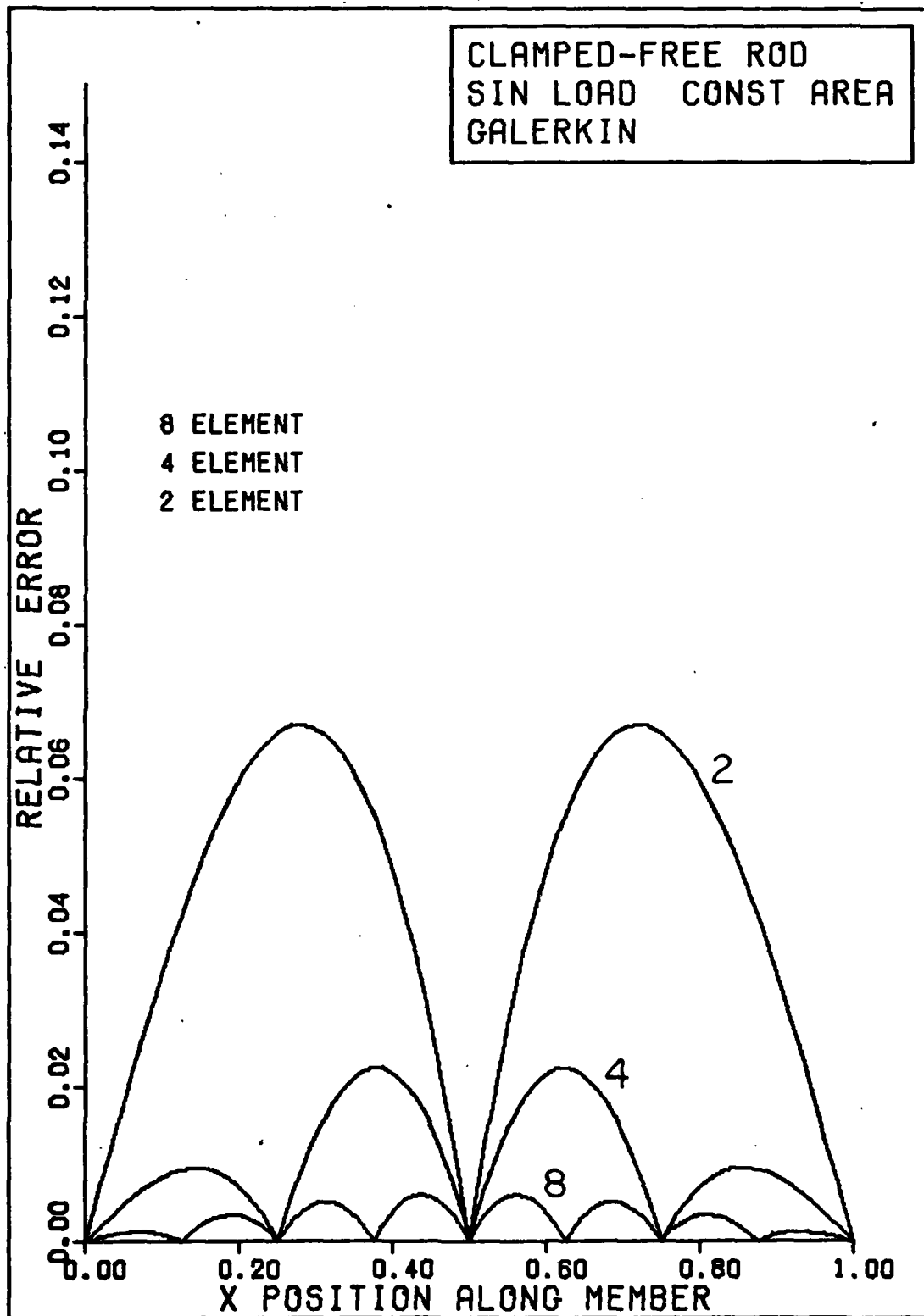


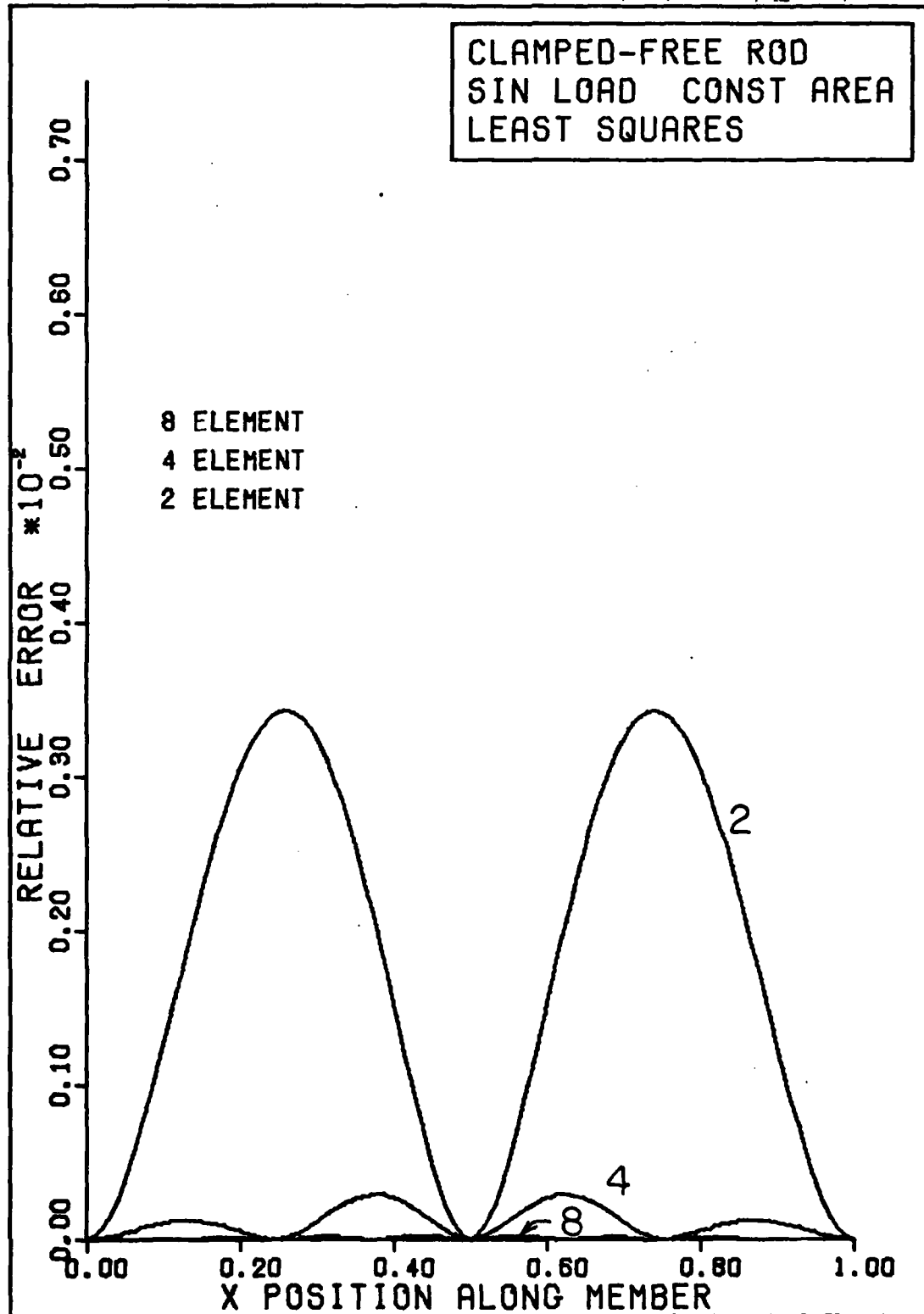


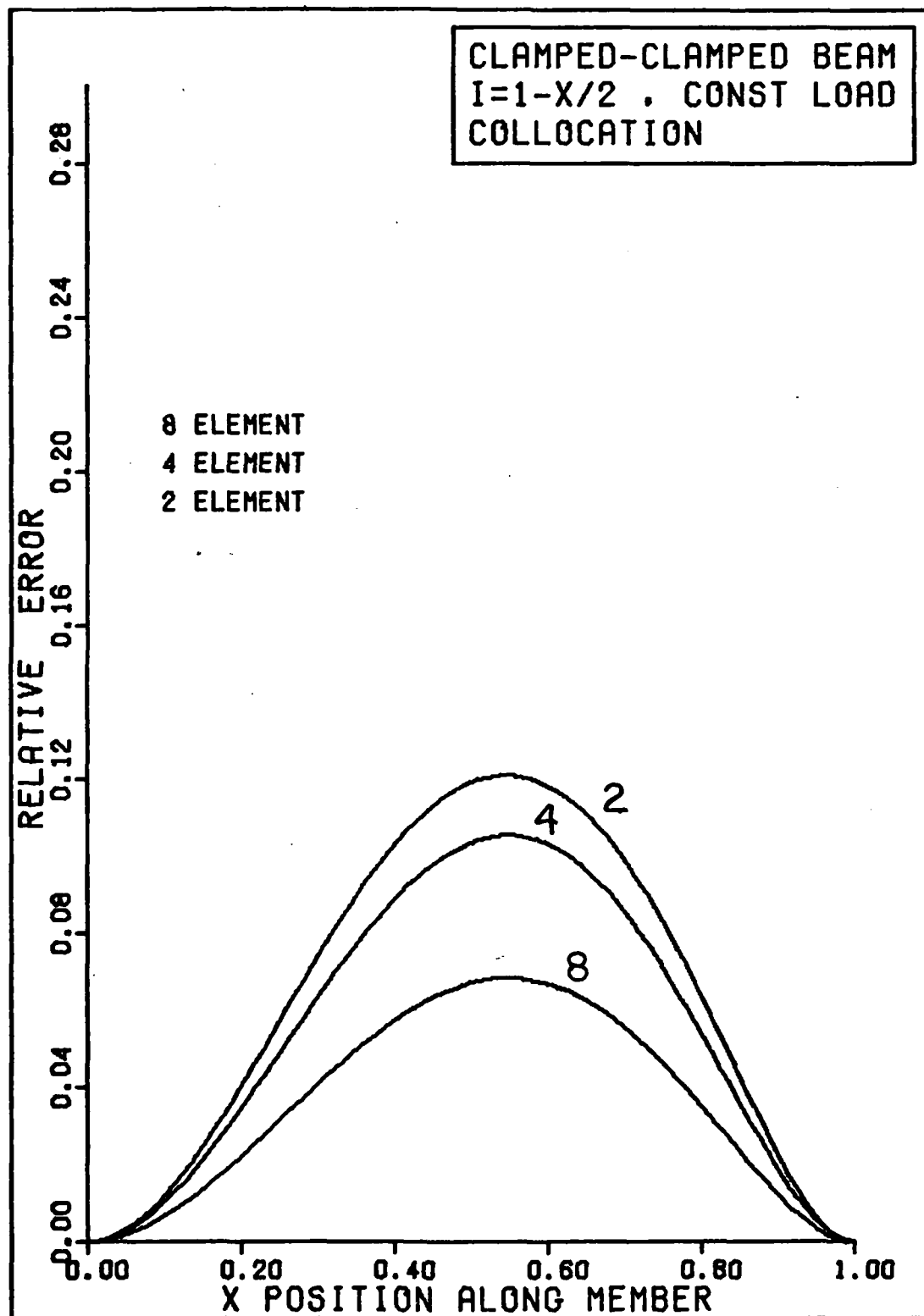


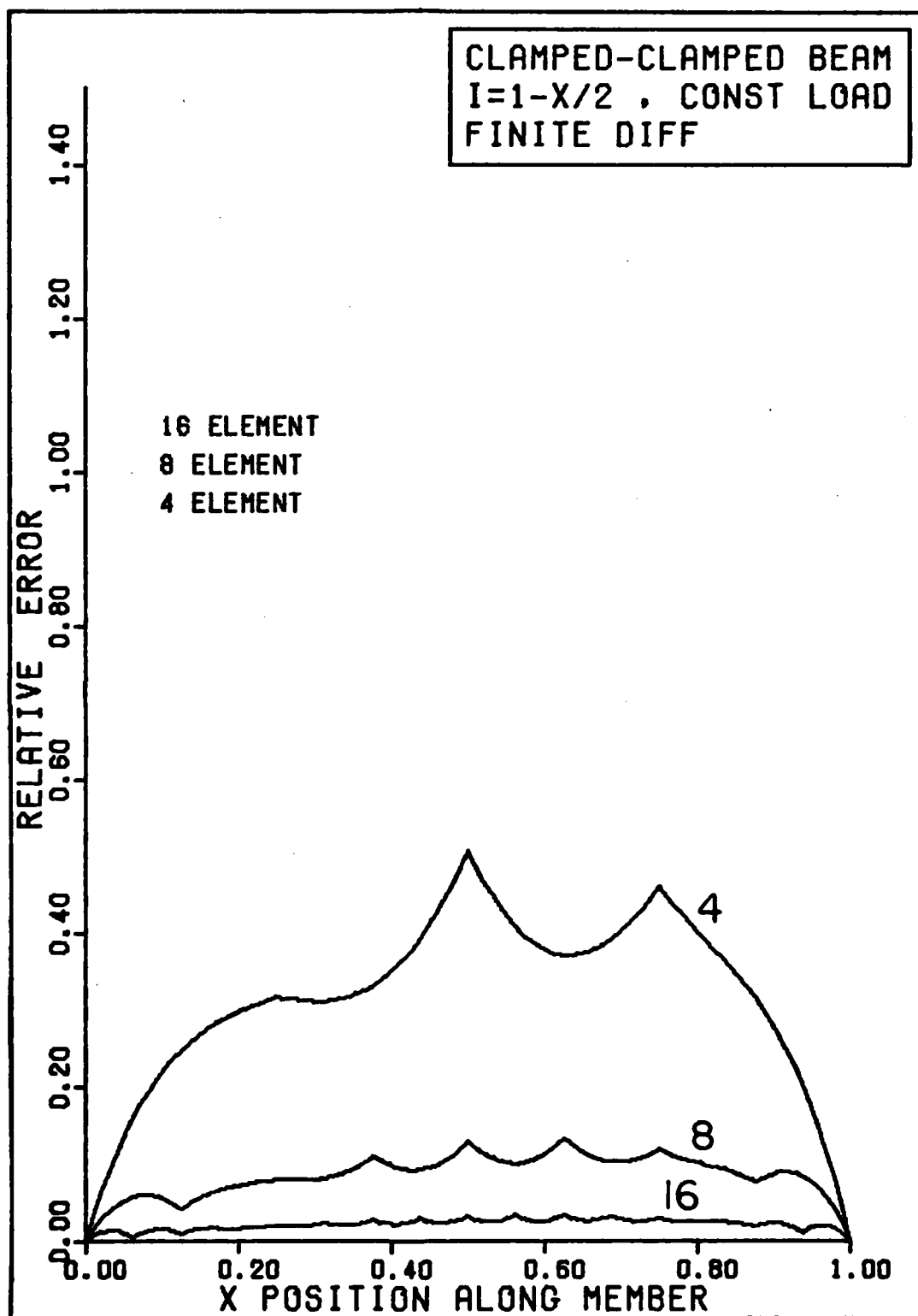


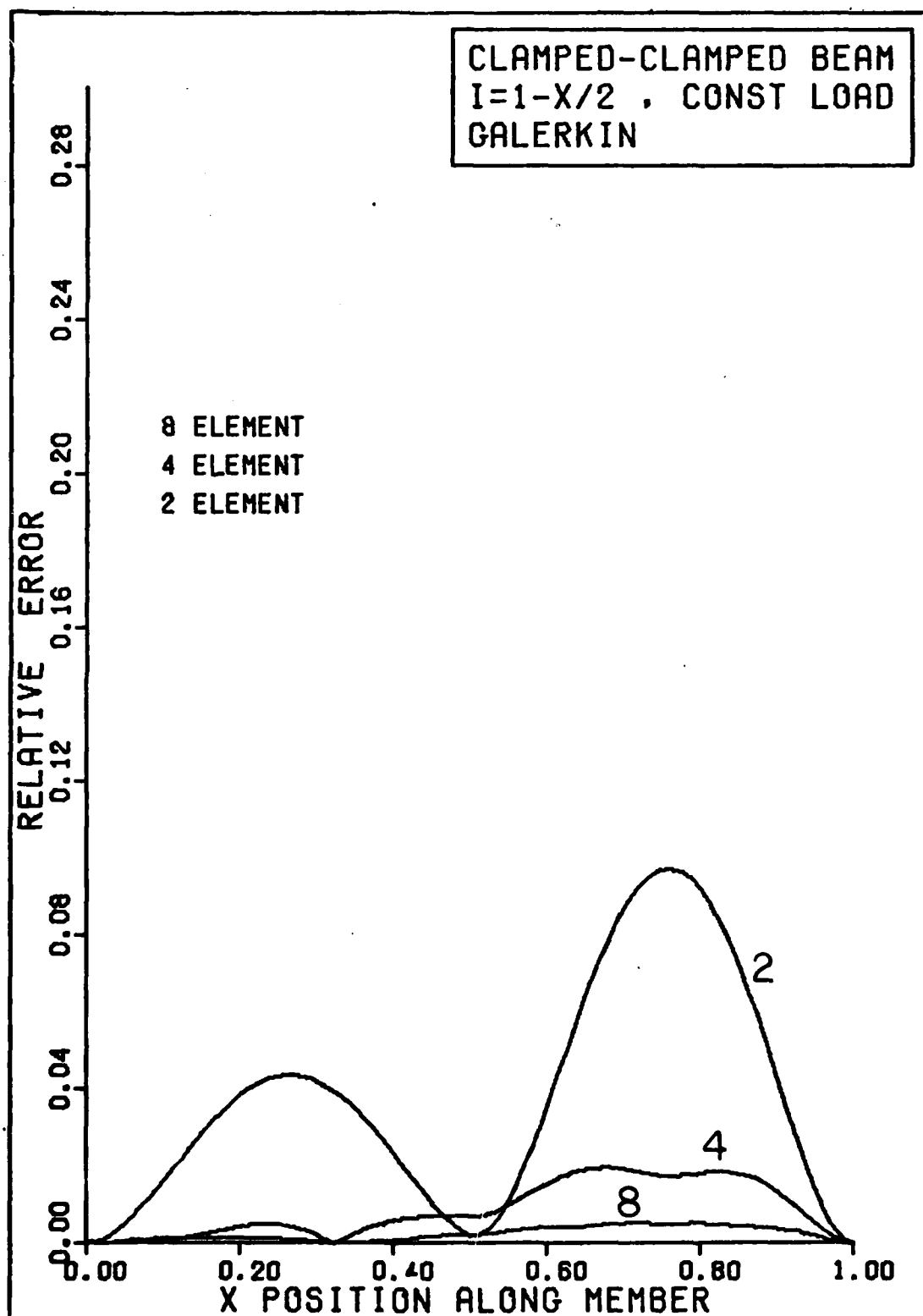


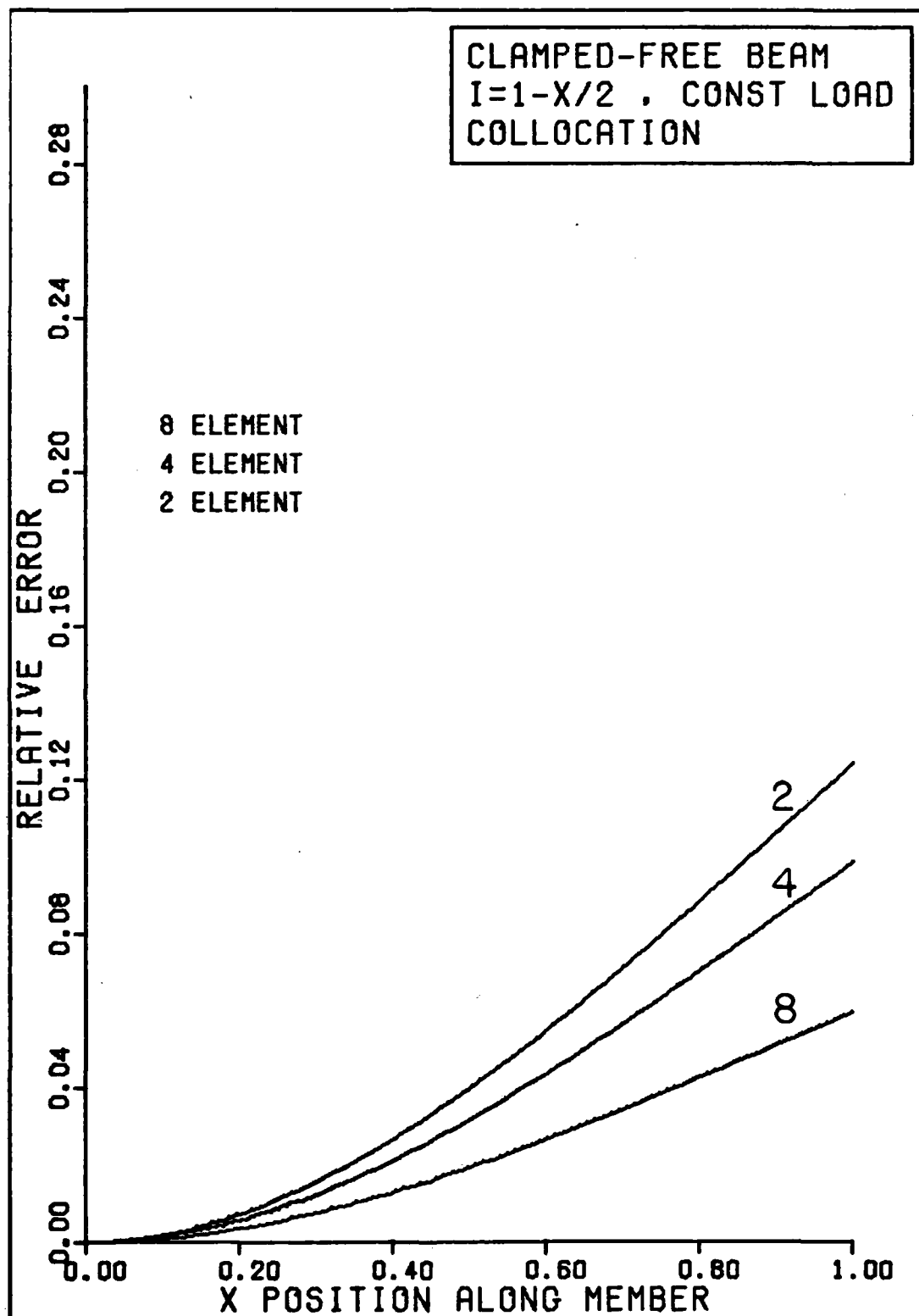


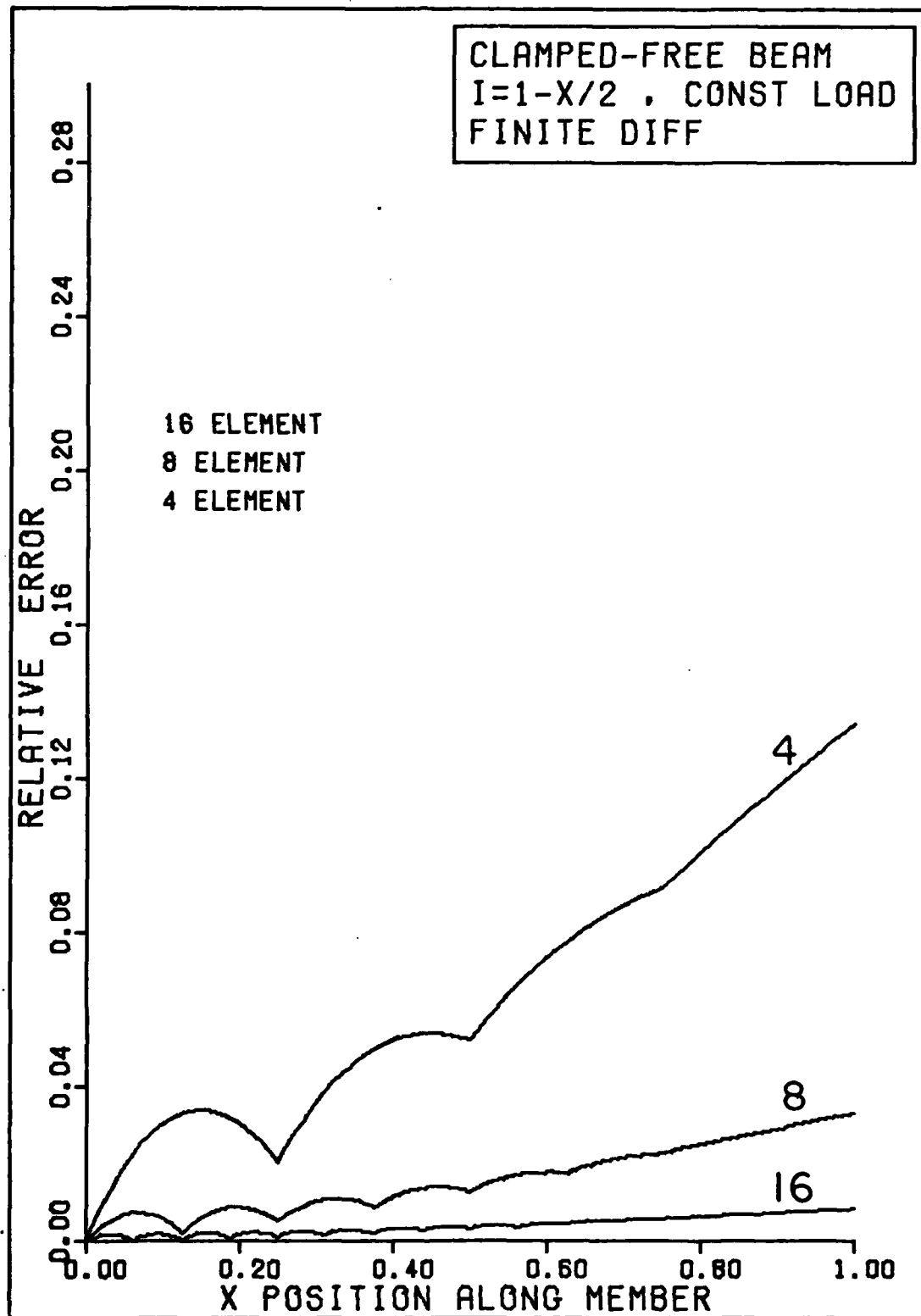


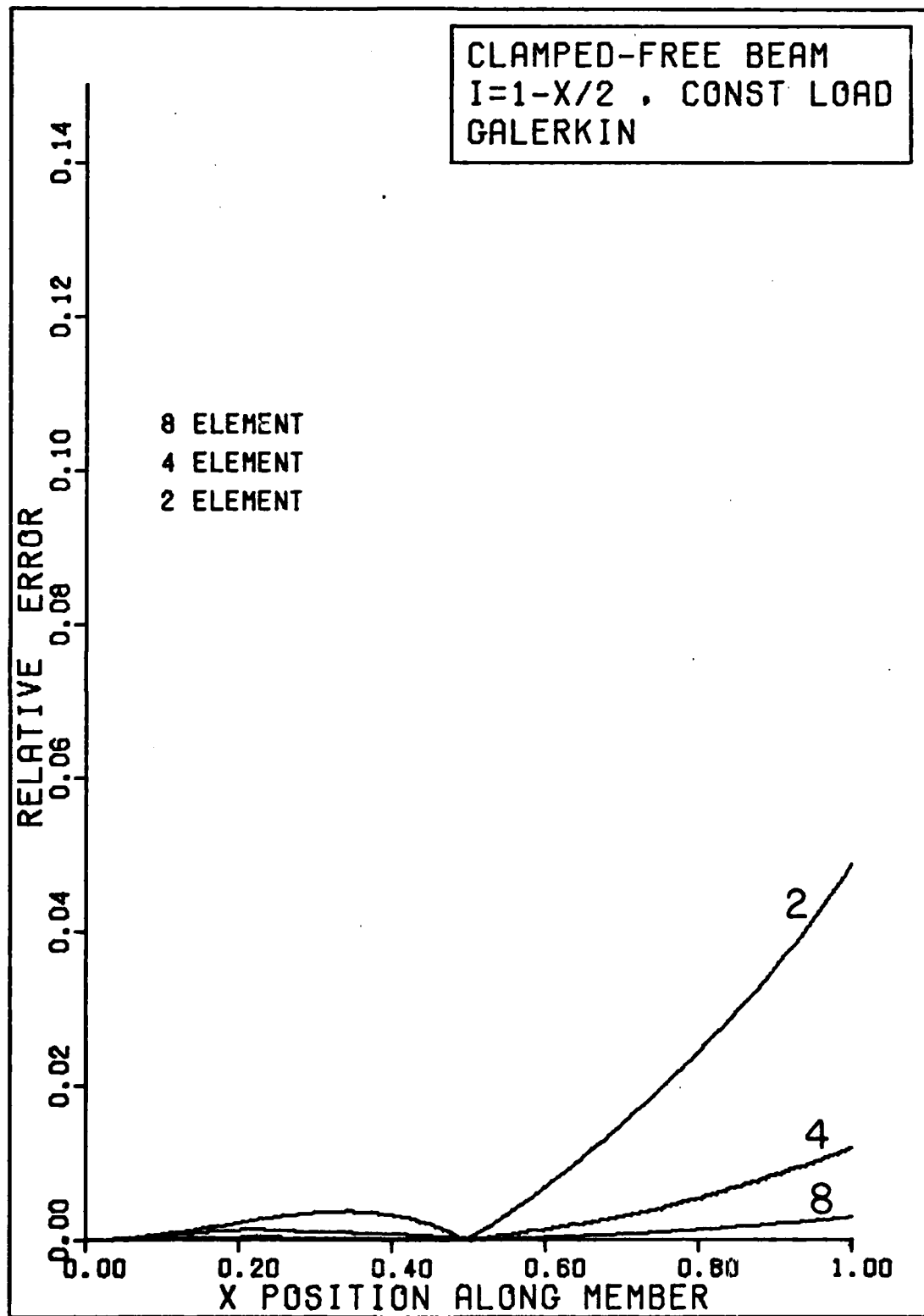












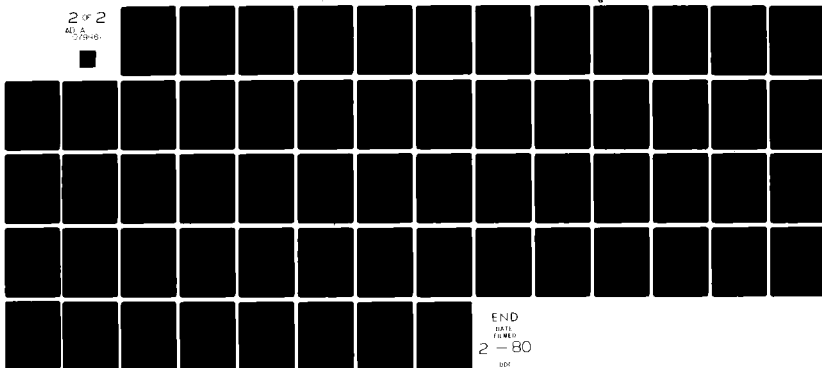
AD-A079 861

AIR FORCE INST OF TECH WRIGHT-PATTERSON AFB OH SCHOO--ETC F/8 12/1
COMPARISON OF NUMERICAL ANALYSIS METHODS FOR SOLVING ONE-DIMENS--ETC(U)
DEC 79 R A SMITH
AFIT/6AE/AA/79D-17

UNCLASSIFIED

NL

2 of 2
ALL A
CIRCUIT



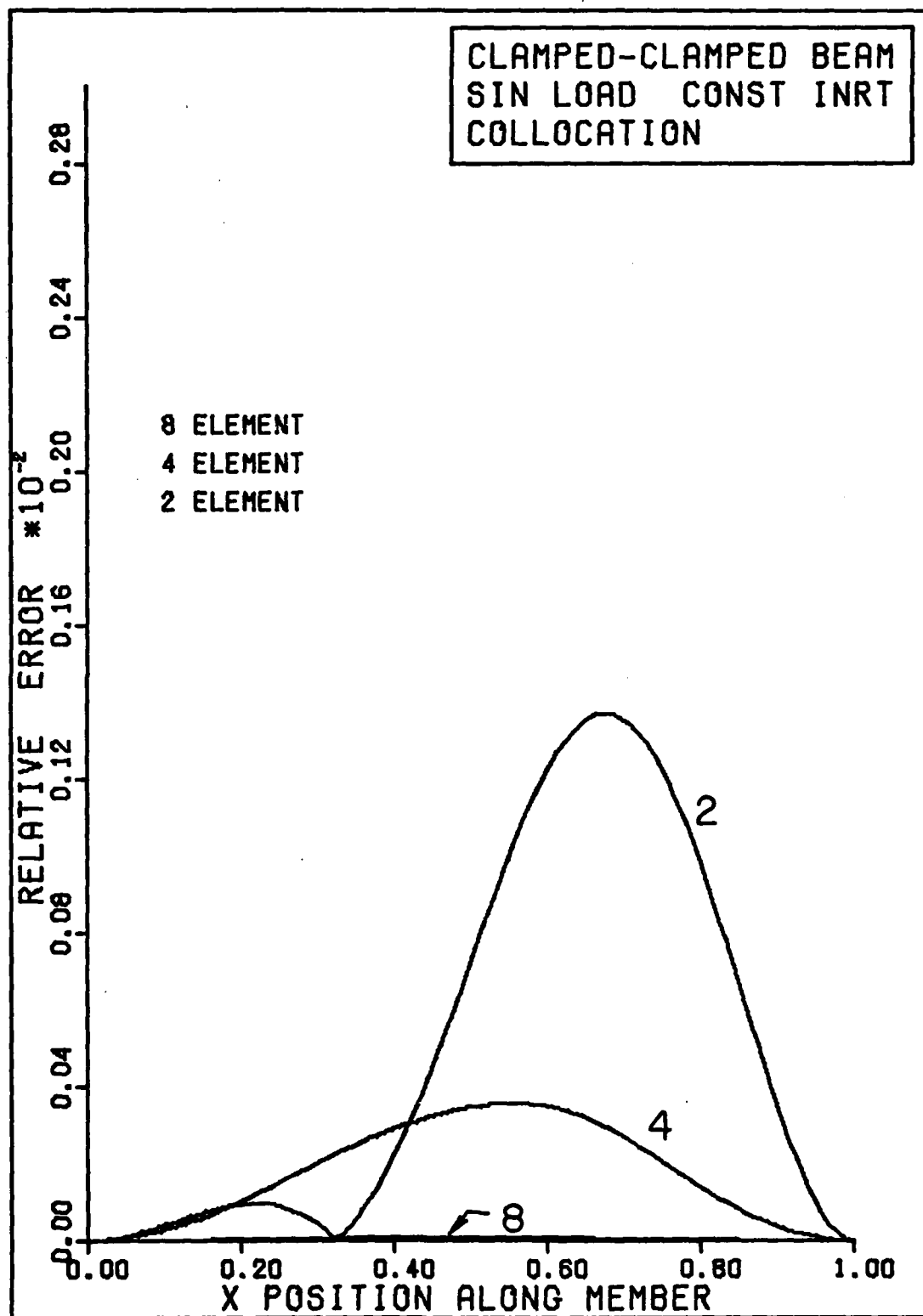
END

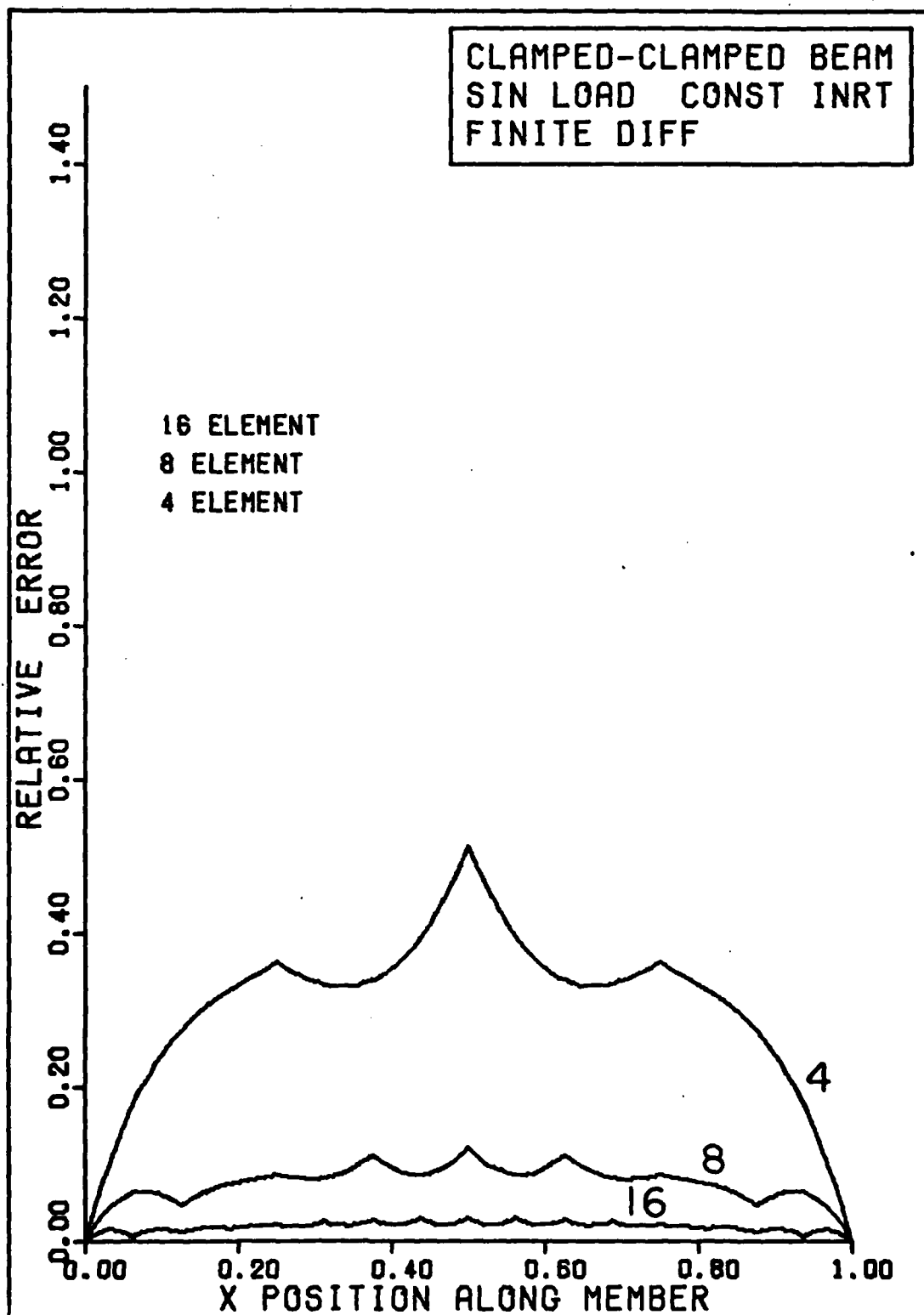
DATE

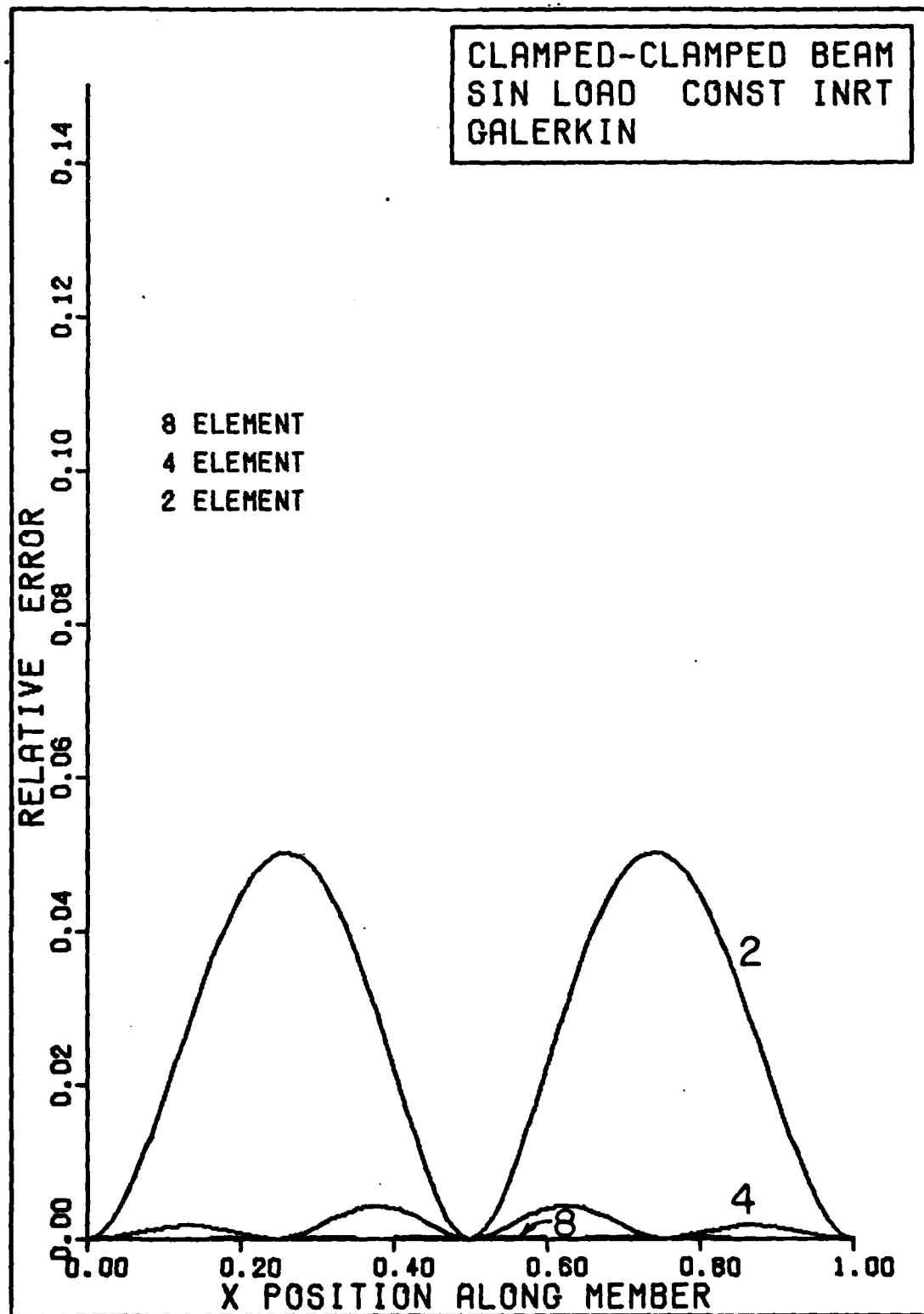
FILED

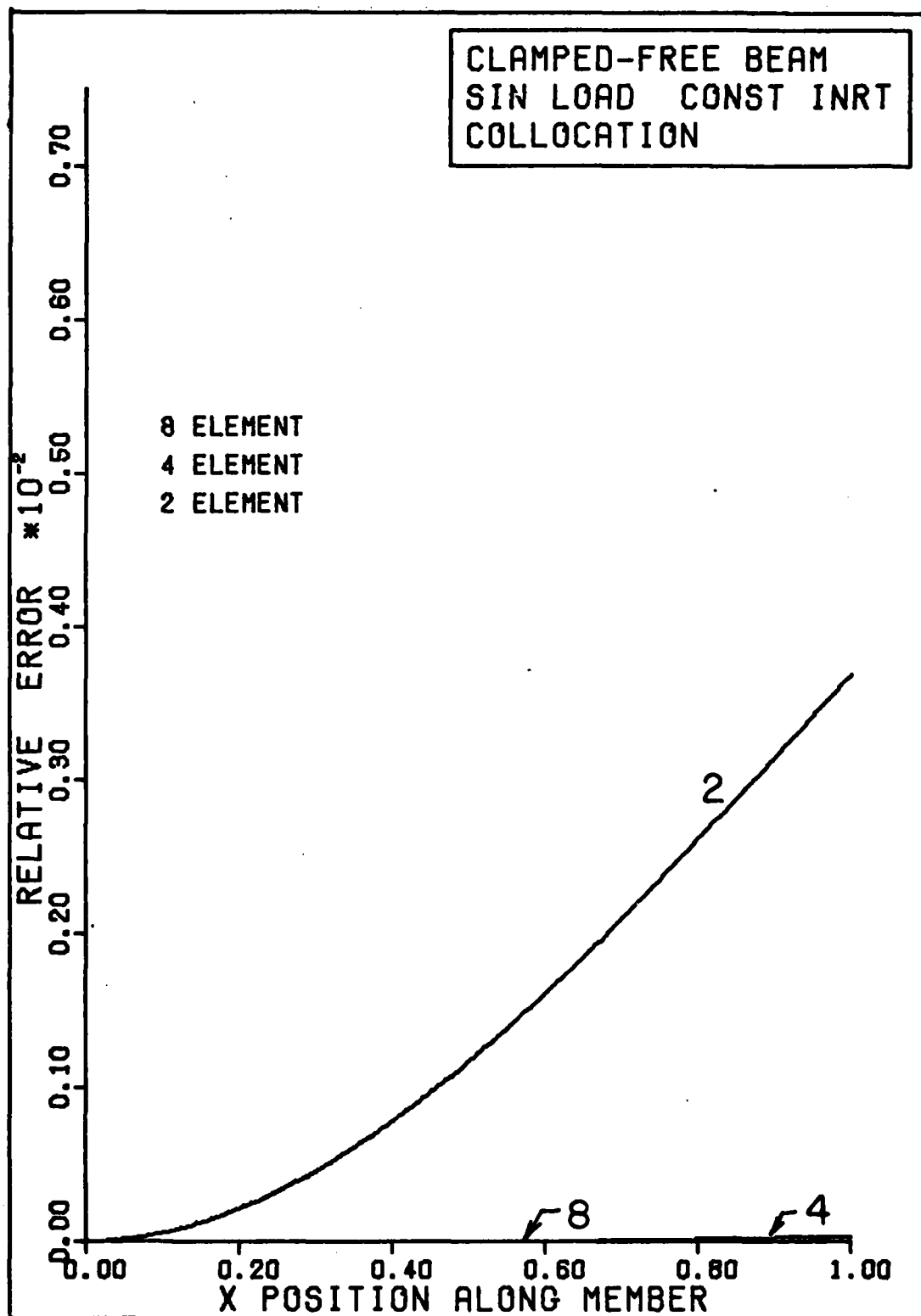
2 - 80

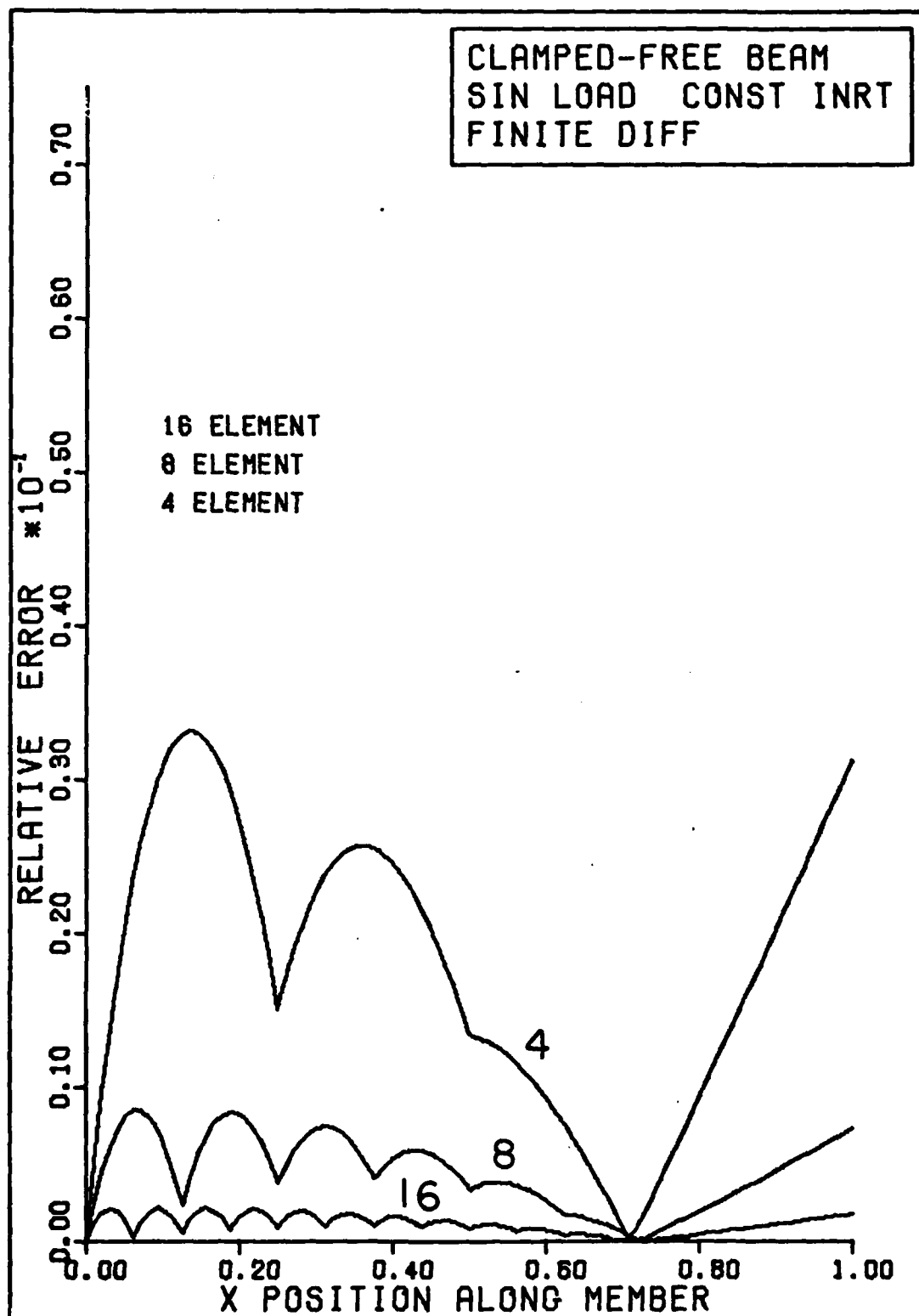
DDI

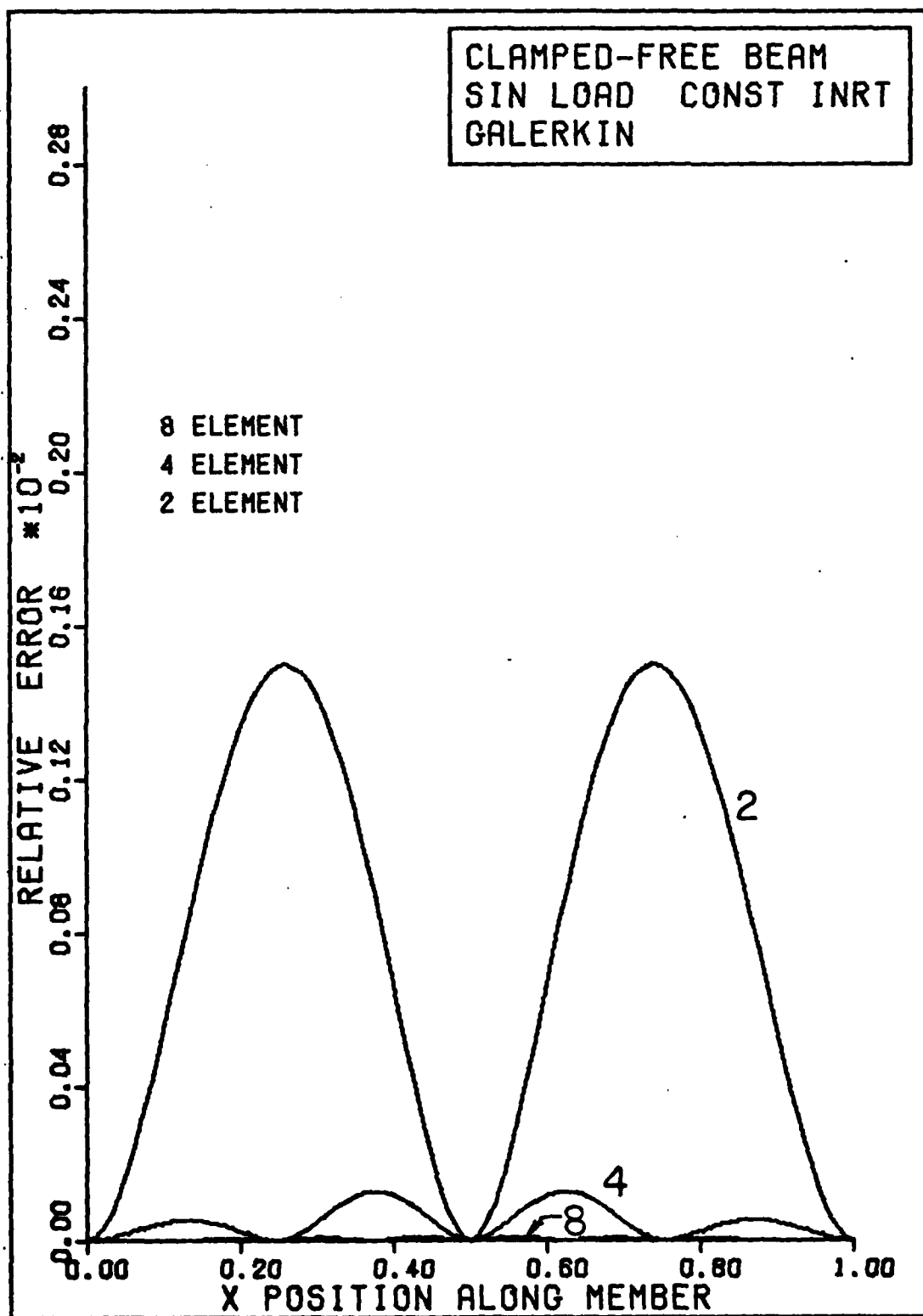












Appendix B

Finite Difference Expressions and Sample Problems

The finite difference method uses difference quotients to approximate the derivatives in a differential equation. These quotients are formed at $N+1$ (a finite number) grid points in the problem domain. For the one-dimensional problems in this study the domain is discretized as shown in Fig B-1.

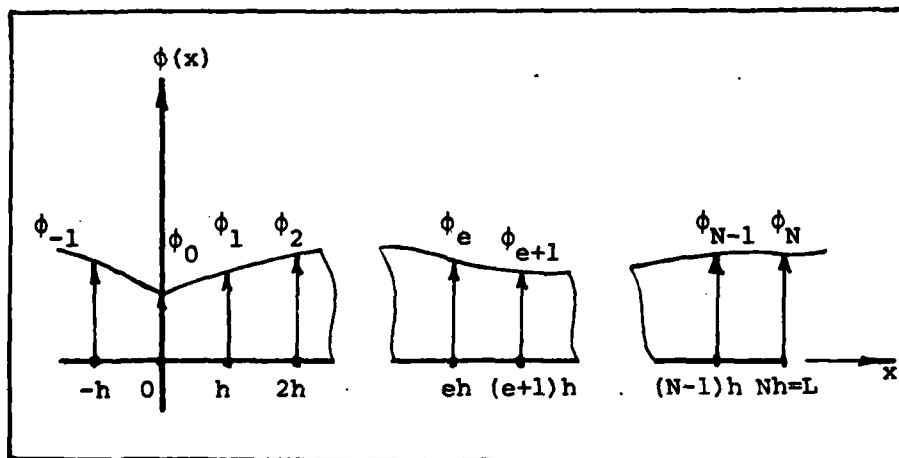


Fig B-1. Discretization of One-Dimensional Domain for Finite Difference Method

Near the boundaries the difference quotients may require that a "false" node exist outside the domain. This situation can easily be handled if symmetry about the boundary

is assumed (Ref 8:143). This situation is illustrated in Fig B-2.

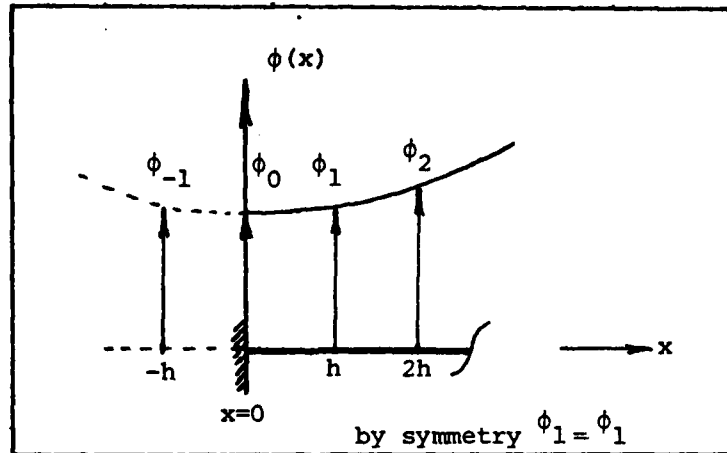


Fig B-2. Symmetry of Approximate Displacement About a Clamped End

Axial Rod

The governing differential equation for the axial rod is

$$\frac{d}{dx} \left\{ A(x) E \frac{du}{dx} \right\} = -F(x) \quad (B-1)$$

which after differentiation becomes

$$A(x) E \frac{d^2 u}{dx^2} + \frac{dA(x)}{dx} E \frac{du}{dx} = -F(x) \quad (B-2)$$

The two second-order central-difference quotients needed are

$$D^2(y_i) = \frac{1}{h^2} (y_{j-1} - 2y_j + y_{j+1}) + \left(-\frac{1}{12} h^2 y_i^{IV}\right) \quad (B-3)$$

$$D(y_i) = \frac{1}{2h} (-y_{j-1} + y_{j+1}) + \left(-\frac{1}{6} h^2 y_j^{III}\right) \quad (B-4)$$

Substituting Eqs (B-3) and (B-4) into Eq (B-2) gives the result

$$\begin{aligned} & [-A(x_{j-1}) - 4A(x_j) + A(x_{j+1})] u_{j-1} + 8A(x_j) u_j \\ & + [A(x_{j-1}) - 4A(x_j) - A(x_{j+1})] u_{j+1} = -\frac{4F(x_j) h^2}{E} \\ & j=0,1,\dots,N \quad (B-5) \end{aligned}$$

For a uniform rod Eq (B-5) reduces to

$$\begin{aligned} -u_{j-1} + 2u_j - u_{j+1} &= -\frac{F(x_j) h^2}{EA} \\ j=0,1,\dots,N \quad (B-6) \end{aligned}$$

where $F(x_j) = P$ for the uniform load case and $F(x_j) = P \sin\left(\frac{\pi x_j}{L}\right)$ for the half-sin load distribution, and $A(x_j) = (1 - \alpha \frac{x_j}{L})$. In this study only two boundary conditions are studied, they are:

$$u(x_k) = 0 - \text{zero displacement} \quad (B-7)$$

$$A(x_k)E \frac{du}{dx}(x_k) = 0 - \text{zero axial force} \quad (\text{B-8})$$

To account for the boundary conditions, the equations associated with nodes near the end of the rod are modified as follows:

1. For a clamped end at $x_k=0$, then $u_0=0$ in row 1 and in row 2

$$8A(x_1)u_1 + [A(x_0)-4A(x_1)-A(x_2)]u_2 = -\frac{4F(x_1)h^2}{E} \quad (\text{B-9})$$

2. For a clamped end at $x_k=L$, then $u_N=0$ in row $N+1$ and in row N

$$8A(x_{N-1})u_{N-1} + [A(x_{N-1})-4A(x_{N-2})-A(x_{N-3})]u_{N-2} = -\frac{4F(x_{N-1})h^2}{E} \quad (\text{B-10})$$

3. For a free end at $x_k=L$, then in row $N+1$

$$8A(x_N)u_N - 8A(x_{N-1})u_{N-1} = -\frac{4F(x_N)h^2}{E} \quad (\text{B-11})$$

Sample Problem B-1. A clamped-free uniform rod is loaded with a half-sin distribution of uniaxial tension. The rod is discretized with five grid points. After the boundary conditions are applied, the system equations become

$$\begin{bmatrix} 8 & -4 & 0 & 0 \\ -4 & 8 & -4 & 0 \\ 0 & -4 & 8 & -1 \\ 0 & 0 & -8 & 8 \end{bmatrix} \begin{Bmatrix} u_1 \\ u_2 \\ u_3 \\ u_4 \end{Bmatrix} = \begin{Bmatrix} .18 \\ .25 \\ .18 \\ 0 \end{Bmatrix}$$

The approximate solution compared with the exact solution is

$$\begin{array}{c} \text{approximate} \\ \left\{ \begin{array}{c} u_1 \\ u_2 \\ u_3 \\ u_4 \end{array} \right\} = \frac{PL^2}{AE} \left\{ \begin{array}{c} .15088 \\ .25758 \\ .30178 \\ .30178 \end{array} \right\} \end{array} \quad \begin{array}{c} \text{exact} \\ \left\{ \begin{array}{c} u_1 \\ u_2 \\ u_3 \\ u_4 \end{array} \right\} = \frac{PL^2}{AE} \left\{ \begin{array}{c} .15122 \\ .26048 \\ .31038 \\ .31831 \end{array} \right\} \end{array}$$

Beam in Bending

The governing differential equation for the beam in bending is

$$\frac{d^2}{dx^2} \left\{ I(x) E \frac{d^2 w}{dx^2} \right\} = F(x) \quad (B-12)$$

After differentiation it becomes

$$I(x) \frac{d^4 w}{dx^4} + 2 \frac{dI(x)}{dx} \frac{d^3 w}{dx^3} + \frac{d^2 I(x)}{dx^2} \frac{d^2 w}{dx^2} = F(x) \quad (B-13)$$

The fourth-order central-difference quotients needed are

$$D(y_j) = \frac{1}{12h} (y_{j-2} - 8y_{j-1} + 8y_{j+1} - y_{j+2}) + \left(\frac{1}{30} h^4 y_j^{(4)} \right) \quad (B-14)$$

$$D^2(y_j) = \frac{1}{12h^2}(-y_{j-2} + 16y_{j-1} - 30y_j + 16y_{j+1} - y_{j+2}) + \left(\frac{1}{90} h^4 y_j^{VI}\right) \quad (B-15)$$

$$D^3(y_j) = \frac{1}{2h^3}(-y_{j-2} + 2y_{j-1} - 2y_{j+1} + y_{j+2}) + \left(-\frac{1}{4} h^2 y_j^V\right) \quad (B-16)$$

$$D^4(y_j) = \frac{1}{h^4}(y_{j-2} - 4y_{j-1} + 6y_j - 4y_{j+1} + y_{j+2}) + \left(-\frac{1}{6} h^2 y_j^{VI}\right) \quad (B-17)$$

If the moment of inertia $I(x)$ is assumed to be a constant or a linear function then Eq (B-14) simplifies to

$$I(x) \frac{d^4 w}{dx^4} + 2 \frac{dI(x)}{dx} \frac{d^3 w}{dx^3} = \frac{F(x)}{E}$$

Substituting the central-difference expressions for the derivatives gives

$$I(x_{j-1})w_{j-2} - 2[I(x_{j-1}) + I(x_j)]w_{j-1} + [I(x_{j-1}) + 4I(x_j) + I(x_{j+1})]w_j$$

$$- 2[I(x_j) + I(x_{j+1})]w_{j+1} + I(x_{j+2})w_{j+2} = \frac{F(x)h^4}{E}$$

$$j=0, 1, \dots, N$$

where $F(x_j) = P$ (constant) for the uniform load distribution and $F(x_j) = P \sin\left(\frac{\pi x_j}{L}\right)$ for the half-sin load distribution.

The boundary conditions modify the set of system equations as follows:

1. For a clamped end at $x_k=0$, then $w_0=0$ in row 1,

and

$$[2I(x_0)+4I(x_1)+I(x_2)]w_1-2[I(x_1)+I(x_2)]w_2$$

$$+ I(x_2)w_3 = \frac{F(x_1)h^4}{E} \quad \text{in row 2, and}$$

$$-2[I(x_0)+I(x_1)]w_1+[I(x_2)+4I(x_2)+I(x_3)]w_2$$

$$-2[I(x_2)+I(x_3)]w_3+I(x_3)w_4 = \frac{F(x_2)h^4}{E} \quad \text{in row 3}$$

2. For a clamped end at $x_k=L$, then $w_N=0$ in row $N+1$,

and

$$I(x_{N-2})w_{N-3}-2[I(x_{N-2})+I(x_{N-1})]w_{N-2}$$

$$+ [2I(x_N)+4I(x_{N-1})+I(x_{N-2})]w_{N-1} = \frac{F(x_{N-1})h^4}{E} \quad \text{in row N,}$$

and

$$I(x_{N-3})w_{N-4}-2[I(x_{N-2})+I(x_{N-3})]w_{N-3}$$

$$+ [I(x_{N-1})+4I(x_{N-2})+I(x_{N-3})]w_{N-2}-2[I(x_{N-2})$$

$$+ I(x_{N-1})]w_{N-1} = \frac{F(x_{N-2})h^4}{E} \quad \text{in row N-1}$$

3. For a free end at $x_k=L$, then

$$2I(x_{N-1})w_{N-2}-4I(x_{N-1})w_{N-1}+2I(x_N)w_N = \frac{F(x_N)h^4}{E}$$

in row $N+1$, and

$$I(x_{N-2})w_{N-3} - 2[I(x_{N-2}) + (x_{N-1})]w_{N-2}$$

$$+ [I(x_{N-2}) + 4I(x_{N-1})]w_{N-1} - 2I(x_{N-1})w_N \text{ in row } N$$

Sample Problem B-2. A clamped-free uniform beam is subjected to a half-sin transverse load distribution. The beam is discretized with five grid points. After the boundary conditions are applied, the system equations become

$$\begin{bmatrix} 7 & -4 & 1 & 0 & 0 \\ -4 & 6 & -4 & 1 & 0 \\ 1 & -3 & 6 & -4 & 1 \\ 0 & 0 & 2 & -4 & 2 \end{bmatrix} \begin{Bmatrix} w_2 \\ w_3 \\ w_4 \\ w_5 \end{Bmatrix} = \begin{Bmatrix} 0.002762 \\ 0.003906 \\ 0.002762 \\ 0.0 \end{Bmatrix}$$

The approximate solution compared with the exact solution is

$$\begin{array}{c} \text{approximate} \\ \begin{Bmatrix} w_2 \\ w_3 \\ w_4 \\ w_5 \end{Bmatrix} = \frac{PL^4}{IE} \begin{Bmatrix} 0.00943 \\ 0.02829 \\ 0.04991 \\ 0.07154 \end{Bmatrix} \end{array} \quad \begin{array}{c} \text{exact} \\ \begin{Bmatrix} w_2 \\ w_3 \\ w_4 \\ w_5 \end{Bmatrix} = \frac{PL^4}{IE} \begin{Bmatrix} 0.00831 \\ 0.02729 \\ 0.05021 \\ 0.07385 \end{Bmatrix} \end{array}$$

Appendix C
Derivation of Finite Element Equations for the
Axial Rod with Sample Problems

The governing differential equation for the axial rod under the influence of an uniaxially distributed force is given as

$$\frac{d}{dx} \left\{ A(x) E \frac{du(x)}{dx} \right\} = -F(x) \quad (C-1)$$

Discretizing the domain into \bar{E} elements with $\bar{E}+1$ nodes, the solution can be approximated as

$$u(x) = N_j(x) u_j \quad j=1,2,\dots,M$$

where M = number of nodal parameters, and the repeated index implies summation.

The differential equation will not be satisfied exactly. The residual error ϵ is thus defined as

$$\epsilon(x) = \frac{d}{dx} \left\{ A(x) E \frac{dN_j}{dx} u_j \right\} + F(x) \neq 0$$

$$j=1,2,\dots,M \quad (C-2)$$

The method of weighted residuals (Ref 12) forces the residual error to be zero, in some weighted average sense, over the domain Ω . For each method this is achieved by performing the following integrations.

Collocation:

$$I = \int_0^L \epsilon(x) \delta(x-x_i) dx = 0 \quad (C-3)$$

Galerkin:

$$I = \int_0^L \epsilon(x) N_i(x) dx = 0 \quad (C-4)$$

Least Squares:

$$I = \int_0^L \epsilon(x) \frac{\partial \epsilon(x)}{\partial u_i} dx = 0 \quad (C-5)$$

Collocation Method

The evaluation of the integral for the collocation method is carried out by first discretizing the domain into \bar{E} elements, each of length h . The integral is thus:

$$I = \sum_{e=1}^{\bar{E}} \int_{(e-1)h}^{eh} \epsilon(x) \delta(x-x_i) dx = 0 \quad (C-6)$$

This integral can be simplified by using local coordinates \bar{x} , where

$$x = (e-1)h + \bar{x}, \quad \begin{array}{l} 0 \leq \bar{x} \leq h \\ 0 \leq x \leq L \end{array} \quad (C-7)$$

The \bar{E} elemental integrals with this transformation become very similar; that is:

$$I_e = \int_0^h \epsilon(\bar{x}) \delta(\bar{x} - \bar{x}_i) d\bar{x} = 0 \quad (C-8)$$

Substituting Eq (C-2) into Eq (C-8) along with the coordinate transformation gives

$$I_e = \int_0^h \left\{ \frac{d}{d\bar{x}} \left[A(\bar{x}) E \frac{dN_j(\bar{x})}{d\bar{x}} u_i \right] + F(\bar{x}) \right\} \delta(\bar{x} - \bar{x}_i) d\bar{x} = 0$$

$$\begin{aligned} j &= 1, 2, \dots, m \\ i &= 1, 2, \dots, m \end{aligned} \quad (C-9)$$

where $N_j(\bar{x})$ are the local shape functions (tabulated in Appendix D) and m is the number of nodal parameters per element.

Integration of Eq (C-9) gives

$$I_e = \left\{ \frac{d}{d\bar{x}} \left[A(\bar{x}) E \frac{dN_j(\bar{x})}{d\bar{x}} u_j \right] + F(\bar{x}) \right\} \bigg|_{\bar{x}=\bar{x}_i} = 0$$

$$j=1, 2, \dots, m \quad (C-10)$$

Suppose the area $A(\bar{x})$ is assumed to vary linearly in the domain, then it can be expressed as

$$A(\bar{x}) = A \left\{ 1 - \frac{\alpha}{L} [(e-1) + \bar{x}] \right\} \quad (C-11)$$

where

A = area of element at left end ($\bar{x}=0$), and

α = taper ratio ($0 \leq \alpha \leq 1.0$).

Substituting Eq (C-11) into Eq (C-10) and differentiating yields

$$I_e = \left\{ \left\{ 1 - \frac{\alpha}{L}[(e-1)h + \bar{x}] \right\} AE \frac{d^2 N_j}{d\bar{x}^2} u_j - \frac{\alpha}{L} AE \frac{dN_j}{d\bar{x}} u_j + F(\bar{x}) \right\} \bigg|_{\bar{x}=\bar{x}_i} = 0$$

$$\begin{aligned} i &= 1, 2, \dots, m \\ j &= 1, 2, \dots, m \\ e &= 1, 2, \dots, \bar{E} \end{aligned} \quad (C-12)$$

where N_j must be such that $\frac{d^2 N_j}{d\bar{x}^2}$ is non-zero. In this thesis N_j is chosen to be the cubic shape functions associated with the C^1 line element (see Table E-I). For this class of functions there are four nodal parameters per element (m equals four). With cubic shape functions (Eq (C-12)) can be written for element e as

$$K_{ij} u_j + F_i = 0 \quad \begin{aligned} i &= 1, \dots, 4 \\ j &= 1, \dots, 4 \\ e &= 1, \dots, \bar{E} \end{aligned} \quad (C-13)$$

where

K_{ij} = elemental stiffness matrix,

u_j = vector of element nodal parameters, and

F_i = vector of element equivalent forces.

In the local coordinate system, the elemental stiffness matrix has elements of the form

$$K_{i1} = \frac{AE}{h^2} \left\{ 1 - \frac{\alpha}{L} \left[(e-1)h + \bar{x}_i \right] \right\} \left[-6 + 12 \frac{\bar{x}_i}{h} \right] - \frac{\alpha AE}{Lh} \left[-6 \frac{\bar{x}_i}{h} + 6 \left(\frac{\bar{x}_i}{h} \right)^2 \right]$$

$$K_{i2} = \frac{AE}{h} \left\{ 1 - \frac{\alpha}{L} \left[(e-1)h + \bar{x}_i \right] \right\} \left[-4 + 6 \frac{\bar{x}_i}{h} \right] - \frac{\alpha AE}{L} \left[1 - 4 \frac{\bar{x}_i}{h} + 3 \left(\frac{\bar{x}_i}{h} \right)^2 \right] \quad (C-14)$$

$$K_{i3} = -K_{i1}$$

$$K_{i4} = \frac{AE}{h} \left\{ 1 - \frac{\alpha}{L} \left[(e-1)h + \bar{x}_i \right] \right\} \left[-2 + 6 \frac{\bar{x}_i}{h} \right] - \frac{\alpha AE}{L} \left[-2 \frac{\bar{x}_i}{h} + 3 \left(\frac{\bar{x}_i}{h} \right)^2 \right]$$

where $i=1,2,3,4$ and the \bar{x}_i have been chosen as the equally spaced points $\bar{x}_i = [0, \frac{h}{3}, \frac{2h}{3}, h]$.

The choice of equally spaced points over Gaussian points was due to the conclusion of Houstis (Ref 5:327) "that equally spaced points give slightly better accuracy for rectangular domains." Theoretically the Gauss points give better results according to Prenter (Ref 10:304-314). He showed that "collocation at Gaussian points using a basis of piecewise cubic Hermite polynomials gives an order h^4 algorithm for approximating the unique solution $x(t)$ to the equation

$$-x''(t) + \sigma(t)x(t) = f(t) \quad a \leq t \leq b$$

$$x(a) = x(b) = 0$$

For a uniform rod the taper ratio α equals zero.
This greatly simplifies the stiffness matrix.

Thus:

$$[K] = \frac{AE}{h} \begin{bmatrix} 6 & -4h & 6 & -2h \\ -2 & -2h & 2 & 0 \\ 2 & 0 & -2 & 2h \\ 6 & 2h & -6 & 4h \end{bmatrix} \quad (C-15)$$

In the local coordinate system, the local nodal unknowns are related to the global unknowns as follows:

$$\begin{array}{c} \text{local} \\ \left\{ \begin{array}{c} u_1 \\ u_2 \\ u_3 \\ u_4 \end{array} \right\} = \left\{ \begin{array}{c} u(0) \\ \frac{du}{dx}(0) \\ u(h) \\ \frac{du}{dx}(h) \end{array} \right\} = \begin{array}{c} \text{global} \\ \left\{ \begin{array}{c} u_{e-1} \\ u_e \\ u_{e+1} \\ u_{e+2} \end{array} \right\} = \left\{ \begin{array}{c} u((e-1)h) \\ \frac{du}{dx}((e-1)h) \\ u(eh) \\ \frac{du}{dx}(eh) \end{array} \right\} \end{array} \quad (C-16)$$

The local and global force vectors are related in the same manner.

$$\begin{array}{c} \text{local} \\ \left\{ \begin{array}{c} F_1 \\ F_2 \\ F_3 \\ F_4 \end{array} \right\} = \left\{ \begin{array}{c} F(0) \\ F(\frac{h}{3}) \\ F(\frac{2h}{3}) \\ F(h) \end{array} \right\} = \begin{array}{c} \text{global} \\ \left\{ \begin{array}{c} F_{e-1} \\ F_e \\ F_{e+1} \\ F_{e+2} \end{array} \right\} = \left\{ \begin{array}{c} F((e-1)h) \\ F((e-1)h+h/3) \\ F((e-1)h+2h/3) \\ F(eh) \end{array} \right\} \end{array} \quad (C-17)$$

where $F(x) = F(\bar{x}) = P$ (constant) for the case of uniform load; and $F(x) = P \sin \left(\frac{\pi x}{L} \right)$ for the case of a half-sin load distribution.

When elements are connected together the shape functions chosen guarantee continuity of the function and its first derivative in the interval $(0, L)$. Therefore, when forming the global equations, the local equations are added so that their local nodal parameters coincide with the appropriate global parameters as defined in Eq (C-16).

Sample Problem C-1. A clamped-free uniform rod with a half-sin load distribution is discretized with two C^1 line elements. The nodal parameters are as illustrated in Fig C-1.

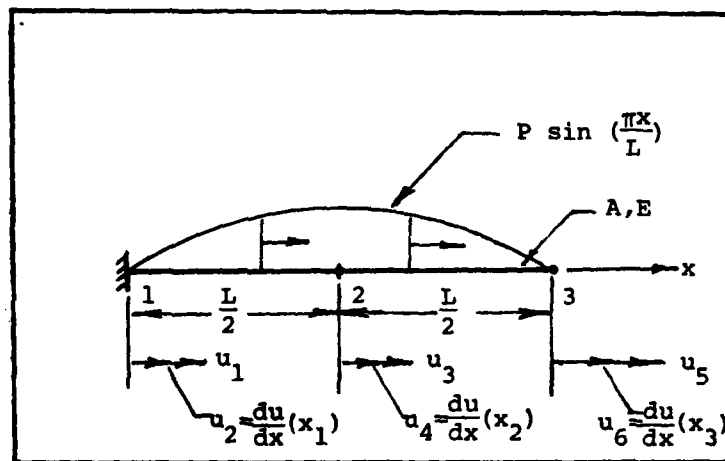


Fig C-1. Global Illustration of a Clamped-Free Uniform Rod Approximated by Two C^1 Line-Elements with a Half-Sin Load Distribution

The unreduced global equations are

$$\frac{AE}{(\frac{L}{2})^2} \begin{bmatrix} 6 & -2L & 6 & -L & 0 & 0 \\ -2 & -L & 2 & 0 & 0 & 0 \\ 2 & 0 & 4 & -L & 6 & -L \\ 6 & L & -8 & L & 2 & 0 \\ 0 & 0 & 2 & 0 & -2 & L \\ 0 & 0 & 6 & L & -6 & 2L \end{bmatrix} \begin{Bmatrix} u_1 \\ u_2 \\ u_3 \\ u_4 \\ u_5 \\ u_6 \end{Bmatrix} = P \begin{Bmatrix} \sin(0) + 0 \\ \sin(\frac{\pi}{6}) + 0 \\ \sin(\frac{\pi}{3}) + \sin(\frac{\pi}{2}) \\ \sin(\frac{\pi}{2}) + \sin(\frac{2\pi}{3}) \\ 0 + \sin(\frac{5\pi}{6}) \\ 0 + \sin(\pi) \end{Bmatrix}$$

These equations can be reduced by using the boundary conditions. At the left end, the displacement u_1 is zero; and at the right end, the axial force $AE u_6$ is zero. Therefore rows one and six and the corresponding columns can be eliminated from the system of equations. The result is

$$\frac{4AE}{L^2} \begin{bmatrix} -L & 2 & 0 & 0 \\ 0 & 4 & -L & 6 \\ L & -8 & L & 2 \\ 0 & 2 & 0 & -2 \end{bmatrix} \begin{Bmatrix} u_2 \\ u_3 \\ u_4 \\ u_5 \end{Bmatrix} = P \begin{Bmatrix} .5 \\ 1.866 \\ 1.866 \\ .5 \end{Bmatrix}$$

The approximate solution compared with the exact is

approximate

exact

$$\begin{Bmatrix} u_2 \\ u_3 \\ u_4 \\ u_5 \end{Bmatrix} = \frac{PL^2}{AE} \begin{Bmatrix} .6443 \\ .2597 \\ .3222 \\ .3222 \end{Bmatrix} ; \quad \begin{Bmatrix} u_2 \\ u_3 \\ u_4 \\ u_5 \end{Bmatrix} = \frac{PL^2}{AE} \begin{Bmatrix} .6366 \\ .2605 \\ .3183 \\ .3183 \end{Bmatrix}$$

Galerkin Method

Galerkin's Method is expressed by Eq (C-4). That is:

$$I = \int_0^L \left\{ \frac{d}{dx} \left[A(x) E \frac{du(x)}{dx} \right] + F(x) \right\} N_i dx = 0$$

$i=1,2,\dots,M$

Integration by parts of the first term

$$I = - \int_0^L A(x) E \frac{dN_i}{dx} \frac{dN_j}{dx} u_j dx + A(x) E \frac{du}{dx} N_i \Big|_0^L + \int_0^L F(x) N_i dx = 0$$

$i=1,2,\dots,M$
 $j=1,2,\dots,M$ (C-18)

The boundary term $A(x) E \frac{du}{dx} N_i \Big|_0^L$ vanishes for both cases of

boundary conditions studied in this thesis. Therefore

Eq (C-18) becomes

$$I = \int_0^L A(x) E \frac{dN_i}{dx} \frac{dN_j}{dx} dx u_j - \int_0^L F(x) N_i dx = 0$$

$i=1,2,\dots,M$
 $j=1,2,\dots,M$

Since the domain is discretized into \bar{E} elements the integral I can be written as

$$I = \sum_{e=1}^{\bar{E}} I_e = \sum_{e=1}^{\bar{E}} \int_{(e-1)h}^{eh} \left\{ A(x) E \frac{dN_i}{dx} \frac{dN_j}{dx} u_j - F(x) N_i \right\} dx = 0$$

$$\begin{aligned} i &= 1, 2, \dots, m \\ j &= 1, 2, \dots, m \end{aligned} \quad (C-19)$$

For these integrals to exist the shape functions N_i must be at least C^0 continuous. They are chosen in this study to be the linear shape functions associated with the C^0 line element described in Appendix E. For the Galerkin method Eq (C-11) is more conveniently expressed as

$$A(\bar{x}) = (1 - \frac{\bar{x}}{h}) A_L + (\frac{\bar{x}}{h}) A_R \quad (C-20)$$

where

$$A_L = A \left[1 - \frac{\alpha(e-1)h}{L} \right]$$

$$A_R = A \left[1 - \frac{\alpha eh}{L} \right]$$

Equation (C-7) can be used to transform Eq (E-19) to a local coordinate system. With the substitution of Eq (C-20) the element integral I_e becomes

$$I_e = \int_0^h \left\{ (1 - \frac{\bar{x}}{h}) A_L + (\frac{\bar{x}}{h}) A_R \right\} E \begin{bmatrix} 1 & -1 \\ -1 & 1 \end{bmatrix} \begin{Bmatrix} u_e \\ u_{e+1} \end{Bmatrix} d\bar{x} - \int_0^h F(\bar{x}) \begin{Bmatrix} 1 - \frac{\bar{x}}{h} \\ \frac{\bar{x}}{h} \end{Bmatrix} d\bar{x} = 0$$

$$e=1, 2, \dots, \bar{E} \quad (C-21)$$

where $F(\bar{x}) = P$ (constant) for the uniform load distribution; and $F(\bar{x}) = P \sin \left(\frac{\pi}{L}[e-1]h + \bar{x} \right)$ for the half-sin load distribution. For the half-sin load distribution Eq (C-21) becomes

$$I_e = \frac{(A_L + A_R)E}{2h} \begin{bmatrix} 1 & -1 \\ -1 & 1 \end{bmatrix} \begin{Bmatrix} u_e \\ u_{e+1} \end{Bmatrix} + \frac{PL\bar{E}}{\pi^2} \left(\sin \frac{\pi e}{\bar{E}} - \sin \frac{\pi(e-1)}{\bar{E}} \right) \begin{Bmatrix} 1 \\ -1 \end{Bmatrix} + \frac{PL}{\pi} \begin{Bmatrix} -\cos \frac{\pi(e-1)}{\bar{E}} \\ \cos \frac{\pi e}{\bar{E}} \end{Bmatrix} = \begin{Bmatrix} 0 \\ 0 \end{Bmatrix}$$

$e=1, 2, \dots, \bar{E} \quad (C-22)$

For the uniform load case and constant area A, Eq (C-21) becomes

$$I_e = \frac{AE}{h} \begin{bmatrix} 1 & -1 \\ -1 & 1 \end{bmatrix} \begin{Bmatrix} u_e \\ u_{e+1} \end{Bmatrix} - \frac{Ph}{2} \begin{Bmatrix} 1 \\ 1 \end{Bmatrix} = \begin{Bmatrix} 0 \\ 0 \end{Bmatrix}$$

$e=1, 2, \dots, \bar{E} \quad (C-23)$

These equations are identical to the equations for the standard finite difference method detailed in Appendix B.

Sample Problem C-2. A constant area clamped-free axial rod is loaded with a half-sin distribution of uni-axial force. This problem is approximated with two C^0 line elements as shown in Fig C-2.

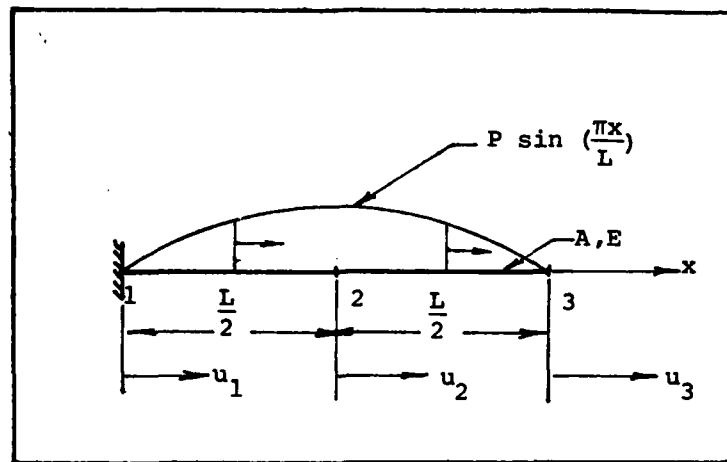


Fig C-2. Global Illustration of a Clamped-Free Uniform Rod Approximated by Two C^0 Line Elements with a Half-Sin Load Distribution

The assembled global equations are

$$\frac{2AE}{L} \begin{bmatrix} 1 & -1 & 0 \\ -1 & 2 & -1 \\ 0 & -1 & 1 \end{bmatrix} \begin{Bmatrix} u_1 \\ u_2 \\ u_3 \end{Bmatrix} = \frac{2PL}{\pi^2} \begin{Bmatrix} -1 + 0 \\ 1 + 1 \\ 0 - 1 \end{Bmatrix} + \frac{PL}{\pi} \begin{Bmatrix} 1 + 0 \\ 0 + 0 \\ 0 + 1 \end{Bmatrix}$$

Since $u_1=0$ by virtue of the boundary conditions the equation reduces to

$$\frac{2AE}{L} \begin{bmatrix} 2 & -1 \\ -1 & 1 \end{bmatrix} \begin{Bmatrix} u_2 \\ u_3 \end{Bmatrix} = PL \begin{Bmatrix} .40528 \\ .11567 \end{Bmatrix}$$

The solution is

$$\begin{Bmatrix} u_2 \\ u_3 \end{Bmatrix} = \frac{PL}{AE} \begin{Bmatrix} .2605 \\ .3183 \end{Bmatrix}$$

which matches the exact solution.

Least Squares Method

The least squares technique of forming finite element equations relies on the evaluation of Eq (C-5). Substituting Eq (C-2) into Eq (C-5) yields

$$I = \int_0^L \left\{ \frac{d}{dx} \left[A(x) E \frac{dN_j}{dx} u_j \right] + F(x) \right\} \frac{d}{dx} \left[A(x) E \frac{dN_i}{dx} \right] dx = 0$$

$i=1,2,\dots,M$
 $j=1,2,\dots,M$ (C-24)

Multiplying and differentiating terms in the integrand gives

$$I = E^2 \int_0^L \left\{ A^2(x) \frac{d^2 N_i}{dx^2} \frac{d^2 N_j}{dx^2} + 2 \frac{dA(x)}{dx} \frac{dN_i}{dx} \frac{dN_j}{dx} \right\} dx u_j$$

$$+ E \int_0^L F(x) \left\{ A(x) \frac{d^2 N_i}{dx^2} + \frac{dA(x)}{dx} \frac{dN_i}{dx} \right\} dx = 0$$

$i=1,2,\dots,M$
 $j=1,2,\dots,M$ (C-25)

This integral can be written as the sum of the elemental integrals in a local coordinate system. The transformation from global to local is given by Eq (C-7). The global shape functions N_i could also be transformed, but the linear shape functions of Table E-1 have all the required properties of the local shape functions desired. To simplify the algebra the derivatives of the shape functions

are written as

$$\frac{dN_i}{d\bar{x}} = h \left[\alpha_i + A_i \left(\frac{\bar{x}}{h} \right) + \frac{B_i}{2} \left(\frac{\bar{x}}{h} \right)^2 \right] \quad i=1,2,\dots,4$$

$$\frac{d^2N_i}{d\bar{x}^2} = A_i + B_i \left(\frac{\bar{x}}{h} \right) \quad i=1,2,\dots,4$$

where

$$\alpha_i = [0, \frac{1}{h}, 0, 0]$$

$$A_i = \frac{1}{h^2} [-6, -4h, 6, -2h]$$

$$B_i = \frac{1}{h^2} [12, 6h, -12, 6h]$$

The final result after integrating the polynomial terms with $F(x) = P$ (constant) can be written for element e in the form

$$I_e = K_{ij} u_j + F_i = 0 \quad \begin{array}{l} i=1,2,\dots,4 \\ j=1,2,\dots,4 \\ e=1,2,\dots,\bar{E} \end{array} \quad (C-26)$$

where

$$\begin{aligned} K_{ij} = E \{ & \alpha_i \alpha_j [A_L^2 - 2A_L A_R + A_R^2] \\ & + (\alpha_i A_j + A_i \alpha_j) [-A_L A_R + A_R^2] \\ & + (\alpha_i B_j + B_i \alpha_j) [-\frac{1}{2} A_L A_R + \frac{1}{2} A_R^2] \\ & + A_i A_j [\frac{1}{60} (20A_L^2 - 40 A_L A_R + 80A_R^2)] \end{aligned}$$

$$+(A_i B_j + B_i A_j) \left[\frac{1}{60} (5A_L^2 - 20A_L A_R + 45A_R^2) \right]$$

$$+B_i B_j \left[\frac{1}{60} (2A_L^2 - 9A_L A_R + 27A_R^2) \right] \}$$

$$i=1,2,3,4$$

$$j=1,2,3,4$$

$$F_i = P [\alpha_i (A_R - A_L) + (A_i + \frac{1}{2} B_i) A_R]$$

and

$$u_j = \begin{Bmatrix} u_{e-1} \\ u_e \\ u_{e+1} \\ u_{e+2} \end{Bmatrix} = \begin{Bmatrix} u \frac{\pi(e-1)}{\bar{E}} \\ \frac{du}{dx} \frac{\pi(e-1)}{\bar{E}} \\ u \frac{\pi e}{\bar{E}} \\ \frac{du}{dx} \frac{\pi e}{\bar{E}} \end{Bmatrix}$$

For a uniform rod the elemental stiffness matrix K_{ij} is simplified considerably due to the fact that $\frac{dA(x)}{dx} = 0$.

Thus Eq (C-26) has the following terms for a half-sin load distribution:

$$K_{ij} = \frac{A^2 E}{h^3} \begin{bmatrix} 12 & 4h & -12 & 6h \\ 6h & 4h^2 & -6h & 2h^2 \\ -12 & -6h & 12 & -6h \\ 6h & 2h^2 & -6h & 4h^2 \end{bmatrix}$$

$$F_i = \frac{PA\bar{E}}{\pi} \left\{ \begin{array}{l} -\frac{6}{h} (CL + CO) + \frac{12\bar{E}}{\pi h} (SL - SO) \\ -2 (CL + 2CO) + \frac{6\bar{E}}{\pi} (SL - SO) \\ \frac{6}{h} (CL + CO) - \frac{12\bar{E}}{\pi h} (SL - SO) \\ -2 (2CL + CO) + \frac{6\bar{E}}{\pi} (SL - SO) \end{array} \right\}$$

where

$$CL = \cos \frac{\pi e}{\bar{E}}, \quad CO = \cos \frac{\pi (e-1)}{\bar{E}},$$

$$SL = \sin \frac{\pi e}{\bar{E}}, \quad SO = \sin \frac{\pi (e-1)}{\bar{E}}$$

Sample Problem C-3. A uniform clamped-free rod is subjected to a half-sin distribution of uniaxial tension. This problem is discretized into two elements as illustrated in Fig C-1. The reduced global equations as formed by the least squares technique are

$$\frac{8AE}{L^3} \begin{bmatrix} 4h^2 & -6h & 2h^2 & 0 \\ -6h & 24 & 0 & -12 \\ 2h^2 & 0 & 8h^2 & -6h \\ 0 & -12 & -6h & 12 \end{bmatrix} \begin{Bmatrix} u_2 \\ u_3 \\ u_4 \\ u_5 \end{Bmatrix} = P \begin{Bmatrix} .11 + 0 \\ 2.1 + 2.1 \\ -1.2 + 1.2 \\ 0 - 2.1 \end{Bmatrix}$$

The solution to these equations is

$$\begin{Bmatrix} u_2 \\ u_3 \\ u_4 \\ u_5 \end{Bmatrix} = \frac{PL^2}{AE} \begin{Bmatrix} .6366 \\ .2605 \\ .3183 \\ .3183 \end{Bmatrix}$$

which agrees with the exact solution.

Appendix D
Derivation of Finite Element Equations
for the Beam in Bending

A beam in bending has a fourth-order linear differential equation governing its transverse displacement. The equation is

$$\frac{d^2}{dx^2} \left\{ I(x) E \frac{d^2 w(x)}{dx^2} \right\} = F(x) \quad (D-1)$$

If $w(x)$ is approximated by $w(x) = N_j(x) W_j$; where $j=1,2,\dots,M$; the residual error in the discretized domain will be of the form

$$\epsilon(x) = \frac{d^2}{dx^2} \left\{ I(x) E \frac{d^2 N_j}{dx^2} \right\} W_j - F(x) \neq 0$$

$i=1,2,\dots,M \quad (D-2)$

The method of weighted residuals is also used for this problem to derive the finite element equations. The integral equations associated with each of the following finite element techniques are repeated here for convenience.

Collocation:

$$I = \int_0^L \epsilon(x) \delta(x-x_i) dx = 0 \quad (C-3)$$

Galerkin:

$$I = \int_0^L \epsilon(x) N_i(x) dx = 0 \quad (C-4)$$

Least Squares:

$$I = \int_0^L \epsilon(x) \frac{\partial \epsilon(x)}{\partial w_i} dx = 0 \quad (C-5)$$

Collocation

Substituting Eq (D-2) into Eq (C-3) yields

$$I = \int_0^L \left\{ E \left[I(x) \frac{d^4 N_j}{dx^4} + 2 \frac{dI(x)}{dx} \frac{d^3 N_j}{dx^3} + \frac{d^2 I(x)}{dx^2} \frac{d^2 N_j}{dx^2} \right] w_j - F(x) \right\} \delta(x-x_i) dx = 0$$

$j=1,2,\dots,M \quad (D-3)$

The transformation from a global coordinate system to a local coordinate system is identical to that for the axial rod as detailed in Appendix C. In this study the moment of inertia $I(x)$ was assumed to be either constant or linear. That is:

$$I(x) = I(1 - \alpha \frac{x}{L}) \quad (0 \leq \alpha \leq 1.0) \quad (D-4)$$

Therefore

$$\frac{dI(x)}{dx} = - \frac{\alpha}{L}$$

and $\frac{d^2 I(x)}{dx^2} = 0$ for all x

Thus the integrated I_e associated with element e becomes

$$I_e = \left\{ \left\{ 1 - \frac{\alpha}{L} [(e-1)h + \bar{x}] \right\} IE \frac{d^4 N_j}{d\bar{x}^4} w_j - \frac{\alpha}{L} IE \frac{d^3 N_j}{d\bar{x}^3} w_j - F(\bar{x}) \right\} \bigg|_{\bar{x}=\bar{x}_i} = 0$$

$$i=1,2,\dots,m$$

$$j=1,2,\dots,m$$

$$e=1,2,\dots,\bar{E} \quad (D-5)$$

where the local shape functions N_j must now be such that

$\frac{d^4 N_j}{d\bar{x}^4}$ is non-zero. The functions chosen are the septic shape functions ($m=8$) for a C^3 line element. (See Appendix E.) The elemental equation for element e can be written in the form

$$I_e = K_{ij} w_j - F_i = 0 \quad (D-6)$$

where K_{ij} is defined for section as $K_{ij}^{(4)} + K_{ij}^{(3)}$; $K_{ij}^{(4)}$

is the part of the stiffness matrix associated with the

$\frac{d^4 N_j}{d\bar{x}^4}$ terms; and $K_{ij}^{(3)}$ is the part associated with the

$\frac{d^3 N_j}{d\bar{x}^3}$ terms.

Let $I_i = \left\{ 1 - \frac{\alpha}{L} [(e-1)h + \bar{x}_i] \right\}$ and $x = \frac{\bar{x}}{h}$, then:

$$K_{i1}^{(4)} = \frac{I_i E}{h^4} [-840 + 10080x - 25200x^2 + 16800x^3]$$

$$K_{i2}^{(4)} = \frac{I_i E}{h^3} [-480 + 5900x - 12960x^2 + 8400x^3]$$

$$K_{i3}^{(4)} = \frac{I_i E}{h^2} [-120 + 1200x - 2700x^2 + 1680x^3]$$

$$K_{i4}^{(4)} = \frac{I_i E}{h} [-16 + 120x - 240x^2 + 140x^3]$$

(D-7)

$$K_{i5}^{(4)} = \frac{I_i E}{h^4} [840 - 10080x + 25200x^2 - 16800x^3]$$

$$K_{i6}^{(4)} = \frac{I_i E}{h^3} [-360 + 4680x - 12240x^2 + 8400x^3]$$

$$K_{i7}^{(4)} = \frac{I_i E}{h^2} [60 - 840x + 2340x^2 - 1680x^3]$$

$$K_{i8}^{(4)} = \frac{I_i E}{h} [-4 + 60x - 180x^2 + 140x^3]$$

and

$$K_{i1}^{(3)} = -\frac{2\alpha x E}{h^2} [-840 + 5040x - 8400x^2 + 4200x^3]$$

$$K_{i2}^{(3)} = -\frac{2\alpha x E}{h} [-480 + 2700x - 4320x^2 + 2100x^3]$$

$$K_{i3}^{(3)} = -2\alpha x E [-120 + 600x - 900x^2 + 420x^3]$$

$$K_{i4}^{(3)} = -2\alpha x E h [-16 + 60x - 80x^2 + 35x^3] - 3\alpha E h$$

$$K_{i5}^{(3)} = -\frac{2\alpha x E}{h^2} [840 - 5040x + 8400x^2 - 4200x^3] \quad (D-8)$$

$$K_{i6}^{(s)} = - \frac{2\alpha x E}{h} [-360 + 2340x - 4060x^2 + 2100x^3]$$

$$K_{i7}^{(s)} = - 2\alpha x E [60 - 420x + 780x^2 - 420x^3]$$

$$K_{i8}^{(s)} = - 2\alpha x E h [-4 + 30x - 60x^2 + 35x^3]$$

The force vector F_i is given by $F_i = P$ (constant), $i=1,2,\dots,8$, for the uniform load distribution, and $F_i = P \sin \left\{ \frac{\pi}{L} (e-1)h + \bar{x}_i \right\}$ for the half-sin load distribution. As with the axial rod, the collocation points \bar{x}_i have been chosen as the equally spaced points; $x_i = \frac{(i-1)}{7} h$, $i=1,2,\dots,8$.

Galerkin

For the Galerkin method Eq (D-2) is substituted into Eq (C-4) and the stiffness term is integrated by parts twice. The result is:

$$\begin{aligned} I = \int_0^L (EI(x) \frac{d^2 N_j}{dx^2} \frac{d^2 N_i}{dx^2} w_j dx - EI(x) \frac{d^2 w}{dx^2} \frac{dN_i}{dx} \Big|_0^L \\ + \frac{d}{dx} (EI(x) \frac{d^2 w}{dx^2}) N_i \Big|_0^L - \int_0^L F(x) N_i dx = 0 \end{aligned}$$

$i=1,2,\dots,M$
 $j=1,2,\dots,M$ (D-9)

The two boundary terms

$$EI(x) \frac{d^2 w}{dx^2} \frac{dN_i}{dx} \Big|_0^L$$

and

$$EI(x) \frac{d^3 w}{dx^3} + E \frac{DI(x)}{dx} \frac{d^2 w}{dx^2} N_i \Big|_0^L$$

both vanish for the boundary conditions studied. The following conditions give this result. Since the cubic shape functions N_i satisfy the clamped end geometric boundary conditions ($w = \frac{dw}{dx} = 0$), the boundary terms vanish for clamped ends. The boundary conditions for a free right end are

$$I(x)E \frac{d^2 w}{dx^2} \Big|_{x=L} = I(x)E \frac{d^3 w}{dx^3} \Big|_{x=L} = 0$$

These conditions correspond to zero moment and zero shear force respectively. Therefore if the right end is free the boundary terms again vanish. Equation (D-9) is thus simplified; and if the same coordinate transformation is performed as for the axial rod, the result for element e can be written in the form of Eq (D-6) where

$$K_{ij} = \frac{(I_L + I_R)E}{2h^3} \begin{bmatrix} 12 & 2h & -12 & 6h \\ 6h & 4h^2 & -6h & 2h^2 \\ -12 & -6h & 12 & -6h \\ 6h & 2h^2 & -6h & 4h^2 \end{bmatrix} \quad (D-10)$$

and for the uniform load distribution $F(x) = P$ (constant)

$$F_i = P \begin{Bmatrix} h/2 \\ h^2/6 \\ h/2 \\ -h^2/6 \end{Bmatrix} \quad (D-11)$$

The half-sin load distribution $F(x) = P \sin \left(\frac{\pi x}{L} \right)$ gives an equivalent force vector of

$$F_i = \frac{PL}{\pi} \left\{ \begin{array}{l} 6 \left(\frac{\bar{E}}{\pi} \right)^2 (CL+CO) + CO + 12 \left(\frac{\bar{E}}{\pi} \right)^3 (SL-SO) \\ 2 \left(\frac{\bar{E}}{\pi} \right)^2 h (CL+CO) + 6 \frac{L\bar{E}^2}{\pi^3} (SO-SL) - \frac{L}{\pi} SO \\ 6 \left(\frac{\bar{E}}{\pi} \right)^2 (CL+CO) - CL + 12 \left(\frac{\bar{E}}{\pi} \right)^3 (SL-SO) \\ 2 \left(\frac{\bar{E}}{\pi} \right)^2 h (2CL+CO) + 6 \frac{L\bar{E}^2}{\pi^3} (SO-SL) + \frac{L}{\pi} SL \end{array} \right\} \quad (D-12)$$

where

$$CL = \cos \frac{\pi e}{\bar{E}}, \quad SL = \sin \frac{\pi e}{\bar{E}}$$

$$CO = \cos \frac{\pi(e-1)}{\bar{E}}, \quad SO = \sin \frac{\pi(e-1)}{\bar{E}}$$

Least Squares

For the least squares method Eq (D-2) is substituted into Eq (C-5) and the result is:

$$I = \int_0^L \left\{ \left[EI(x) \frac{d^4 N_j}{dx^4} + E \frac{dI(x)}{dx} \frac{d^3 N_j}{dx^3} + E \frac{d^2 I(x)}{dx^2} \frac{d^2 N_j}{dx^2} \right] w_j \right. \\ \left. - F(x) \left\{ EI(x) \frac{d^4 N_i}{dx^4} + E \frac{dI(x)}{dx} \frac{d^3 N_i}{dx^3} + E \frac{d^2 I(x)}{dx^2} \frac{d^2 N_i}{dx^2} \right\} \right\} dx = 0 \quad (D-13)$$

Since $I(x) = I(1 - \alpha \frac{x}{L})$, $\frac{d^2 I(x)}{dx^2} = 0$

If Eq (D-13) is written in local coordinates for a domain that is discretized into \bar{E} elements, the integral for element e is

$$I_e = \int_0^h \left\{ \left[EI(\bar{x}) \frac{d^4 N_j}{d\bar{x}^4} + E \frac{dI(\bar{x})}{d\bar{x}} \frac{d^3 N_j}{d\bar{x}^3} \right] w_j - F(\bar{x}) \right\} \left\{ EI(\bar{x}) \frac{d^4 N_i}{d\bar{x}^4} + E \frac{dI(\bar{x})}{d\bar{x}} \frac{d^3 N_i}{d\bar{x}^3} \right\} d\bar{x} = 0$$

$$i=1,2,\dots,m$$

$$j=1,2,\dots,m$$

$$e=1,2,\dots,\bar{E} \quad (D-14)$$

For this method the septic shape functions are chosen (see Appendix E), and let

$$\frac{d^3 N_j}{d\bar{x}^3} = \alpha_i + hx \left[A_i + \frac{x}{2} B_i + \frac{x^2}{3} C_i + \frac{x^3}{4} D_i \right]$$

$$\frac{d^4 N_j}{d\bar{x}^4} = A_i + B_i x + C_i x^2 + D_i x^3 \quad (D-15)$$

where $x = \frac{\bar{x}}{h}$, and

$$\alpha_i = [0, 0, 0, 1, 0, 0, 0, 0]$$

$$A_i = \frac{1}{h^4} [-840, -480h, -120h^2, -16h^3, 840, -360h, 60h^2, -4h^3]$$

$$B_i = \frac{1}{h^4} [10080, 5400h, 1200h^2, 120h^3, -10080, 4680h, -840h^2, 60h^3]$$

$$C_i = \frac{1}{h^4} [-25200, -12960h, -2700h^2, -240h^3, 25200, -12240h, 2340h^2, -180h^3]$$

$$D_i = \frac{1}{h^4} [16800, 8400h, 1680h^2, 140h^3, -16800, 8400h, -1680h^2, 140h^3]$$

$$\text{Let } I(\bar{x}) = I_L (1 - \frac{\bar{x}}{h}) + I_R (\frac{\bar{x}}{h})$$

Then Eq (D-14) can be written in the form of Eq (D-6)

where

$$\begin{aligned} K_{ij} = Eh \{ & 8(I_L^2 - 2I_L I_R + I_R^2) \alpha_i \alpha_j \\ & + (I_L^2 - 4I_L I_R + I_R^2) (\alpha_i A_j + A_i \alpha_j) \\ & + \frac{1}{3} (I_L^2 - 5I_L I_R + 4I_R^2) (\alpha_i B_j + B_i \alpha_j) \\ & + \frac{1}{6} (I_L^2 - 6I_L I_R + 5I_R^2) (\alpha_i C_j + C_i \alpha_j) \\ & + \frac{1}{10} (I_L^2 - 7I_L I_R + 6I_R^2) (\alpha_i D_j + D_i \alpha_j) \\ & + (I_L^2 - 3I_L I_R + 3I_R^2) A_i A_j \\ & + (\frac{2}{15} I_L^2 - \frac{3}{5} I_L I_R + \frac{4}{5} I_R^2) B_i B_j \\ & + (\frac{13}{315} I_L^2 - \frac{5}{21} I_L I_R + \frac{25}{63} I_R^2) C_i C_j \\ & + (\frac{1}{56} I_L^2 - \frac{1}{8} I_L I_R + \frac{1}{4} I_R^2) D_i D_j \\ & + (\frac{1}{3} I_L^2 - \frac{4}{3} I_L I_R + \frac{3}{2} I_R^2) (A_i B_j + B_i A_j) \\ & + (\frac{1}{6} I_L^2 - \frac{5}{6} I_L I_R + I_R^2) (A_i C_j + C_i A_j) \end{aligned}$$

$$\begin{aligned}
& + \left(\frac{1}{10} I_L^2 - \frac{3}{5} I_L I_R + \frac{3}{4} I_R^2 \right) (A_i D_j + D_i A_j) \\
& + \left(\frac{13}{180} I_L^2 - \frac{17}{45} I_L I_R + \frac{5}{9} I_R^2 \right) (B_i C_j + C_i B_j) \\
& + \left(\frac{19}{420} I_L^2 - \frac{23}{84} I_L I_R + \frac{3}{7} I_R^2 \right) (B_i D_j + D_i B_j) \\
& + \left(\frac{3}{112} I_L^2 - \frac{29}{168} I_L I_R + \frac{5}{16} I_R^2 \right) (C_i D_j + D_i C_j) \} \\
& \qquad \qquad \qquad i=1,2,\dots,8 \\
& \qquad \qquad \qquad j=1,2,\dots,8 \\
& \qquad \qquad \qquad e=1,2,\dots,\bar{E} \quad (D-16)
\end{aligned}$$

The force vector for the uniform load case $F(x) = P$ is given by

$$\begin{aligned}
F_i = Ph \left\{ (I_R - I_L) 2\alpha_i + (3I_R - I_L) \frac{A_i}{2} \right. \\
\left. + (4I_R - I_L) \frac{B_i}{6} + (5I_R - I_L) \frac{C_i}{12} + (6I_R - I_L) \frac{D_i}{20} \right\} \\
\qquad \qquad \qquad i=1,2,\dots,8 \\
\qquad \qquad \qquad e=1,2,\dots,\bar{E} \quad (D-17)
\end{aligned}$$

The uniform beam has $I_L = I_R = I$ and $\alpha = 0$; therefore Eq (D-16) reduces to

$$\begin{aligned}
K_{ij} = EI^2 h \left\{ A_i B_j + \frac{1}{2} (A_i B_j + B_i A_j) + \frac{1}{3} (B_i B_j + A_i C_j + C_i A_j) \right. \\
+ \frac{1}{4} (B_i C_j + C_i B_j + A_i D_j + D_i A_j) + \frac{1}{5} (C_i C_j + B_i D_j + D_i B_j) \\
\left. + \frac{1}{6} (C_i D_j + D_i C_j) + \frac{1}{7} D_i D_j \right\} \\
\qquad \qquad \qquad i=1,2,\dots,8 \\
\qquad \qquad \qquad j=1,2,\dots,8 \\
\qquad \qquad \qquad e=1,2,\dots,\bar{E} \quad (D-18)
\end{aligned}$$

and Eq (D-17) reduces to

$$F_i = PIh \left\{ A_i + \frac{1}{2} B_i + \frac{1}{3} C_i + \frac{1}{4} D_i \right\} \quad (D-19)$$

Substituting the appropriate constants in Eqs (D-18) and (D-19) gives the result for I_e shown in Eq (D-20). The half-sin load distribution results in an equivalent force vector which was quite unexpected. The force vector is given by the following equation

$$F_i = K_{ij} E_j \quad \begin{array}{l} i=1,2,\dots,8 \\ j=1,2,\dots,8 \end{array}$$

where

K_{ij} = uniform beam stiffness matrix from Eq (D-20)

and

$$E_j = \frac{PL}{\pi} \left\{ \begin{array}{l} \left(\frac{L}{\pi}\right)^3 \sin \frac{\pi(e-1)}{\bar{E}} \\ \left(\frac{L}{\pi}\right)^2 \cos \frac{\pi(e-1)}{\bar{E}} \\ -\frac{L}{\pi} \sin \frac{\pi(e-1)}{\bar{E}} \\ - \cos \frac{\pi(e-1)}{\bar{E}} \\ \left(\frac{L}{\pi}\right)^3 \sin \frac{\pi e}{\bar{E}} \\ \left(\frac{L}{\pi}\right)^2 \cos \frac{\pi e}{\bar{E}} \\ -\frac{L}{\pi} \sin \frac{\pi e}{\bar{E}} \\ - \cos \frac{\pi e}{\bar{E}} \end{array} \right\}$$

$$I_e = \frac{EI}{h^7} \begin{bmatrix} 100800 & 50400h & 10080h^2 & 840h^3 & -100800 & 50400h & -10080h^2 & 840h^3 \\ 50400h & 25920h^2 & 5400h^3 & 480h^4 & -50400h & 24480h^2 & -4680h^3 & 360h^4 \\ 10080h^2 & 5400h^3 & 1200h^4 & 120h^5 & -10080h^2 & 4680h^3 & -840h^4 & 60h^5 \\ 840h^3 & 480h^4 & 120h^5 & 16h^6 & -840h^3 & 360h^4 & -60h^5 & 4h^6 \\ -100800 & -50400h & -10080h^2 & -840h^3 & 100800 & -50400h & 10080h^2 & -840h^3 \\ 50400h & 24480h^2 & 4680h^3 & 360h^4 & -50400h & 25920h^2 & -5400h^3 & 480h^4 \\ -10080h^2 & -4680h^3 & -840h^4 & -60h^5 & 10080h^2 & -5400h^3 & 1200h^4 & -120h^5 \\ 840h^3 & 360h^4 & 60h^5 & 4h^6 & -840h^3 & 480h^4 & -120h^5 & 16h^6 \end{bmatrix} \begin{Bmatrix} w_{e-3} \\ w_{e-2} \\ w_{e-1} \\ w_e \\ w_{e+1} \\ w_{e+2} \\ w_{e+3} \\ w_{e+4} \end{Bmatrix} = \begin{Bmatrix} 0 \\ 0 \\ 0 \\ h \\ 0 \\ 0 \\ 0 \\ -h \end{Bmatrix}$$

$$I_e = \frac{EI}{h^7}$$

(D-20)

Appendix E

Shape Functions and Several Derivatives

The shape functions used for a particular finite element technique determine the nature of the approximate solution (Ref 6:131). These functions as used in this study can be formed from the familiar Hermite Polynomials (Ref 6:152-155). Unfortunately, this method does not convey the physical nature of the functions.

A linear approximation of the field variable within an element is given by $\phi(\bar{x}) = [1 \ \bar{x}] \begin{Bmatrix} a_1 \\ a_2 \end{Bmatrix}$. For a line element, as depicted in Fig E-1, the nodal parameters ϕ_1 and ϕ_2 are given by

$$\begin{Bmatrix} \phi_1 \\ \phi_2 \end{Bmatrix} = \begin{bmatrix} 1 & 0 \\ 1 & h \end{bmatrix} \begin{Bmatrix} a_1 \\ a_2 \end{Bmatrix}$$

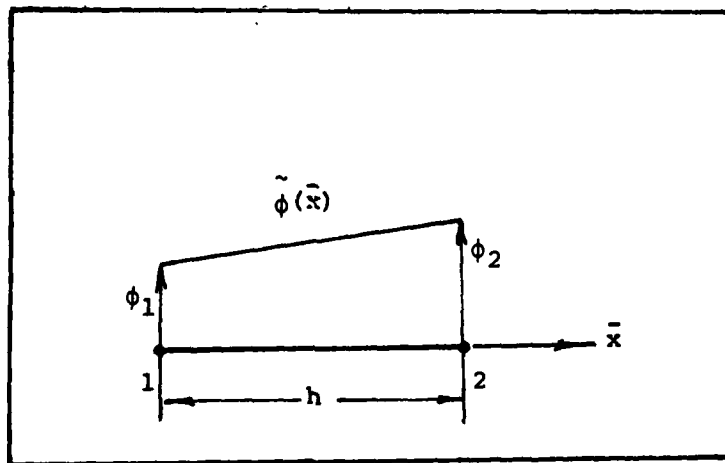


Fig E-1. C^0 Line Element

Inverting this relation and substituting a_1 and a_2 into the approximation equation gives

$$\tilde{\phi}(\bar{x}) = [1 \quad \bar{x}] \begin{bmatrix} 1 & 0 \\ -\frac{1}{h} & \frac{1}{h} \end{bmatrix} \begin{Bmatrix} \phi_1 \\ \phi_2 \end{Bmatrix}$$

The product of the two matrices is defined as the vector of shape functions N_j , where j denotes the shape function associated with nodal parameter ϕ_j . The approximation equation is now of the form:

$$\tilde{\phi}(x) = \sum_{j=1}^m N_j \phi_j \quad j=1,2,\dots,m$$

where m = number of nodal parameters associated with the element.

This type of element is said to have C^0 continuity because only the function is continuous between two connected elements. The linear shape functions are given in Fig E-2. These shape functions exhibit properties of the "kronecker" delta function. That is:

$$N_j(\bar{x}_i) = \delta_{ij} \equiv \begin{cases} 1 & i=j \\ 0 & i \neq j \end{cases}$$

A line element possessing C^1 continuity will have continuous first derivatives of the field variable between two connected elements. This requires a cubic approximation of the field variable. By duplicating the process followed for the linear shape functions one can transform

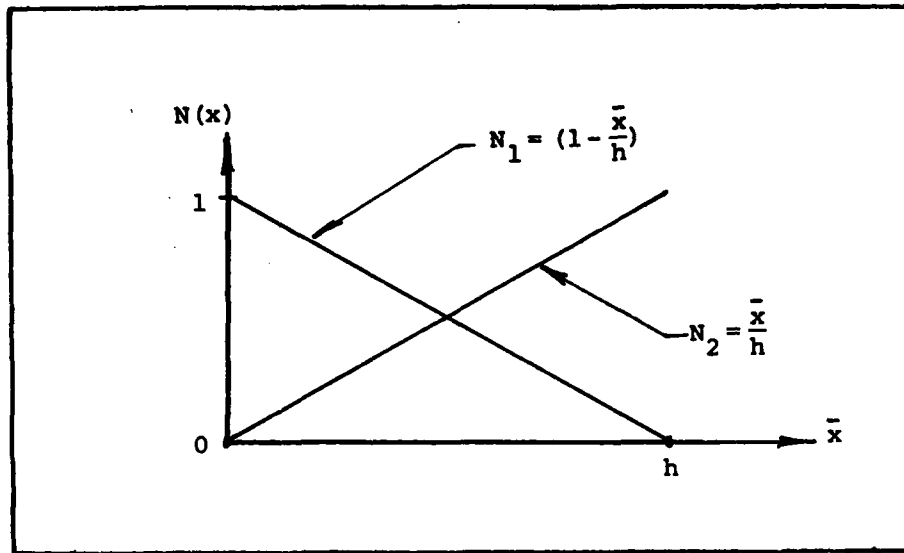


Fig. E-2. Linear Shape Functions (Ref 5:154)

the equation $\tilde{\phi}(\bar{x}) = a_1 + a_2\bar{x} + a_3\bar{x}^2 + a_4\bar{x}^3$ into

$$\tilde{\phi}(\bar{x}) = \sum_{j=1}^4 N_j \phi_j$$

where the nodal parameters ϕ_j are illustrated in Fig E-3.

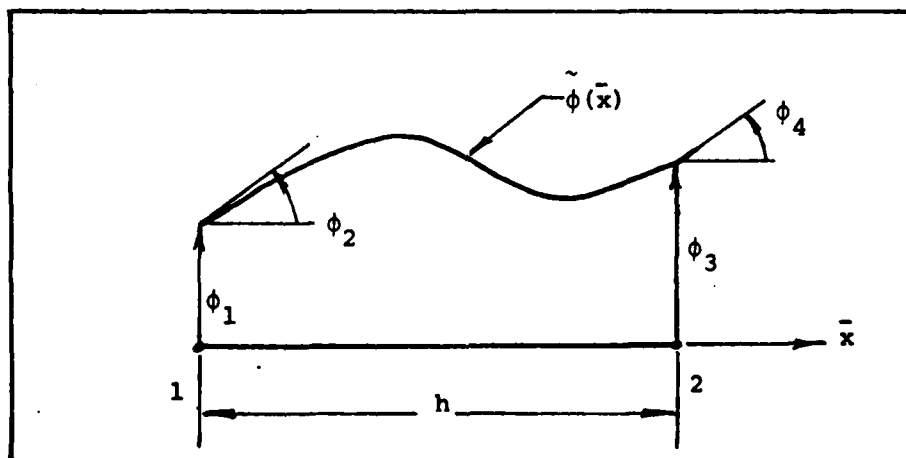


Fig. E-3. C^1 Line Element

The cubic shape functions associated with the C^1 line element are given in Fig E-4. The linear and cubic shape functions are summarized in Table E-I.

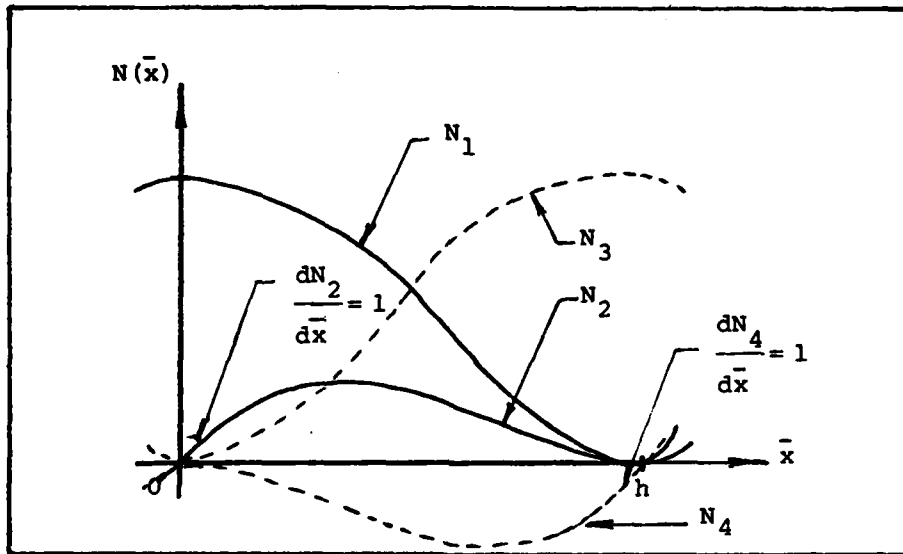


Fig. E-4. Cubic Shape Functions (Ref 6:154)

The highest order element used in this thesis is a C^3 line element. It allows continuity of the third derivative of the field variable between elements. The approximation equation is $\tilde{\phi}(\bar{x}) = a_1 + a_2\bar{x} + a_3\bar{x}^2 + a_4\bar{x}^3 + a_5\bar{x}^4 + a_6\bar{x}^5 + a_7\bar{x}^6 + a_8\bar{x}^7$. Since there are eight undetermined parameters the C^3 line element must be defined with four nodal parameters at each of its two nodes. Thus the ϕ_j vector is

Table E-1

Linear and Cubic Shape Functions with
Derivatives of Specific Interest

(a) Linear: $0 \leq x = \frac{\bar{x}}{h} \leq 1$

$$\{N\}^T = \begin{Bmatrix} 1 - x \\ x \end{Bmatrix} \quad \{B\}^T = \left\{ \frac{dN}{d\bar{x}} \right\}^T = \begin{Bmatrix} -\frac{1}{h} \\ \frac{1}{h} \end{Bmatrix}$$

(b) Cubic: $0 \leq x = \frac{\bar{x}}{h} \leq 1$

$$\{N\}^T = \begin{Bmatrix} 1 - 3x^2 + 2x^3 \\ h[x - 2x^2 + x^3] \\ 3x^2 - 2x^3 \\ h[-x^2 + x^3] \end{Bmatrix} \quad \{B\}^T = \left\{ \frac{d^2N}{d\bar{x}^2} \right\}^T = \begin{Bmatrix} \frac{6}{h^2} [2x-1] \\ \frac{2}{h} [3x-2] \\ -\frac{6}{h^2} [2x-1] \\ \frac{2}{h} [3x-1] \end{Bmatrix}$$

$$\begin{Bmatrix} \phi_1 \\ \phi_2 \\ \phi_3 \\ \phi_4 \\ \phi_5 \\ \phi_6 \\ \phi_7 \\ \phi_8 \end{Bmatrix} = \begin{Bmatrix} \phi(0) \\ \phi, \bar{x}(0) \\ \phi, \bar{x}\bar{x}(0) \\ \phi, \bar{x}\bar{x}\bar{x}(0) \\ \phi(h) \\ \phi, \bar{x}(h) \\ \phi, \bar{x}\bar{x}(h) \\ \phi, \bar{x}\bar{x}\bar{x}(h) \end{Bmatrix}$$

The third and seventh parameters are proportional to the bending moment in a beam at $\bar{x}=0$ and $\bar{x}=h$. The fourth and eighth parameters are proportional to the transverse shear force. The septic shape functions are given in Table E-II, along with their fourth derivatives. Shape functions N_1 through N_4 are shown in Fig E-5; the other four shape functions are simply a reflection about the point $\bar{x}=h/2$.

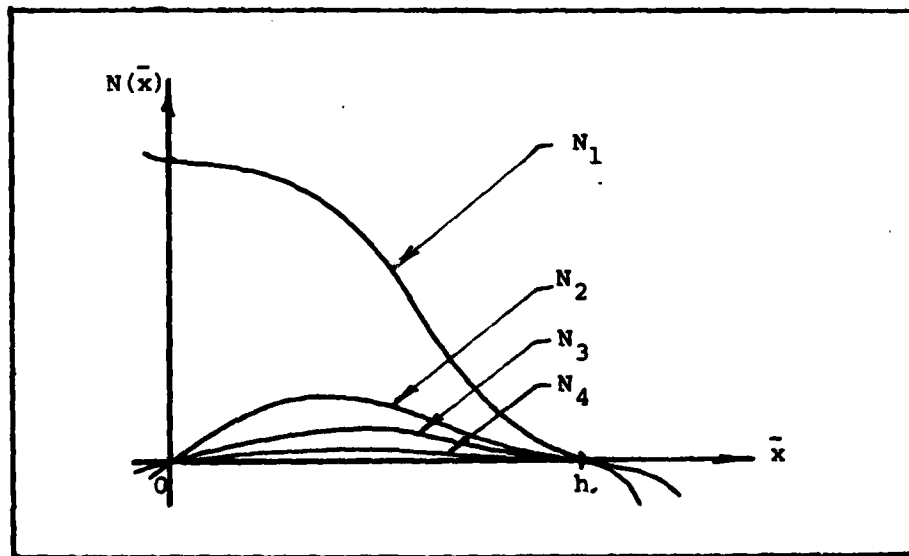


Fig E-5. Septic Shape Functions (Ref 5:155)

Table E-II

Septic Shape Functions with Derivatives
of Specific Interest

$$\begin{aligned} \{N\}^T &= \left\{ \begin{aligned} &1-35x^4 + 85x^5 - 70x^6 + 20x^7 \\ &h[x-20x^4 + 45x^5 - 36x^6 + 10x^7] \\ &h^2 \left[\frac{1}{2}x^2 - 5x^4 + 10x^5 - \frac{15}{2}x^6 + 2x^7 \right] \\ &h^3 \left[\frac{1}{6}x^3 - \frac{2}{3}x^4 + x^5 - \frac{2}{3}x^6 + \frac{1}{6}x^7 \right] \\ &35x^4 - 84x^5 + 70x^6 - 20x^7 \\ &h[-15x^4 + 39x^5 - 34x^6 + 10x^7] \\ &h^2 \left[\frac{5}{2}x^4 - 7x^5 + \frac{13}{2}x^6 - 2x^7 \right] \\ &h^3 \left[-\frac{1}{6}x^4 + \frac{1}{2}x^5 - \frac{1}{2}x^6 + \frac{1}{6}x^7 \right] \end{aligned} \right\} \\ \{B\}^T = \left\{ \frac{d^4 N}{dx^4} \right\}^T &= \left\{ \begin{aligned} &\frac{1}{h^4}[-840 + 10080x - 25200x^2 + 16800x^3] \\ &\frac{1}{h^3}[-480 + 5400x - 12960x^2 + 8400x^3] \\ &\frac{1}{h^2}[-120 + 1200x - 2700x^2 + 1680x^3] \\ &\frac{1}{h}[-16 + 120x - 240x^2 + 140x^3] \\ &\frac{1}{h^4}[840 - 10080x + 25200x^2 - 16800x^3] \\ &\frac{1}{h^3}[-360 + 4680x - 12240x^2 + 8400x^3] \\ &\frac{1}{h^2}[60 - 840x + 2340x^2 - 1680x^3] \\ &\frac{1}{h}[-4 + 60x - 180x^2 + 140x^3] \end{aligned} \right\} \end{aligned}$$

where $0 \leq x = \frac{\bar{x}}{h} \leq 1$

Appendix F
Derivation of Finite Element Equations for the
Nonlinear Problem with Sample Calculations

The differential equation given for the nonlinear problem studied is

$$[1-\phi_x]\phi_{xx} = 0 \qquad 0 < x < 1 \qquad (F-1)$$

with the boundary conditions

$$\begin{aligned} \phi(0) &= 0 \\ \phi_x(0) &= 1 \\ \phi(1) &= C_1 \text{ (constant)} \end{aligned} \qquad (F-2)$$

where the subscript x implies differentiation with respect to the independent variable x . Equation (F-1) can be stated in two different but equivalent forms. These are

$$A) \qquad \phi_x - \frac{1}{2} [\phi_x^2]_x = 0 \qquad (F-3)$$

$$B) \qquad -\frac{1}{2} [(1-\phi_x)^2]_x = 0 \qquad (F-4)$$

The domain was discretized into two elements of length h_1 and h_2 respectively, with the global nodal parameters given in Eq (F-5). The two elements are joined at a double node as shown in Fig. F-1.

$$\begin{aligned}
 \phi_1 &= \phi(0) & \phi_5 &= \phi(h_1^+) \\
 \phi_2 &= \frac{d\phi(0)}{dx} & \phi_6 &= \frac{d\phi(h_1^+)}{dx} \\
 \phi_3 &= \phi(h_1^-) & \phi_7 &= \phi(h_1+h_2) \\
 \phi_4 &= \frac{d\phi(h_1^-)}{dx} & \phi_8 &= \frac{d\phi(1)}{dx}
 \end{aligned}
 \tag{F-5}$$

where ϕ_3 and ϕ_4 are the approximate solutions to the displacement (potential function) and the slope (velocity) respectively at the right end of the first element; and ϕ_5 and ϕ_6 are the approximate solutions at the left end of the second element. The discretized domain is shown in Fig. F-1.

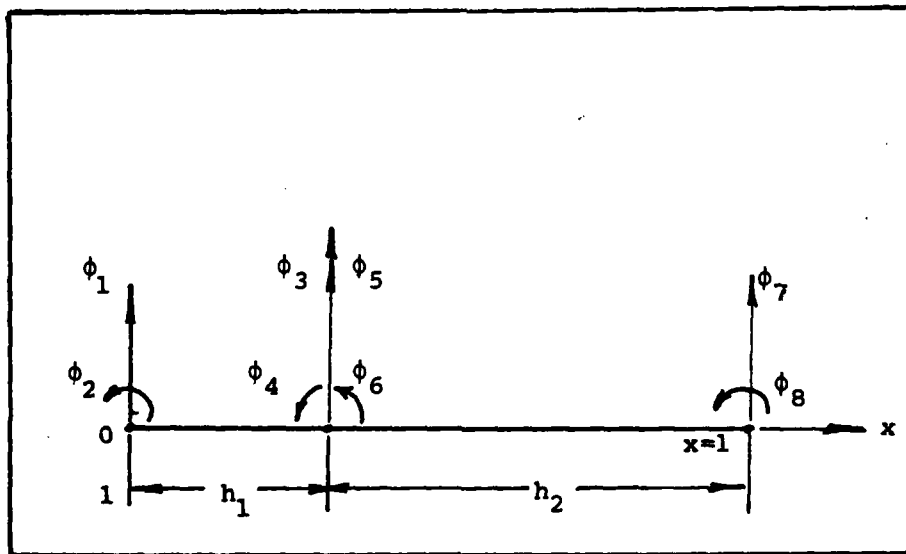


Fig F-1. Discretized Domain for Nonlinear Problem

It is necessary to have at least one double node because the differential equation with the boundary conditions given by Eq (F-2) has exactly one discontinuity. The double node allows the specification of the discontinuity, or jump, in the approximate solution. The jump is modeled by two equations. They are:

$$\begin{aligned}\phi_3 &= \phi_5 \\ \phi_4 &= \phi_6 + \Delta\end{aligned}\tag{F-6}$$

where Δ is the change in slope between elements. The first equation insures continuity of the function across the inter-element boundary; and the second guarantees the required change in slope.

With this discretization, the finite element equations can be derived by the same process as the linear problems. (See Appendices C and D.)

Equation (F-6) is solved by an iterative process. With the substitution $\phi^n(\bar{x}) = N_j(\bar{x}) \phi_j^n$, the iterative equation for element e becomes

$$\int_0^h \left\{ 1 - \frac{1}{2} N_{k\bar{x}} \phi_k^n \right\} N_{i\bar{x}} N_{j\bar{x}} d\bar{x} \phi_j^{n+1} = 0$$

$$\begin{aligned}0 &\leq \bar{x} \leq h & i &= 1, 2, 3, 4 \\ e &= 1, 2 & j &= 1, 2, 3, 4 \\ & & k &= 1, 2, 3, 4\end{aligned}\tag{F-7}$$

where ϕ_j^n are the nodal solutions obtained from the n^{th} iteration.

By the exact same process Eq (F-4) gives

$$\int_0^h \left\{ 1 - N_{k\bar{x}} \phi_k^n \right\} N_{i\bar{x}} N_{j\bar{x}} d\bar{x} \phi_j^{n+1} = \int_0^h (1 - N_{k\bar{x}} \phi_k^n) N_{i\bar{x}} d\bar{x}$$

$$\begin{array}{ll} 0 \leq \bar{x} \leq h & i=1,2,3,4 \\ e=1,2 & j=1,2,3,4 \\ & k=1,2,3,4 \end{array} \quad (\text{F-8})$$

The shape functions chosen are the cubic functions given in Appendix E. The local shape function derivatives can be written in the form

$$N_{i\bar{x}} = \left(\frac{\bar{x}}{h} \right) \left\{ A_i + B_i \left(\frac{\bar{x}}{h} \right) \right\}$$

$$\begin{array}{ll} 0 \leq \bar{x} \leq h & i=1,2,3,4 \end{array} \quad (\text{F-9})$$

where

$$A_i = \left[-\frac{6}{h}, -4, \frac{6}{h}, -2 \right]$$

$$B_i = \left[\frac{6}{h}, 3, -\frac{6}{h}, 3 \right].$$

With $N_{i\bar{x}}$ in this form Eqs (F-7) and (F-8) can be written in the following form for $h_1 = h_2 = h$

$$K_{ij} \phi_j^{n+1} = F_i$$

$$\begin{array}{l} i=1,2,\dots,4 \\ j=1,2,\dots,4 \\ e=1,2 \end{array}$$

where

$$K_{ij} = \frac{h}{420} [A_i A_j \Gamma_1 + (A_i B_j + B_i A_j) \Gamma_2 + B_i B_j \Gamma_3] \quad (F-9)$$

$$\Gamma_1 = 84\beta_1 + 105\beta_2 + 140$$

$$\Gamma_2 = 70\beta_1 + 84\beta_2 + 105 \quad (F-10)$$

$$\Gamma_3 = 60\beta_1 + 70\beta_2 + 84$$

and for Eq (F-7) - formulation A

$$\beta_1 = -\frac{3}{2h} [2(\phi_1^n - \phi_3^n) + h(\phi_2^n + \phi_4^n)]$$

$$\beta_2 = \frac{1}{h} [3(\phi_1^n - \phi_3^n) + h(2\phi_2^n + \phi_4^n)]$$

$$F_i = 0 \quad i=1,2,3,4 \quad (F-11)$$

and for Eq (F-8) - formulation B

$$\beta_1 = -\frac{3}{h} [2(\phi_1^n - \phi_3^n) + h(\phi_2^n + \phi_4^n)]$$

$$\beta_2 = \frac{2}{h} [3(\phi_1^n - \phi_3^n) + h(2\phi_2^n + \phi_4^n)]$$

$$F_1 = -\frac{1}{60} (18\beta_1 + 30\beta_2 + 60) \quad (F-12)$$

$$F_2 = -\frac{h}{60} (24\beta_1 + 35\beta_2 + 60)$$

$$F_3 = \frac{1}{60} (18\beta_1 + 30\beta_2 + 60)$$

$$F_4 = \frac{h}{60} (6\beta_1 + 5\beta_2)$$

The products of A_i and B_i in matrix form are as follows for $h = 1/2$.

$$[AA] = [A_i A_j] = \begin{bmatrix} 144 & 48 & -144 & 24 \\ & 16 & -48 & 8 \\ & & 144 & -24 \\ \text{(symmetric)} & & & 4 \end{bmatrix}$$

$$[AB] = [A_i B_j + B_i A_j] = \begin{bmatrix} -288 & -84 & 288 & -60 \\ & -24 & 84 & -18 \\ & & -288 & 60 \\ \text{(symmetric)} & & & 12 \end{bmatrix}$$

$$[BB] = [B_i B_j] = \begin{bmatrix} 144 & 36 & -144 & 36 \\ & 9 & -36 & 9 \\ & & 144 & -36 \\ \text{(symmetric)} & & & 9 \end{bmatrix}$$

Sample Problem F-1. The nonlinear problem for $\Delta=2$ is solved by formulation A. The initial guess is $\phi_i^0 = [0, 1, 1, 1, 1, -1, 0, -1]$

For element 1:

$$\beta_1 = 3, \beta_2 = -3$$

$$\Gamma_1 = 77, \Gamma_2 = 63, \Gamma_3 = 54$$

thus,

$$K_{ij} = \frac{1}{840} \begin{bmatrix} 720 & 348 & -720 & 12 \\ & 206 & -348 & -32 \\ & & 720 & -12 \\ \text{(symmetric)} & & & 38 \end{bmatrix}$$

For element 2:

$$\beta_1 = -3, \beta_2 = 3$$

$$\Gamma_1 = 203, \Gamma_2 = 147, \Gamma_3 = 114$$

$$K_{ij} = \frac{1}{840} \begin{bmatrix} 3312 & 1500 & -3312 & 156 \\ & 746 & -1500 & 4 \\ & & 3312 & -156 \\ \text{(symmetric)} & & & 74 \end{bmatrix}$$

Assembling the elemental matrices in the global system equations gives

$$\begin{bmatrix} 720 & 748 & -720 & 12 & 0 & 0 & 0 & 0 \\ & 206 & -348 & -32 & 0 & 0 & 0 & 0 \\ & & 720 & -12 & 0 & 0 & 0 & 0 \\ & & & 38 & 0 & 0 & 0 & 0 \\ & & & & 3312 & 1500 & -3312 & 156 \\ & & & & & 746 & -1500 & 4 \\ & & & & & & 3312 & -156 \\ \text{(symmetric)} & & & & & & & 74 \end{bmatrix} \begin{Bmatrix} \phi_1^1 \\ \phi_2^1 \\ \phi_3^1 \\ \phi_4^1 \\ \phi_5^1 \\ \phi_6^1 \\ \phi_7^1 \\ \phi_8^1 \end{Bmatrix} = \{0\}$$

Substituting the jump conditions and the boundary conditions gives the reduced system equations. They are

$$\begin{bmatrix} 720 & -12 & 0 & 0 & 0 \\ -12 & 38 & 0 & 0 & 0 \\ 1 & 0 & -1 & 0 & 0 \\ 0 & 1 & 0 & -1 & 0 \\ 0 & 0 & 156 & 4 & 74 \end{bmatrix} \begin{Bmatrix} \phi_3^1 \\ \phi_4^1 \\ \phi_5^1 \\ \phi_6^1 \\ \phi_8^1 \end{Bmatrix} = \begin{Bmatrix} 348 \\ 32 \\ 0 \\ 2 \\ 0 \end{Bmatrix}$$

Solving this equation gives the following which matches the exact solution.

$$\phi_i^1 = [0, 1, 0.5, 1, 0.5, -1, 0, -1]$$

The next iteration is performed with $\phi_i^n = \phi_i^1$ which gives ϕ_i^2 . This second iteration gives the same numerical results as the first, implying convergence of the algorithm.

Collocation

The domain is discretized in the same manner as for the Galerkin's method. The derivation of the finite element equations is by the same procedure as followed in Appendices C and D for this method. The two formulations give the following global equations for element e.

Formulation A:

$$\left\{ \left(1 - \frac{1}{2} N_{k\bar{x}} \phi_k^h \right) N_{j\bar{x}\bar{x}} - \frac{1}{2} N_{j\bar{x}} N_{k\bar{x}\bar{x}} \phi_k^n \right\} \bigg|_{\bar{x}=\bar{x}_i} \phi_j^{n+1} = 0$$

$$\begin{array}{ll} 0 \leq \bar{x} \leq h & i=1,2,\dots,m \\ e=1,2 & j=1,2,\dots,m \\ & k=1,2,\dots,m \end{array} \quad (F-13)$$

Formulation B:

$$\left\{ \begin{array}{l} -(1-N_{k\bar{x}}\phi_k^n)N_{j\bar{x}\bar{x}} + N_{j\bar{x}}N_{k\bar{x}\bar{x}}\phi_k^n \end{array} \right\} \phi_j^{n+1} = N_{k\bar{x}\bar{x}} \phi_k^n \bigg|_{\bar{x}=\bar{x}_i}$$

$$\begin{array}{ll} 0 \leq \bar{x} \leq h & i=1,2,\dots,m \\ e=1,2 & j=1,2,\dots,m \\ & k=1,2,\dots,m \end{array} \quad (F-14)$$

The cubic shape functions given in Eq (F-9) are used for this method also.

Vita

Randy A. Smith was both on 27 February 1956 in East Stroudsburg, Pennsylvania. He graduated from high school in the same town in June 1974. He then attended Lehigh University and received a Bachelor of Science degree in Mechanical Engineering in May 1978. Upon graduation, he received a USAF commission through the ROTC program. He then entered the School of Engineering, Air Force Institute of Technology, in June 1978.

Permanent Address: 40 Grandview Street
East Stroudsburg, Pennsylvania
18301

UNCLASSIFIED

SECURITY CLASSIFICATION OF THIS PAGE (When Data Entered)

REPORT DOCUMENTATION PAGE		READ INSTRUCTIONS BEFORE COMPLETING FORM
1. REPORT NUMBER AFIT/GAE/AA-79D-17	2. GOVT ACCESSION NO.	3. RECIPIENT'S CATALOG NUMBER
4. TITLE (and Subtitle) COMPARISON OF NUMERICAL ANALYSIS METHODS FOR SOLVING ONE-DIMENSIONAL ELLIPTIC DIFFERENTIAL EQUATIONS		5. TYPE OF REPORT & PERIOD COVERED MS Thesis
7. AUTHOR(s) Randy A. Smith 2nd Lt, USAF		6. PERFORMING ORG. REPORT NUMBER
9. PERFORMING ORGANIZATION NAME AND ADDRESS Air Force Institute of Technology (AFIT/EN) Wright-Patterson AFB, Ohio 45433		8. CONTRACT OR GRANT NUMBER(s)
11. CONTROLLING OFFICE NAME AND ADDRESS		10. PROGRAM ELEMENT, PROJECT, TASK AREA & WORK UNIT NUMBERS
14. MONITORING AGENCY NAME & ADDRESS (if different from Controlling Office)		12. REPORT DATE December 1979
		13. NUMBER OF PAGES 156
		15. SECURITY CLASS. (of this report) UNCLASSIFIED
		15a. DECLASSIFICATION/DOWNGRADING SCHEDULE
16. DISTRIBUTION STATEMENT (of this Report) Approved for public release; distribution unlimited		
17. DISTRIBUTION STATEMENT (of the abstract entered in Block 20, if different from Report)		
18. SUPPLEMENTARY NOTES Approved for public release; IAW AFR 190-17 JOSEPH P. HIPPS, Major, USAF Director, Office of Public Affairs		
19. KEY WORDS (Continue on reverse side if necessary and identify by block number) Numerical Analysis Finite Element Method Ordinary Differential Equations Finite Difference Method		
20. ABSTRACT (Continue on reverse side if necessary and identify by block number) Four numerical methods are used to solve a specific set of problems and then the methods are compared for accuracy and efficiency. The methods are: standard finite differences, collocation, Galerkin, and least squares. The latter three methods are finite element methods which use either Lagrange linear, Hermite cubic, or Hermite septic piecewise polynomials as interpolation functions.		

DD FORM 1473

EDITION OF 1 NOV 65 IS OBSOLETE

UNCLASSIFIED

SECURITY CLASSIFICATION OF THIS PAGE (When Data Entered)

UNCLASSIFIED

SECURITY CLASSIFICATION OF THIS PAGE(When Data Entered)

The problem set consists of second- and fourth-order, linear and nonlinear, differential equations with constant and variable coefficients. The linear equations govern elementary structural members and the nonlinear equation is a one-dimensional analog for transonic flow past an airfoil.

The three major conclusions are: (1) the least squares method with Hermite cubic polynomials was the method of choice for the second order linear equations, (2) the collocation method was chosen over the Galerkin and the finite difference methods for the fourth-order equations, and (3) Galerkin method was chosen over the collocation method for the nonlinear problem.

UNCLASSIFIED

SECURITY CLASSIFICATION OF THIS PAGE(When Data Entered)